

SPECIFIC FUNCTIONS OF THE TUMOR SUPPRESSOR P53  
ARE ACTIVATED BY P73 AND VHL

Eric R. Wolf

Submitted to the faculty of the University Graduate School  
in partial fulfillment of the requirements  
for the degree  
Doctor of Philosophy  
in the Department of Biochemistry and Molecular Biology,  
Indiana University

July 2019

Accepted by the Graduate Faculty of Indiana University, in partial fulfillment of the requirements for the degree of Doctor of Philosophy.

Doctoral Committee

---

Lindsey Mayo, PhD, Chair

---

Mark Goebel, PhD

May 9, 2019

---

Mircea Ivan, PhD

---

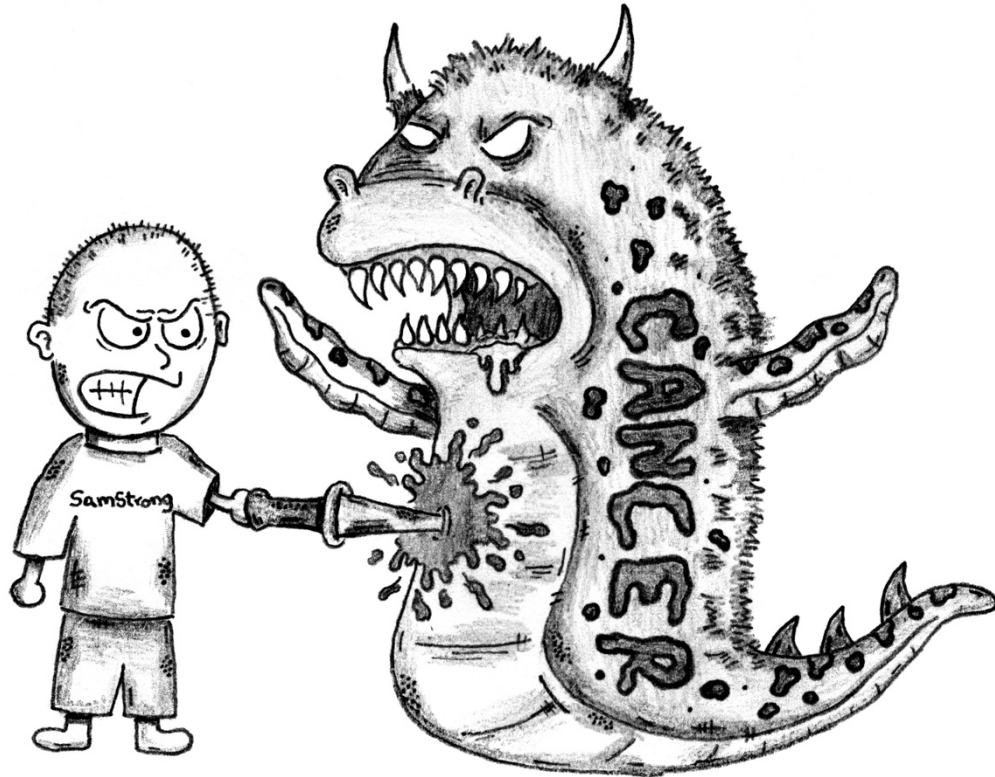
Marc Mendonca, PhD

---

Clark Wells, PhD

## DEDICATION

For Sam – your relentless drive to improve the lives of those who followed you has been an immense source of motivation for me.



Drawing by Sam Featherstone. Printed with permission from SamStrong.

## ACKNOWLEDGEMENTS

I want to acknowledge the people in my life who have helped, inspired, and motivated me. Emily and Jack – for always believing in me and keeping me grounded. My parents, Tom and Shelly, and brother, Alex – for teaching me to be curious about everything and providing an environment that fostered learning. My teachers and professors, Mrs. Ball, Mrs. Steffenhagen, and Dr. Na – for entertaining my questions and instilling in me an appreciation for the sciences. Additionally, I want to acknowledge the role that many relatives and friends have played in inspiring and motivating me through their own battles with cancer – my grandparents Dick and Elvira Wolf, my grandparents Harrison and Jessie Hicks, my uncle Gary Patrick, my uncle Joe Hicks, my sister-in-law Libby Storkman, my friend Sam Featherstone, my aunt-in-law Julie Mills, and my mom, Shelly Wolf.

I would like to thank my advisor, Dr. Lindsey Mayo – for his mentorship and guidance during my graduate career. I would also like to acknowledge the members of my committee – Dr. Mark Goebel, Dr. Mircea Ivan, Dr. Marc Mendonca, and Dr. Clark Wells for their time, knowledge, and helpful insights throughout my research. I want to thank the past members of the Mayo lab as well – Dr. Paula Hauck, for training me at the bench and providing valuable technical advice; Dr. David Olivos, for our stimulating scientific conversations; and Ciaran McAtarsney, for being a great colleague.



Eric R. Wolf

SPECIFIC FUNCTIONS OF THE TUMOR SUPPRESSOR P53  
ARE ACTIVATED BY P73 AND VHL

The transcription factor and tumor suppressor protein p53 critically regulates cell survival or death in response to cellular stress. p53 can activate genes involved in a wide variety of processes, including apoptosis, cell cycle arrest, angiogenesis, metabolism, and senescence. Mutations in p53 are common in cancer and alter its interactions with other proteins, but there are other mechanisms and posttranslational modifications that can alter these interactions as well. In some tumors, such as renal cell carcinoma, p53 is commonly inactive even though mutations to *TP53* are rare. This suggests that there are other biochemical mechanisms of inhibition, which we explore in this study.

Mutations in the DNA-binding domain of p53 result in conformational changes that enable p53 to interact with and inhibit its family member p73, thereby promoting cell survival instead of apoptosis. In contrast, it has been reported that wild-type p53 does not bind to p73. We found that JNK-mediated phosphorylation of Thr81 in the proline-rich domain (PRD) of p53 enabled wild-type p53 to form a complex with p73. The dimerization of wild-type p53 with p73 facilitated the expression of apoptotic target genes such as *PUMA* and *BAX*, as well as the induction of apoptosis. In addition to the apoptotic function of p53, the tumor suppressor also plays a major role in the inhibition of angiogenesis.

Here we also report a new mechanism where the Mdm2 oncoprotein can indirectly inactivate p53 through the regulation of the tumor suppressor VHL. In response to hypoxia, VHL can bind p53, which results in activation of several anti-angiogenic

targets of p53 such as *THBS1* and *COL18A1*. Mdm2 regulates the VHL-p53 interaction by conjugating nedd8 to VHL within a region that is important for the VHL-p53 interaction, blocking the induction of anti-angiogenic genes and resulting in a proangiogenic phenotype. Due to its positive regulation of major proangiogenic proteins and its negative regulation of potent inhibitors of angiogenesis, we propose that the oncoprotein Mdm2 is the angiogenic switch. These findings refine our understanding of p53 interactions and activation, specifically for p53-p73 induced cell death and p53-VHL inhibition of angiogenesis.

Lindsey Mayo, PhD, Chair

## TABLE OF CONTENTS

List of Tables .....	ix
List of Figures .....	x
List of Abbreviations .....	xii
1. Background .....	1
1.1. The p53 tumor suppressor family .....	1
1.2. The p53-Mdm2 autoregulatory feedback loop .....	2
1.3. The p53-independent roles of Mdm2 in cancer .....	7
1.3.1. Introduction .....	7
1.3.2. Mdm2 in tumorigenesis .....	9
1.3.3. Mdm2 promotes an aggressive cell cycle .....	12
1.3.4. Mdm2 inhibits the DNA damage response .....	17
1.3.5. Mdm2 promotes metastasis .....	19
1.3.6. Conclusion .....	20
1.4. VHL-HIF pathway .....	21
2. Materials and Methods .....	25
2.1. Cell culture .....	25
2.2. Transient transfection .....	25
2.3. Plasmid generation .....	25
2.4. Protein purification .....	27
2.5. Western blotting .....	27
2.6. I-TASSER protein structure prediction .....	27
2.7. Immunofluorescence microscopy .....	30
2.8. Colony forming assay .....	30
2.9. GFP fluorescence assay .....	30
2.10. Thrombospondin-1 reporter assay .....	31
2.11. Secreted thrombospondin-1 assay .....	31
2.12. Generation of shp53 786-O and RCC4 cell lines .....	33
2.13. Enzyme-linked immunosorbent assay .....	33
2.14. Immunoprecipitation .....	33
2.15. GFP HUVEC tube formation assay .....	33
2.16. Bioinformatics analysis of clinical data .....	34
2.17. His-nedd8 pulldown .....	34
2.18. in vitro neddylation assay .....	34
3. Mutant and wild-type p53 form complexes with p73 upon phosphorylation by the kinase JNK .....	37
3.1. Introduction .....	37
3.2. The phosphorylation of p53 by JNK results in the induction of the apoptotic protein PUMA .....	38
3.3. The predicted structure of a Thr <sup>81</sup> phosphomimic shows a potential mode of binding to p73 .....	43
3.4. Phosphorylation of Thr <sup>81</sup> of p53 promotes a p53-p73 complex .....	46
3.5. The JNK-initiated p53-p73 pathway is important for apoptosis .....	56
3.6. Discussion .....	61
4. Mdm2 functions as an angiogenic switch through its regulation of VHL .....	64

4.1. Introduction .....	64
4.2. p53 target genes for apoptosis and angiogenesis are altered by VHL status .....	66
4.3. Mdm2 binds to VHL and inhibits VHL-p53 complex formation under hypoxia.....	71
4.4. Neddylation of VHL by Mdm2 interferes with VHL-p53 complex formation.....	75
4.5. VHL colocalizes with p53 under hypoxia or with treatment of MLN4924.....	80
4.6. VHL increases the acetylation of p53 under hypoxia, leading to increased transcription and secretion of TSP-1.....	85
4.7. p53 and TSP-1 inhibit Human Umbilical Vein Endothelial Cell network formation.....	88
4.8. Discussion.....	92
5. Discussion and Future Directions .....	96
5.1. Contributions to the field and status of research .....	96
5.2. Evidence for an Mdm2-VHL feedback loop .....	102
5.3. Conclusions and summary of findings.....	113
References.....	116
Curriculum Vitae	

## LIST OF TABLES

Table 1: VHL Disease types .....	24
Table 2: Oligonucleotides used for the site directed mutagenesis of p53.....	26
Table 3: Description of cell lines used.....	28
Table 4: List of antibodies .....	29
Table 5: List of miscellaneous reagents.....	33
Table 6: Description buffers used.....	35
Table 7: Manders' coefficients for microscopy colocalization analysis.....	54

## LIST OF FIGURES

Figure 1: Mdm2 is involved in several hallmarks of cancer.....	11
Figure 2: A map of the domains and interactions of the Mdm2 protein.....	16
Figure 3: Mdm2 impacts the Rb signaling pathway .....	18
Figure 4: Phosphorylation of Thr <sup>81</sup> of mutant p53 in response to JNK activation .....	40
Figure 5: Phosphorylation of Thr <sup>81</sup> in cell lines with wild-type p53 .....	41
Figure 6: U87 cell death.....	42
Figure 7: Predicted structure of a Thr <sup>81</sup> phosphomimic reveals a possible mode of binding to p73 .....	45
Figure 8: p53-p73 complex formation and activity .....	48
Figure 9: The effect of T81E on p53-p73 complex formation.....	49
Figure 10: p53 activation and colocalization with p73 in MDA-MB-157 cells .....	51
Figure 11: p53 activation and colocalization with p73 in HME1 cells.....	52
Figure 12: p53 activation and colocalization with p73 in TMD231 cells.....	53
Figure 13: JNK activation or inhibition in HME, MDA157, and TMD231 cell lines.....	54
Figure 14: Downstream effects of the p53-p73 pathway.....	57
Figure 15: Effects of the p53-p73 pathway on cell survival.....	58
Figure 16: Cell fate is dictated by the formation of a p53-p73 complex .....	60
Figure 17: p53 target genes for apoptosis and angiogenesis are altered by VHL status .....	68
Figure 18: VHL increases transcription of <i>THBS1</i> and secretion of TSP-1 .....	69
Figure 19: Angiogenesis array with conditioned media from 786-O cells under hypoxia.....	70
Figure 20: Mdm2 binds to VHL and inhibits VHL-p53 complex formation under hypoxia.....	72
Figure 21: Schematic of VHL protein .....	73
Figure 22: Mdm2 inhibits VHL-p53 complex formation under hypoxia .....	74
Figure 23: Neddylation impacts p53-VHL complex formation.....	77
Figure 24: Mdm2 binds directly to the alpha domain of VHL and neddylates VHL at K159.....	78
Figure 25: Neddylation of VHL by Mdm2 reduces VHL-p53 complex formation.....	79
Figure 26: VHL colocalizes with p53 under hypoxia or with treatment of MLN4924 .....	82
Figure 27: K159E VHL colocalizes with p53 in normoxia and hypoxia, but also with treatment of MLN4924 .....	83
Figure 28: VHL colocalizes with p53 under hypoxia or with treatment of MLN4924 in Caki-1 cells .....	84
Figure 29: VHL increases the acetylation of p53 under hypoxia, leading to increased transcription of TSP-1.....	86
Figure 30: VHL increases the secretion of TSP-1 through p53 transactivation .....	87
Figure 31: p53 and TSP-1 inhibit Human Umbilical Vein Endothelial Cell network formation through VHL .....	89
Figure 32: p53 and TSP-1 inhibit Human Umbilical Vein Endothelial Cell network formation.....	90
Figure 33: Schematic of the p53-VHL pathway being inhibited by Mdm2 .....	91
Figure 34: Mdm2 promotes epithelial to mesenchymal transition .....	93

Figure 35: Phosphorylation of Mdm2 by Src increases binding to MdmX.....	100
Figure 36: MdmX increases the Mdm2-mediated neddylation of VHL.....	101
Figure 37: <i>MDM2</i> mRNA levels are affected by the mutation status of VHL .....	103
Figure 38: VHL inhibits the P2 promoter of <i>MDM2</i> in normoxia and hypoxia .....	104
Figure 39: VHL and hypoxia cause the expression of an alternatively spliced isoform of <i>MDM2</i> mRNA.....	106
Figure 40: VHL and hypoxia cause the expression of an alternatively spliced isoform of Mdm2 protein.....	108
Figure 41: Mdm2 ubiquitinates VHL .....	109
Figure 42: Schematic of the VHL-Mdm2 alternative feedback loop .....	112

## LIST OF ABBREVIATIONS

Abl	Abelson tyrosine-protein kinase
AD	Acidic Domain
Akt/PKB	Protein Kinase B
AP1	Transcription factor AP-1
APPBP1/UBA3	Amyloid Precursor Protein Binding Protein 1/Ubiquitin-like Protein-Activating Enzyme 3
ARF	ADP Ribosylation Factor
ARF-BP1	ARF-Binding Protein 1 \
ATCC	American Type Culture Collection
ATM	Serine-protein kinase ATM
ATR	Ataxia telangiectasia and Rad3-related protein
BAI-1	Brain-specific Angiogenesis Inhibitor 1
BAX	Bcl-2 Associated X protein
BBC3	Bcl-2 Binding Component 3
BLG	Beta-Lactoglobulin
c-Src	Cellular Src kinase
CA-Src	Constitutively Active Src kinase
ccRCC	Clear Cell Renal Cell Carcinoma
CD36	Cluster of differentiation 36
CDK	Cyclin Dependent Kinase
CDKN1A	Cyclin Dependent Kinase Inhibitor 1A
COL18A1	Collagen Type XVIII Alpha 1



Cop1	Constitutive photomorphogenesis protein 1
Cul2	Cullin 2
DAPI	4',6-diamidino-2-phenylindole
DBD	DNA Binding Domain
DDR	DNA Damage Response
DMEM	Dulbecco's Modified Eagle Media
DMSO	Dimethyl Sulfoxide
DNA	Deoxyribonucleic Acid
DP1	Protein product of Transcription Factor Dp-1 ( <i>TFDP1</i> )
dpc	Days Post Coitum
DSB	Double Strand Break
E2F1-4	E2F Transcription Factor 1-4
EBM-2	Endothelial Cell Growth Basal Medium-2
ECM	Extracellular Matrix
EGM-2	Endothelial Cell Growth Medium-2
ELISA	Enzyme-Linked Immunosorbent Assay
EMT	Epithelial to Mesenchymal Transition
ER	Estrogen Receptor
ETS2	Protein C-ets-2
FASTA	Fast-All
FN	Fibronectin
FOXO1	Forkhead Box Protein O1
FOXO3A	Forkhead Box Protein O3

G1	Gap 1 phase
GAPDH	Glyceraldehyde 3-Phosphate Dehydrogenase
GFP	Green Fluorescent Protein
GFR	Growth Factor Reduced
GST	Glutathione S-Transferase
HA	Hemagglutinin
HAT	Histone Acetyltransferase
HIF1 $\alpha$	Hypoxia Inducible Factor 1 $\alpha$
HIF1 $\beta$ /ARNT	Hypoxia Inducible Factor 1 $\beta$ /Aryl Hydrocarbon Receptor Nuclear Translocator
HIF2 $\alpha$	Hypoxia Inducible Factor 2 $\alpha$
HIPK2	Homeo-domain Interacting Protein Kinase 2
HME	Human Mammary Epithelial Cell
HUVEC	Human Umbilical Vein Endothelial Cell
IB	Immunoblot
IGF-1	Insulin-like Growth Factor 1
IgG	Immunoglobulin G
IP	Immunoprecipitation
I-TASSER	Iterative Threading ASSEmbly Refinement
JNK	c-Jun N-terminal Kinase
kDa	kilo Dalton
LFS	Li Fraumeni Syndrome
MAPK	Mitogen Activated Protein Kinase

Mdm2	Mouse Double Minute 2
MdmX (Mdm4)	Mouse Double Minute X (Mouse Double Minute 4)
MMP-9	Matrix Metalloproteinase 9
Mre11	Double-strand break repair protein MRE11
MRN	Protein complex consisting of Mre11, Rad50, and Nbs1
mRNA	Messenger Ribonucleic Acid
Mtp53	Mutant p53
Nedd8	Neural Precursor Cell Expressed, Developmentally Down-regulated 8
NEM	N-Ethylmaleimide
NES	Nuclear Export Signal
Ni-NTA	Nickel – Nitrilotriacetic Acid agarose
NLS	Nuclear Localization Signal
NoLS	Nucleolar targeting Sequence
ODD	Oxygen Dependent Degradation domain
p53	Protein product of <i>TP53</i>
p63	Protein product of <i>TP63</i>
p73	Protein product of <i>TP73</i>
p90Rsk	p90 Ribosomal S6 Kinase
PBS	Phospho Buffered Saline
PBST	Phospho Buffered Saline with Tween-20
PHD	Plant Homeodomain
PHD	Prolyl Hydroxylase

PI3K	Phosphoinositide 3-kinase
Pirh2	p53-induced RING-H2 protein
PRD	Proline Rich Domain
PTEN	Phosphatase and Tensin Homolog
PTM	Post Translational Modification
PUMA	p53 Upregulated Modulator of Apoptosis
PVDF	Polyvinylidene Difluoride
Rad50	DNA repair protein Rad50
Rb	Retinoblastoma protein
Rbx1	RING-box protein 1
REG	Regulator domain
RING	Really Interesting New Gene
SCF <sup>SKP2</sup>	Skp1, Cull1, F-box protein, S-phase kinase-associated protein 2
SDS-PAGE	Sodium Dodecyl Sulfate – Polyacrylamide Gel Electrophoresis
SERPINE1	Serpin Family E Member 1
SIAH1	E3 ubiquitin-protein ligase SIAH1
shRNA	Short Hairpin RNA
siRNA	Small Interfering RNA
SNP	Single Nucleotide Polymorphism
Sp1	Transcription factor Sp1
Src	Proto-oncogene tyrosine-protein kinase SRC
TAD1	Transactivation Domain 1
TAD2	Transactivation Domain 2

TET	Tetramerization Domain
THBS1	Thrombospondin-1 precursor
TNBC	Triple Negative Breast Cancer
Trim24	Transcription intermediary factor 1-alpha
TSP-1	Thrombospondin-1
Ub	Ubiquitin
UbcH12	Nedd8 Conjugating Enzyme Ubc12
UTR	Untranslated Region
VEC	VHL, Elongin B/C, Rbx1, and Cul2 E3 Ligase Complex
VEGF	Vascular Endothelial Growth Factor
VHL	Von Hippel-Lindau tumor suppressor
WCL	Whole cell lysate
WD40	40 amino acid motif terminating in a tryptophan-aspartic acid (W-D) dipeptide
WWE	Protein domain with conserved tryptophan and glutamate (W and E) residues

## **1. Background**

### ***1.1 The p53 tumor suppressor family***

The first evidence of an ancestor to the p53 family of proteins comes in sea anemones [2]. This ancestral gene more closely resembles p53 family members, p63 and p73, but its function was akin to the modern day p53 – to protect cells from DNA damage. It is likely that these organisms evolved to have this ancestral protein due to the high levels of UV they are exposed to near the surface of water. As evolution progressed, the appearance of the first gene that closely represents p53 came about in cartilaginous fish, when somatic stem cells were first used by organisms to regenerate adult tissues [2]. Later, with the dawn of bony fish, the p63/p73 like gene evolved to become two separate genes that share similarity with both p63 and p73. While all of these family members share similarities, they have distinct functions and protein domains as well. For instance, p63 has been linked to development of epithelial cells, p73 plays a role in the development of the immune and nervous systems, and p53 plays a major role in most cells in the DNA damage response [2]. p63 and p73 are both needed for a full apoptotic response to DNA damage. Indeed, p63 is present on promoters of p53 target genes in the absence of p53, but p53 is not present on a subset of these gene promoters in the absence of p63 and p73 [3]. This regulation suggests that p53 alone is not sufficient to promote tumor suppression.

*TP53* is the most mutated gene in all human cancers, and has been called the ‘Guardian of the Genome’ for its many functions in maintaining the integrity of DNA. Interestingly, p63 and p73 are very rarely mutated in cancer [4]. The p53 protein functions as a dimer of dimers, with tight regulation of its tetramerization domain [5]. As

a tetramer, p53 can bind to p53-responsive sequences in the promoter region of many genes involved in apoptosis, cell cycle arrest, metabolism, and angiogenesis [6]. p73 and p53 can both activate some, but not all, genes with the consensus p53-responsive sequence and they are both induced via DNA damage.

Some interesting insights into p53 have been gained through the analysis of various diseases and species. The Li Fraumeni Syndrome (LFS) is a familial disease associated with germline mutations in *TP53*. Studying families with LFS has given researchers information about the role of various *TP53* mutations in cancer [7, 8]. Patients with Down Syndrome have a reduced occurrence of all cancers. This is due, in part, to the trisomy of chromosome 21 that defines Down Syndrome. The extra copy of a specific gene on chromosome 21, *COL18A1*, has been associated with a 2-fold increase in serum levels of its protein product, endostatin [9]. *COL18A1* is a known target of p53 involved in the inhibition of angiogenesis. Interestingly, elephants and other trunk swinging mammals rarely get cancer. While the mechanisms governing this phenomenon are not entirely understood, it is due at least in part to the fact that the elephant genome encodes 20 copies of *TP53* [10]. The lack of cancer in elephants is part of what is known as ‘Peto’s Paradox’, which states that although larger animals should have an increased incidence in cancer due to the increased cell count, they do not. Instead, these animals have evolved to have a reduced number of oncogenes in their genomes and, like *TP53* in elephants, an increased number of tumor suppressors in their genomes.

### ***1.2 The p53-Mdm2 autoregulatory feedback loop***

Inactivation of p53 can happen in a variety of ways including mutation of the *TP53* gene and the binding of the p53 protein to viral or oncogenic proteins. Mutations of

*TP53* are extremely common in cancer, but there are many tumors that maintain wild type p53. In these tumors, p53 can be inhibited at the protein level by overexpressed cellular oncoproteins or by viral oncogenic proteins. In fact, p53 was originally discovered due to its binding to the SV40 large T antigen [11, 12]. The main cellular oncoprotein that inhibits p53 is the mouse double minute 2 (Mdm2) protein. The interaction of Mdm2 with p53 was initially discovered in rat fibroblasts as a 90 kDa protein complexed with p53 [13]. Importantly, this interaction was only seen when p53 was wild type, and wild type p53 also caused an increase in *MDM2* mRNA [14-16]. Further studies characterized Mdm2 as an inhibitor of p53 through direct transcription inhibition and by targeting p53 for degradation via the 26S proteasome. Mdm2 binds p53 in its transactivation domain and causes an  $\alpha$ -helical conformation change, which has been reported to inhibit the DNA binding activity of p53 [14, 17]. However, other groups have reported that an Mdm2-p53 complex can be found on the chromatin of p53 target genes, suggesting that the binding of Mdm2 to p53 does not completely block the DNA binding activity of p53 [18]. Additionally, Mdm2 is an E3 ubiquitin ligase for p53 and in this manner it signals for proteasomal mediated degradation of p53 [19-24]. While Mdm2 is the most studied E3 ubiquitin ligase for p53, there are over 20 other E3 ligases that regulate p53 in different contexts [25].

There are several reasons to explain the high number of E3 ligases for p53 including differential expression during embryonic development, evolutionary conservation, and differential binding in specific PTM contexts. Trim24 and Cop1 are both expressed in a tissue-specific context at 10.5 dpc, while ARF-BP1 is ubiquitously expressed at 14.5 dpc [25]. Interestingly, deletion of Trim24 in mice caused tumor



formation specific to the liver [26]. Additionally, deletion of the Trim24 ancestor in *Drosophila*, *bonus*, results in widespread cell death due to increased activity of D-p53, the *Drosophila* version of human p53 [27]. Perhaps the most likely reason for this redundancy in E3 ligases is to ensure that post-translationally modified p53 can still be regulated. p53 is highly modified by phosphorylation, acetylation, and methylation so in order to regulate the protein there needs to be a complex system in place to read these PTMs. Bromo structural domains are known to interact with acetylated lysines, and PHD domains with patterns of methylated lysines. Of note, Trim24 contains a PHD-Bromo domain, but its ability to recognize acetylated and/or methylated p53 has not been tested. There are specific phosphorylation sites of p53 that inhibit its binding to Mdm2, so to circumvent these processes there are other E3 ligases that can likely bind to p53 independently of PTMs. Cop1 has a WD40 domain, which facilitates protein-protein interactions that are not dependent on PTMs. Likewise, ARF-BP1 has a WWE domain which functions in a similar manner. Pirh2 is another E3 ligase of p53 that binds preferentially to tetramers of p53, which likely means that it functions in terminating the p53 response [28]. Both Pirh2 and Cop1 are also part of an autoregulatory feedback loop with p53, in a similar manner to Mdm2. Trim24, Cop1, ARF-BP1, and Pirh2 ubiquitination of p53 leads to K48-linked polyubiquitination and subsequent degradation [27, 29]. Mdm2 may have the most diverse regulation of p53, being able to mediate K48-linked polyubiquitination, K63-linked monoubiquitination, and neddylation. Just as the regulation of p53 by Mdm2 is a multifaceted process, the regulation of Mdm2 itself is complex.

In order to regulate p53, Mdm2 must first gain entry to the nucleus. The mechanisms governing the nuclear-cytoplasmic shuttling of Mdm2 are highly regulated and dependent on specific signaling conditions and timing. In response to MAPK activation by IGF-1, the PI3-kinase activates Akt/PKB, which in turn phosphorylates Mdm2 at S166 and S186 [30]. These serines are proximal to the nuclear localization sequence on Mdm2, and phosphorylation of these sites causes rapid translocation of Mdm2 to the nucleus and Mdm2-mediated inhibition of p53 [30]. Interestingly, IGF-1 stimulation of MAPK can also lead to the nuclear export of Mdm2. The downstream kinase of MAPK, p90Rsk, phosphorylates Mdm2 in response to IGF-1 and causes nuclear export of Mdm2 [31]. While the IGF-1/MAPK/PI3K/Akt pathway results in rapid translocation of Mdm2 to the nucleus in under five minutes, the IGF-1/MAPK/p90Rsk pathway acts more slowly and results in export of Mdm2 from the nucleus at around 30 minutes [30, 31]. ATR has also been shown to prevent p53 nuclear export by phosphorylating Mdm2 at S407 in response to DNA damage [32]. p19<sup>ARF</sup> is another protein that interacts with Mdm2 to block the Mdm2-mediated degradation of p53. The exact mechanism of p19<sup>ARF</sup> inhibition of Mdm2 is not known, but it is clear that p53 is stabilized by blocking the nuclear-cytoplasmic shuttling of Mdm2 [33, 34]. It seems that in this context, Mdm2 is stuck in the nucleus by being linked to the nucleolus by p19<sup>ARF</sup> [35]. Another mechanism of both p53 stabilization and Mdm2 degradation is governed by PTEN. Like *MDM2*, *PTEN* is a target of p53 but is induced in response to apoptosis where the *MDM2* gene is not induced. PTEN is capable of inhibiting the PI3K/Akt pathway, which leads to decreased nuclear Mdm2 and increased cytoplasmic Mdm2. When Mdm2 is restricted to the cytoplasm it is degraded and has a reduced half-life [36].

In this manner, PTEN causes an increase in p53 activity and p53 target genes resulting in a sensitization of cells to chemotherapy [36]. Mdm2 is also highly regulated at the promoter level, resulting in varied splice forms and transcript levels of *MDM2* in response to different signaling pathways.

There are two promoter regions in the *MDM2* gene. The P1 promoter is constantly activated, but the P2 promoter contains binding sites for p53. In response to DNA damage, p53 is stabilized and activated and it binds to the P2 promoter of *MDM2* to promote its transcription [15, 37]. While the P1 promoter is basally active, it has been shown that p53 only binds to the P2 promoter in response to stress [38]. Elevated Mdm2 protein then destabilizes p53 either by directly blocking its transcription or through ubiquitination and subsequent degradation. While p53 activation of the P2 promoter feeds into the autoregulatory feedback loop, there are other ways in which the P2 promoter can be activated. In response to TGF- $\beta$ 1 signaling, the Smad3/4 transcription factors bind to the P2 promoter of *MDM2* and activate its transcription [39]. In recent years, many other mechanisms of both activating and inhibiting *MDM2* transcription have been identified. In ER<sup>+</sup> breast cancer cells, ETS2 is able to bind to an AP1-ETS responsive element to activate transcription of *MDM2* [40]. *MDM2* can also be activated by Vitamin D, thyroid hormone receptor, and estrogen, while retinoic acid can inhibit *MDM2* transcription [41-45].

In addition to the ubiquitinating function of Mdm2 in response to genotoxic stress, it has recently been shown that Mdm2 is also able to function as an E3 nedd8 ligase, which was later shown to be in response to phosphorylation by the tyrosine kinase c-Src [46, 47]. Mdm2 can then neddylate p53, but rather than causing degradation as in

the case of ubiquitination, neddylation actually increases the stability of p53, but it is inactive [47]. A related protein to Mdm2, MdmX (also known as Mdm4), is important for Mdm2 mediated ubiquitination and neddylation as it forms a dimer with Mdm2 in order to effectively inhibit p53 [48]. Additionally, MdmX is able to bind directly to p53 to inhibit its tumor suppressive function independently of Mdm2 [49]. The fact that MdmX can inhibit p53 independent of Mdm2 highlights the fact that there are many other protein interactions in the p53-Mdm2 pathway that can either stabilize or destabilize p53. For instance, problems in the retinoblastoma signaling pathway during cell division can result in increased transcription of the *ARF* gene. The ARF protein is an inhibitor of Mdm2, which allows p53 protein levels to increase and causes cell cycle arrest or apoptosis to fix or discard damaged cells [50-52]. While p53 is the most studied target for Mdm2/MdmX mediated ubiquitination and neddylation, there are other targets of the E3 ligase as well, such as the promoter of cellular invasion Slug [53]. These target proteins have opened the door for p53-independent functions of Mdm2 to be explored.

### ***1.3 The p53-independent roles of Mdm2 in cancer***

#### ***1.3.1 Introduction***

Mouse double minute 2 (Mdm2) was first cloned in 1987 from a transformed 3T3 double minute mouse cell line [54]. There were three copies of the gene termed Mdm1, 2 and 3. The second copy was able to transform murine cells with Ha-Ras [54-56]. Furthermore, the human homologue of Mdm2, Hdm2, was able to transform human cells with Ha-RasV12 and the E1A viral oncogene [57]. The protein encoded by the *MDM2* gene is elevated in 40-80% of human tumors [39]. The most studied role of Mdm2 is its downregulation of the tumor suppressor p53. Mdm2 binds and mono-ubiquitinates p53 in

the nucleus in response to DNA damage, leading to the nuclear export and subsequent degradation of p53 [14, 17, 19-22, 37]. The primary reason that this role is considered to be the most prominent role of Mdm2 is due to the fact that knockout of p53 rescues an embryonic lethality of *mdm2*<sup>-/-</sup> mice [58, 59]. Embryonic lethality of *mdm2*<sup>-/-</sup> mice occurs at 6.5 days post coitum (dpc), as Mdm2 plays important roles in the development of many tissue types. At 10.5 dpc, Mdm2 is ubiquitously expressed, but by 12.5 dpc the expression is tissue specific. Interestingly, at 18.5 dpc Mdm2 is expressed in the retina, where tumors are commonly found with defects in the retinoblastoma protein that Mdm2 is able to regulate [60]. This study led many to believe that the regulation of p53 was the only important role of Mdm2, and much of the literature is focused on Mdm2 in the context of its regulation of p53. However, Mdm2 has been studied for its oncogenic effects in many different types of cancers, including those harboring mutations or deletions in p53. Jones et al. were the first to definitively show that Mdm2 had tumor-promoting effects independently of p53. Using a transgenic mouse model that globally expressed high amounts of *mdm2* mRNA they showed that increased expression of *mdm2* led to an increased incidence of tumor formation, regardless of p53 status [61]. Since this groundbreaking study, Mdm2 has been shown to be involved in a plethora of cellular processes that are independent of p53. Mdm2 can disrupt the normal cell cycle [62-69], slow down DNA repair processes [70, 71], increase invasiveness and migration of tumor cells [43, 72-76], and cause cellular transformation [43, 61, 77, 78] all in the absence of functional p53.

It is abundantly clear that Mdm2 can regulate p53. The emergence of so many functions of Mdm2 that occur in the absence of p53 raises the question of what the main

role of Mdm2 is in a tumor setting. It is possible that Mdm2 is able to affect the same proteins and pathways both dependent on and independent of p53, but that the laws of physics are followed and Mdm2 takes the path of least resistance. Alternatively, specific signaling pathways may dictate the activity of Mdm2 and its cellular substrates dependent on extracellular or intracellular cues. As described by Hanahan and Weinberg, there are ten hallmarks of cancer [79]. Currently, Mdm2 is integrated into five of these hallmarks independently of p53 (Figure 1).

### *1.3.2 Mdm2 in tumorigenesis*

After the discovery of the *TP53* gene it quickly became clear that its protein product, p53, was important in the regulation of the cell cycle and apoptosis (reviewed in [80]). After the identification of p53, there was an obvious desire to identify and characterize other proteins that interact with and regulate p53. Momand et al. found that a 90 kDa protein precipitated with p53 and that this 90 kDa protein was able to form a stable complex with p53 *in vivo*. Further characterization showed that the 90 kDa protein was the protein product of the *MDM2* gene [14]. In their analysis, the authors saw that not all p53 was bound by Mdm2 and so they wanted to determine if the same was true of Mdm2. Using a similar approach, they investigated the amount of free p53 and free Mdm2 in cells with well-known growth characteristics. In every cell line that they tested, there was a fraction of Mdm2 that was not in complex with p53 [81]. Notably, in 3T3DM cells, which were the most tumorigenic cells that they tested, over 98% of total Mdm2 was not bound to p53. In the same cells, there was no p53 found outside of complexes with Mdm2. While normal cell lines tested also had high levels of free Mdm2, this still raises the question of what the other 98% of Mdm2 protein is doing in tumor cells.

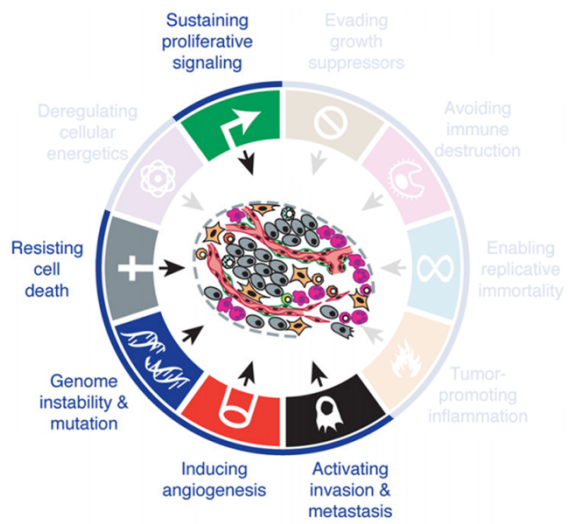


Figure 1. Mdm2 is involved in several hallmarks of cancer. Adapted from [79].

To address the possibility of Mdm2 playing a role in transformation, a mouse model was made where several copies of the entire *mdm2* gene under the control of its native promoter were integrated into the genome [61]. *mdm2* mRNA and protein expression were verified and the mice were monitored for tumor development. Mice overexpressing Mdm2 were susceptible to tumor formation, and the rate of tumor formation was dose dependent on copies of the *mdm2* pseudo-gene. Although the rate of tumor formation between *p53*<sup>-/-</sup> mice and *p53*<sup>-/-</sup>*mdm2*<sup>+/+</sup> mice were almost identical, the types of tumors that developed were very different. *p53*<sup>-/-</sup>*mdm2*<sup>+/+</sup> mice were much more likely to get sarcomas than *p53*<sup>-/-</sup> mice, suggesting that Mdm2 plays a role independent of p53 in the formation of tumors. In order to further investigate the role that Mdm2 plays in the development of tumors, Lundgren et al. developed a model in which *MDM2* expression was regulated by the BLG promoter, which was induced in mammary glands during gestation and lactation [78]. In this model, increased Mdm2 caused a defect in cytokinesis in both p53 positive and p53 null mice. While S phase progressed as usual in these mice, cytokinesis did not occur, leading to large multinucleated cells. Mice that harbored Mdm2 overexpression also developed mammary tumors at a much faster rate than control animals.

### *1.3.3 Mdm2 promotes an aggressive cell cycle*

Progression through the cell cycle is an intricate process with many checkpoints in place to ensure the successful and error free replication of cells. In cancer, the cell cycle becomes dysregulated through many different mechanisms. Neoplastic cells are able to rapidly proliferate by abrogating certain checks during a normal cell cycle. By removing these checks, cancer cells can both grow rapidly and have a higher propensity



for further mutations since there is not as much time for DNA repair processes to take place. Mdm2 is able to influence the cell cycle through a number of mechanisms, through both direct interactions with p53 and by some mechanisms that are completely independent of p53.

Perhaps the most significant way that Mdm2 can affect the cell cycle independently of p53 is through the Rb/E2F pathway. The tumor suppressor Rb binds many E2F transcription factors and inhibits their transcriptional activity, which is important for the cell cycle and apoptosis [82-84]. Mdm2 is able to overcome a blockage of the cell cycle by the tumor suppressor p107, an Rb family member [77]. p107 binds preferentially to E2F4 and causes cells to arrest in the G1 phase, inhibiting the growth of cells and allowing time for DNA repair proteins to function [85]. In the presence of Mdm2, and both with or without p53, the G1 arrest can be overcome in an Mdm2-dependent manner. During the normal progression of the cell cycle, Rb becomes hyperphosphorylated by cyclin-dependent kinases (CDKs) and releases E2Fs. Mdm2 can bind directly to Rb, and release E2F1 to induce downstream genes. Interestingly, Mdm2 binds preferentially to hypophosphorylated Rb, which would ordinarily inhibit E2F1 [68]. Also it has been reported that Mdm2 could bind to E2F1 directly and activate the transcriptional activity of E2F1 [69]. Additional literature suggests that p53 directly regulates the transcription factor E2F1, independent of both Mdm2 and Rb [86]. However, most data points to Mdm2 having a direct impact on the inhibition of E2F1. For instance, one study showed that Mdm2 was able to downregulate E2F1 through a cascade of events initiated by the inhibition of p53 [67]. This may be a key pathway for the inhibition of apoptosis mediated by E2F. Furthermore, the authors showed how

Mdm2 inhibition of p53 resulted in decreased levels of p21. Additionally, Mdm2 has been shown to increase the degradation of p21 independent of ubiquitination [87]. Since p21 inhibits the cyclins/CDKs responsible for hyperphosphorylation of Rb, lower levels of p21 result in more phosphorylation of Rb and a release of E2F. Interestingly, while these authors were investigating the role of Mdm2 on E2F1 signaling, they discovered that MdmX was also able to inhibit E2F1 independently of p53 [88]. This points to a prominent role of Mdm2 and MdmX in the Rb/E2F signaling pathway. Mdm2 has also been shown to bind to E2F1 and inhibit the SCF<sup>SKP2</sup> ligase from ubiquitinating E2F1 [69]. There are many ways in which Mdm2 alters the function of E2F1, but one intriguing mechanism is through DP1, which forms dimers with E2F1. E2F1 has transcriptional activity on its own, but its ability to bind DNA increases when it forms heterodimers with DP1. Separate labs have shown that Mdm2 interacts with DP1 [64, 65]. In their model system, Mdm2 caused a defect in apoptosis only in the presence of DP1, suggesting that DP1 is the regulatory subunit for Mdm2 [64]. When Mdm2 was bound to DP1 there was a change in function of the E2F1/DP1 heterodimers from pro-apoptotic to pro-growth. While one group was able to see an interaction with Mdm2 and E2F1 *in vitro* using recombinant proteins, they were not able to see the same interaction in cells [65]. Though they suggested that the lack of a detectable interaction may be due to low levels of E2F1 in their cells, it is possible that Mdm2 only interacts with DP1 or alterations in the post-translational modifications to either protein is necessary for the E2F interaction. One of the very early papers on E2F1/DP1 heterodimers showed that the adenovirus E4 protein was able to bind to DP1, but not E2F1, and increase the DNA binding capacity of the heterodimer [89]. An overview of the impact of Mdm2 on this

signaling pathway is shown in Figure 3. Mdm2 is also able to overcome a proliferative checkpoint after being induced by estrogen in Estrogen Receptor alpha (ER<sup>+</sup>) positive breast cancer cells [43]. The induction of Mdm2 by estrogen is independent of p53 and results in a more aggressive phenotype in response to estrogen.

Forkhead box proteins O3A and O1 (FOXO3A and FOXO1) are able to inhibit the cell cycle through varying mechanisms. Fu et al. were investigating possible crosstalk between the p53 pathway and the FOXO pathway when they noticed an inverse correlation in the protein levels of Mdm2 and both FOXO3A and FOXO1. They determined through several biochemical assays that Mdm2 bound to and mediated ubiquitination to the FOXO proteins [62]. While the authors suggest that ubiquitination of FOXO proteins by Mdm2 is dependent on p53, the reason was that p53 has the ability to transcribe Mdm2. Since it has been shown that Mdm2 protein levels can still be high in the absence of p53 and that Mdm2 can be transcriptionally activated in the absence of p53 [75, 90, 91], it is highly possible that the regulation of these FOXOs by Mdm2 is also a p53 independent event.

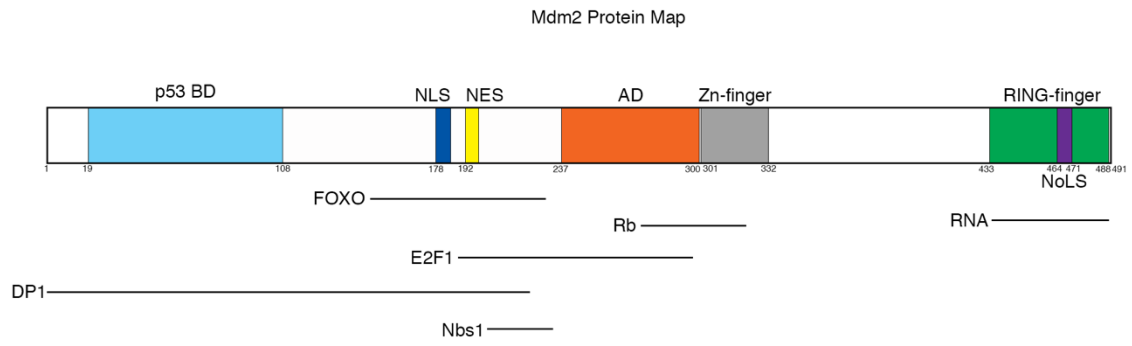


Figure 2. A map of the domains and interactions of the Mdm2 protein. Regions where Foxo, E2F1, DP1, NBS1, Rb and RNA are designated in the specific domains.

#### *1.3.4 Mdm2 inhibits the DNA damage response*

One of the major reasons for checkpoints in the cell cycle is to allow for DNA damage to be repaired before cell division continues. This is one of the main defense mechanisms that cells have against cancer causing mutations. p53 is responsible for a large portion of the DNA damage response (DDR) by causing growth arrest, apoptosis, and DNA repair. Tumor suppression by p53 is accomplished through p53 functioning as a transcription factor for a wide variety of genes, and as mentioned above, is blocked by Mdm2 complexing with p53. In addition to the regulation of p53, Mdm2 has been found to have other effects on the DDR which are independent of p53. Namely, Mdm2 is associated with the Mre11/Rad50/Nbs1 (MRN) complex [70, 71].

The MRN complex is important for repairing double strand DNA breaks (DSBs). Mre11 recognizes sites of DSBs and binds directly to the free ends of DNA. Rad50 is an ATPase and provides the energy for the complex, while Mre11 provides nuclease function. Nbs1 is localized to DSBs through binding to Mre11. Alt et al. demonstrated that Mdm2 is able to bind to Nbs1 at sites of DNA damage, but not to Mre11 or Rad50 [70]. The authors showed that Mdm2 expression resulted in a delay in DNA repair that was independent of both p53 and ARF, but dependent on Nbs1. Another group published a similar study in which they showed that Mdm2 overexpression led to an increase in chromosome and chromatid breaks in addition to a delay in DNA repair dependent on Nbs1 [71]. This group mapped the Mdm2 binding domain for Nbs1 as amino acids 198-228 of Mdm2, in between the nuclear export sequence (NES) and the acidic domain (AD). The binding region of Nbs1, as well as other binding regions of interest in this section, are seen in Figure 2.

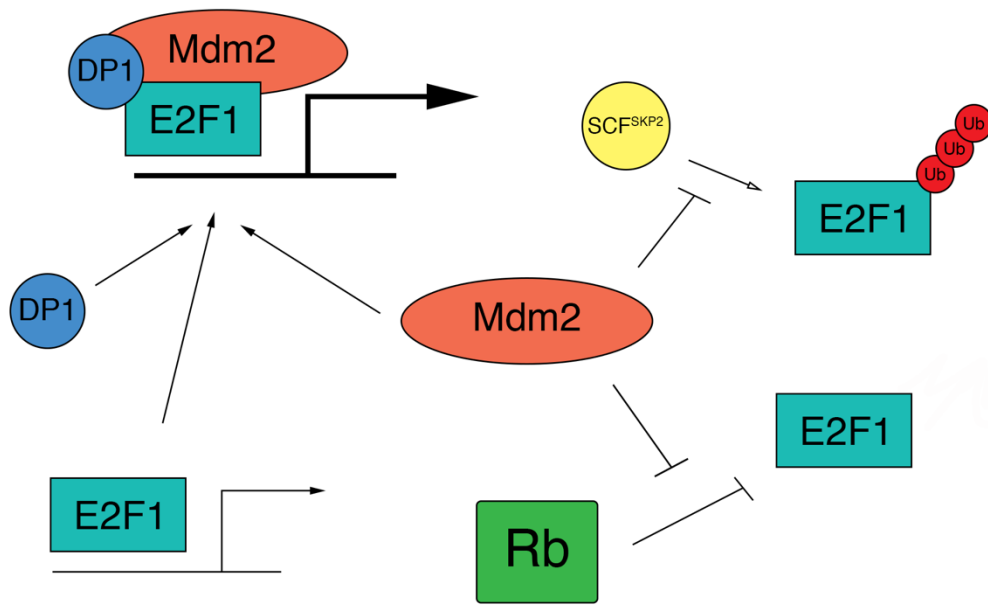


Figure 3. Mdm2 impacts the Rb signaling pathway. The pathway shows how Mdm2 affects transcription of E2F1 target genes and how Mdm2 blocks Rb and SCF.

### *1.3.5 Mdm2 promotes metastasis*

Mdm2 plays an important role in the conditioning of the tumor microenvironment. In order for a tumor to become metastatic, it must circumvent the cellular junctions to migrate away from the primary tumor and intravasate into the blood stream to travel through the circulatory or lymphatic system to reach a distant site. The first step in this process is traveling through the tissue immediately surrounding the tumor. There are many obstacles standing in the way of tumor cell invasion. Mdm2 is able to promote metastasis through many different mechanisms involving the secretion of matrix metalloproteinases [72, 92-94], degradation of cell-cell adhesion proteins [74], and stabilization of proteins involved in angiogenesis [76, 95-97].

Matrix metalloproteinase-9 (MMP-9) is an important regulator of the extracellular matrix (ECM). When activated, MMP-9 functions to digest type IV and V collagen in the ECM, making it easier for cells to travel through this dense space [94]. Multiple groups have shown that Mdm2 was correlated with the expression of MMP-9 in breast [72], pancreatic [93], and lung [92] cancers. Mdm2 expression was correlated with an increase in both mRNA and protein levels of MMP-9 [72]. In an animal model of lung cancer, the correlation between MMP-9 and Mdm2 was the highest in late stage tumors [92]. In addition to the degradation of the ECM, Mdm2 has profound effects on vascularization in tumors in response to hypoxia. It is clear that Mdm2 and hypoxia-inducible factor 1 alpha (HIF1 $\alpha$ ) bind directly to each other in response to hypoxia [95-100]. HIF1 $\alpha$  is stabilized under hypoxic conditions and translocated to the nucleus, where it is free to bind to its partner protein HIF1 $\beta$ . This heterodimeric protein complex is important for activating the transcription of several target genes important for cell survival and the

hypoxic response. Interestingly, there is also a slight increase in Mdm2 protein in response to hypoxia that is independent of p53 [97]. There is some controversy in these studies regarding what the role of Mdm2 is under hypoxia, possibly stemming from the different conditions these groups consider hypoxia. However, the majority of the available data points to Mdm2 stabilizing HIF1 $\alpha$  in response to hypoxia, which in turn causes an increase in the transcription of vascular endothelial growth factor (VEGF) [97]. *VEGF* is one of the major target genes for HIF1 $\alpha$ , and it is a crucial regulator of angiogenesis. In addition to activating the transcription of *VEGF* through the stabilization of HIF1 $\alpha$ , Mdm2 is also able to bind directly to the 3' UTR of *VEGF* mRNA and increase its stability and protein levels [76].

There have been many mechanistic studies showing that Mdm2 increases the metastatic potential of cancers, but the most convincing data comes from studies of human tissue samples. High levels of Mdm2 correlate with metastasis and late-stage tumors in both breast cancer and melanoma [39, 73]. Recent work from our own lab has shown that Mdm2, and not gain of function mutant p53, is required for the early stages of metastasis [101]. This research has been verified by another group, who recently showed that both Mdm2 and MdmX can promote metastasis in TNBC [102]. The intricate roles that Mdm2 plays in metastasis are not fully understood, but these studies provide a clear rationale for the continuation of studies that investigate Mdm2 in metastasis.

### *1.3.6 Conclusion*

Ever since the initial cloning and identification of Mdm2, the focus of subsequent studies has been shackled by its interaction with p53. The overwhelming majority of research surrounding Mdm2 is still centered around its regulation of p53. While the



interaction with p53 is undoubtedly a role for Mdm2, it is clearly not its only function. In addition to p53, there are many other transcription factors that are able to activate transcription of the *MDM2* gene [75, 90, 91]. Since tumor cells have evolved mechanisms to turn on Mdm2 in the absence of p53, there must be an advantage for tumor cells to have high levels of Mdm2. The last decade has seen an increase in the interest of p53-independent effects of Mdm2. This is highly relevant given the immense interest in targeting the Mdm2/p53 interaction to treat cancers. Until the p53-independent effects are better understood these treatments will likely continue to be compromised. Only through the complete study of Mdm2's interacting proteins and the ways in which the *MDM2* gene can be activated will we be able to effectively target this pathway as a cancer treatment.

#### ***1.4 The canonical VHL-HIF pathway***

The hypoxia inducible factors (HIFs) are dimeric protein complexes responsible for the cellular response to low oxygen. They function as transcription factors to turn on genes with hypoxia responsive elements (HREs) that impact a variety of cellular functions including angiogenesis, metabolism, growth, and migration [103]. There are three hypoxia inducible factor  $\alpha$  subunits – HIF1 $\alpha$ , HIF2 $\alpha$ , and HIF3 $\alpha$ . HIF1 $\alpha$  is highly conserved across species and is thought to be the major driver of the hypoxia response. HIF2 $\alpha$  has some overlapping functions with HIF1 $\alpha$ , but differs in that it regulates erythropoietin production in adults [103]. HIF3 $\alpha$  has complementary and inhibitory functions to HIF1 $\alpha$  and HIF2 $\alpha$ , but is less well understood. Recent studies suggest that HIF3 $\alpha$  may actually inhibit HIF1 $\alpha$  and HIF2 $\alpha$  in the inflammatory and hypoxic responses [104-106].

Under normal oxygen, HIF1 $\alpha$  and HIF2 $\alpha$  subunits are hydroxylated by various prolyl hydroxylases (PHDs) at Pro402/564 and Pro405/531, respectively [107-109]. This prolyl hydroxylation allows the von Hippel-Lindau (VHL) protein to recognize these HIF $\alpha$  subunits and target them for degradation via the 26S proteasome [108-111]. VHL serves as the substrate recognition protein in a ubiquitin E3 ligase complex along with elongin B, elongin C, Cul2, and Rbx1 [110, 112]. In low oxygen conditions the PHDs are inactive due to lack of oxygen, which stabilizes HIF $\alpha$  subunits. HIF1 $\alpha$  is most active in acute (less than 24 hours) or severe (less than 0.1% O<sub>2</sub>) hypoxia while HIF2 $\alpha$  is more active under chronic (48-72 hours) or mild (less than 5% O<sub>2</sub>) hypoxia [113, 114]. Stabilized HIF $\alpha$  subunits move into the nucleus to bind with their ubiquitously expressed HIF $\beta$ /ARNT subunits to activate transcription [115, 116].

Pathogenic disruption of VHL/HIF $\alpha$  regulation can be hereditary or spontaneous. In VHL Disease, patients inherit a mutated form of *VHL* that causes a variety of clinical presentations depending on the specific mutation [117-120]. Many, but not all of these mutations have a defect in HIF $\alpha$  binding, which directly relates to the severity of the clinical presentation (Table 1) [121]. Approximately 1 in every 35,000 live births is diagnosed with VHL Disease, and there are over 150 identified germline mutations [120, 122]. These mutations are categorized based on their clinical presentation into Type 1, Type 2A, Type 2B, or Type 2C. Examples of Type 1 VHL Disease include a complete deletion of the *VHL* gene or a C162F point mutation. The C162F mutation results in a mutant VHL that has reduced binding to both HIF1 $\alpha$  and elongin C and loses its ability to regulate HIF $\alpha$  [111]. Type 2A mutants, such as Y98N and Y112H, have also lost their ability to regulate HIF $\alpha$ , but they present with a low risk for renal cell cancer [123]. Type

2B mutants, such as R167Q, are able to regulate HIFs, but still present with a high risk for renal cell cancer [124]. The R167Q mutant has a reduced ability to bind to elongin C, but maintains binding to elongin B, Cul2, and Rbx1. While controversial, it appears that VHL R167Q has a reduced half-life as compared to WT VHL and its ability to regulate HIF2 $\alpha$  is slightly impaired [125]. VHL mutations that result in Type 2C VHL Disease, such as L188V and K159E, maintain their ability to fully regulate HIF1 $\alpha$  and present only with pheochromocytoma [111, 126]. Additionally, *VHL* is commonly mutated in spontaneous renal cell carcinoma [117, 127, 128]. These tumors are highly vascularized and have high expression of HIF protein and gene expression of HIF targets.

<b>VHL Disease Type</b>	<b>Clinical Presentation</b>	<b>Mutations</b>	<b>HIF status</b>
<b>Type 1</b>	RCC, retinal angioma, CNS hemangioblastoma, pancreatic cysts, neuroendocrine tumors, low risk for pheochromocytoma	Truncating or missense	↑↑↑
<b>Type 2A</b>	Pheochromocytoma, retinal angioma, CNS hemangioblastoma, low risk for RCC	Missense	↑
<b>Type 2B</b>	Pheochromocytoma, retinal angioma, CNS hemangioblastoma, pancreatic cysts, neuroendocrine tumors, high risk for RCC	Missense	↑↑
<b>Type 2C</b>	Pheochromocytoma only	Missense	Normal

Table 1. VHL Disease types. Information obtained from [121].

## **2. Materials and Methods**

### ***2.1 Cell culture***

All cell lines were cultured in Dulbecco's modified Eagle medium with 8-10% fetal bovine serum and supplemented with penicillin and streptomycin in a 37° C humidified incubator in 5% CO<sub>2</sub>. Anisomycin, SP600125, and camptothecin were purchased and suspended as described by the manufacturer (Sigma-Aldrich). Anisomycin was used at 30 μM, camptothecin was used at 30 μM, and SP600125 was used at 25 μM unless otherwise noted. For hypoxia experiments, cells were cultured in DMEM/F12 1:1 and placed at 37° C in a humidified incubator with 1% O<sub>2</sub> in a BioSpherix SubChamber System with a ProOx oxygen controller.

### ***2.2 Transient transfection***

Transient transfections were performed using polyethylenimine at 1:1 with DNA. Annexin V and Dead Cell Assay kit from Millipore was used to stain cells that were analyzed on a Muse cytometer.

### ***2.3 Plasmid generation***

We generated the mutant p53 plasmids using the p53-SN<sub>3</sub> plasmid with a site directed mutagenesis kit (Life technologies). The oligonucleotides for these mutations are shown in Table 2. Following mutagenesis in p53-SN<sub>3</sub>, the p53 gene was subcloned into either pRSET A or pNIT (LNITX) using BamH1.

T81E forward	5'-CCAGCAGCTCCTGAACCGGCGGCC-3'
T81E reverse	5'-GGCCGCCGGTTCAGGAGCTGCTGG-3'
T81A forward	5'-CCAGCAGCTCCTGCACCGGCGGCC-3'
T81A reverse	5'-GGCCGCCGGTGCAGGAGCTGCTGG-3'
S46D forward	5'-GATTTGATGCTGGACCCGGACGATATTG-3'
S46D reverse	5'-CAATATCGTCCTGGGCCAGCATCAAATC-3'

Table 2. Oligonucleotides used for the site directed mutagenesis of p53.

#### ***2.4 Protein purification***

Recombinant proteins (p73, p53, GST, GST-alpha VHL, GST-beta VHL, GST-VHL, His-Mdm2, and GST-p300 HAT domain) were produced in BL21DE3 cells and purified as previously described [129, 130]. His-Src was purchased from Millipore and the neddylation reaction components were purchased from Boston Biochem.

#### ***2.5 Far Western and Western blotting***

Far Western was completed by 96 well dot blot system and recombinant proteins were placed in wells and fixed to nitrocellulose by drying. Blot was blocked with 5% nonfat dry milk and incubated with recombinant p73. p73 was then detected by p73 antibody followed by secondary and an enhanced chemiluminescence (ECL) reagent. Western blot analysis used whole cell lysates lysed with Urea Lysis Buffer or immunoprecipitated proteins extracted with IP Lysis Buffer (Table 5). Whole cell lysates, immunoprecipitated proteins, pulldown assays, and in vitro reactions were all subjected to SDS-PAGE and transferred to PVDF membrane. Western blots for all antibodies were performed according to the manufacturers' protocols (Table 3).

#### ***2.6 I-TASSER protein structure prediction***

Amino acid sequences for wild-type p53, R248W p53, T81E p53, S46D, and R248W/T81E p53 were input to the I-TASSER web server as FASTA sequences. Predicted protein structures were generated using a previously described method [131-133] and analyzed using the CCP4 Molecular Graphics Program (CCP4MG) v. 2.10.6 [134]. Structures were superposed using a built in function within the software.

<b>Cell Line</b>	<b>p53 status</b>	<b>VHL status</b>	<b>Notes</b>
H1299	<i>Null</i>	<i>Wild type</i>	<i>Used for transfections</i>
TMD231	<i>R280K</i>	<i>Wild type</i>	<i>Derivative of MDA-MB-231</i>
U87	<i>Wild type</i>	<i>Wild type</i>	
HME1	<i>Wild type</i>	<i>Wild type</i>	
SF767	<i>Wild type</i>	<i>Wild type</i>	
3T3	<i>Wild type</i>	<i>Wild type</i>	<i>Mouse cell line</i>
hTERT BJ	<i>Wild type</i>	<i>Wild type</i>	
MDA-MB-468	<i>R273H</i>	<i>Wild type</i>	
MDA-MB-157	<i>A88fs*52</i>	<i>Wild type</i>	
786-O	<i>P278A/WT</i>	<i>G104fs</i>	<i>p53 status is contested - data suggests it could be wild type.</i>
RCC4	<i>Wild type</i>	<i>Null</i>	
Caki-1	<i>Wild type</i>	<i>Wild type</i>	
MCF7	<i>Wild type</i>	<i>Wild type</i>	
GFP HUVEC	<i>Wild type</i>	<i>Wild type</i>	

Table 3. Description of cell lines used. Data obtained from the Cancer Cell Line Encyclopedia.



Target	Clone	Company	Concentration	Data Type
Actin	C4	SCBT	1:5,000	WB
BAX	2D2	SCBT	1:1,000	WB
GST		SCBT	1:5,000	WB
HA	12CA5	Roche	1:1,000 2 µg/sample	WB IP
HIF1α	H1α67	SCBT	1:1,000	WB
His	HIS.H8	Thermo	1 µg/sample	Pulldown
JNK	D-2	SCBT	1:1,000	WB
pJNK	9251	CST	1:1,000	WB
Mdm2	IF2	Millipore	1:500 2 µg/sample	WB IP
Mdm2	2A10		1:2,000	WB
Mdm2	2A9		1:2,000	WB
Mdm2	4B2		1:2,000	WB
Nedd8	A-812	R&D	1:1,000 2 µg/sample	WB IP
Ac-p53 K373/382	06-758	Millipore	1:1,000	WB
p53	DO-1	SCBT	1:4,000 2 µg/sample 1:100 1:10,000	WB IP IF Far Western
p53	FL-393	SCBT	1:1,000 2 µg/sample	WB IP
p-p53 T81	2676	CST	1:1,000	WB
p73	D3G10	CST	1:1,000 1:100	WB IF
p73	Ab-1	Millipore	1:500 2 µg/sample 1:5,000	WB IP Far Western
p73	Ab-2	Millipore	1:500 2 µg/sample 1:5,000	WB IP Far Western
PUMA		CST	1:500	WB
TSP-1	A6.1	SCBT	1:500 100 ng/sample	Dot Blot Tube forming
VHL	VHL40	SCBT	1:1,000 2 µg/sample 1:100	WB IP IF
VHL	FL-181	SCBT	1:1,000	WB
VHL	IgG 32	BD	2 µg/sample	IP
VHL	S2-647	BD	1:2,000	WB
VHL	NBP2-30070	Novus	1:2,000	WB

Table 4. List of primary antibodies

## ***2.7 Immunofluorescence microscopy***

MDA157, HME, or TMD231 cells were grown on glass coverslips. 786-O, RCC4, or Caki-1 cells were grown on glass coverslips and transfected with WT or K159E VHL. Following transfection for 24 hours, cells were treated with MLN4924 or a control for an additional 16 hours. Cells were fixed in 4% paraformaldehyde in phosphate buffered saline (PBS) for 15 minutes, washed with PBS, and permeabilized in 1% Triton X-100 in PBS for 15 minutes. Coverslips were blocked in 5% bovine serum albumin for 1 hour in PBS/Tween before being stained with the indicated antibodies. Coverslips were then incubated with anti-rabbit AlexaFluor 647 and anti-mouse AlexaFluor 488 secondary antibodies before being fixed to slides with ProLong Diamond Antifade Mountant with DAPI (Life Technologies). Slides were visualized on a Leica SP8 MP microscope. Colocalization analysis was done using Imaris v9.0.2 and colocalized images were created using the “RG2B\_Colocalization” plugin for ImageJ. Scale bar, 25  $\mu\text{m}$  (MDA157, TMD231) or 50  $\mu\text{m}$  (HME).

## ***2.8 Colony forming assay***

Empty Vector and shp53 hTERT BJ cells were plated in triplicate and treated with Anisomycin for 9 hours. Dimethyl sulfoxide (DMSO) was used as a vehicle control. Cells were stained with equal parts methanol and methylene blue for 15 minutes. The plate was then washed 3 times with deionized water to remove any excess stain and left to dry at room temperature.

## ***2.9 GFP fluorescence assay***

Green fluorescent protein (GFP) shp53 and LVTHM Empty Vector control BJ cells were plated in quadruplet and treated with DMSO or 10  $\mu\text{M}$  of Anisomycin for 48

hours. Fluorescence emitted by GFP in each well was measured at 509 nm using a SpectraMax M5 spectrophotometer (Molecular Devices).

### ***2.10 Thrombospondin-1 reporter assay***

H1299, 786-O, RCC4, or Caki-1 cells were transfected with a reporter construct for thrombospondin-1 as previously described [47]. Luciferase activity was measured following transfection for 40 hours, with 16 hours of MLN4924 when noted in the figures (Table 4).

### ***2.11 Secreted thrombospondin-1 assay***

786-O or RCC4 cells were cultured in DMEM for 48 hours. Media was harvested and passed through a nitrocellulose membrane using a Bio-Dot microfiltration apparatus (BioRad). The membrane was then incubated with an antibody for TSP-1 (A6.1, Santa Cruz) and analyzed by Western blot. Resulting images were quantified using the Dot Blot Analyzer plugin for ImageJ.

<b>Reagent</b>	<b>Catalog Number</b>	<b>Company</b>
Angiogenesis Array	ARY007	R&D Systems
Anisomycin	A9789	Sigma-Aldrich
Camptothecin	C9911	Sigma-Aldrich
GFR Matrigel	354230	Corning
Luciferase Assay Substrate	E1501	Promega
Luciferase Control	T1056	Invitrogen
MLN4924	SI9830	Life Sensors
Mouse 2° Antibody AlexaFluor 488	A28175	Invitrogen
Mouse 2° Antibody HRP	1706516	BioRad
Ni-NTA Agarose	30210	Qiagen
Nedd8	UL-812	Boston Biochem
Nedd8 E1	E-312	Boston Biochem
Nedd8 E2	E2-656	Boston Biochem
p53 shRNA	Sc-29435	Santa Cruz
PP1	956025-83-5	Calbiochem
ProLong Diamond Antifade Mountant with DAPI	P36962	Thermo Fisher
Protein G Agarose	20398	Pierce
Rabbit 2° Antibody AlexaFluor 647	A27040	Invitrogen
Rabbit 2° Antibody HRP	1706515	BioRad
SP600125	S5567	Sigma-Aldrich
Src Kinase	14-326	Millipore
TSP-1 ELISA Kit	ELH-TSP1-1	Ray Biotech

Table 5. List of miscellaneous reagents

### ***2.12 Generation of shp53 786-O and RCC4 cell lines***

Lentiviruses encoding shRNA to p53 or a control were transfected in 293 phoenix cells. Supernatant media containing virus was collected at 48 hours, supplemented with 10 µg/mL polybrene, and syringe filtered through a 0.45 µm filter. Media containing virus was added to cells for 48 hours. Transduced cells were selected for by the addition of 2 µg/mL puromycin for one week.

### ***2.13 Enzyme-linked immunosorbent assay***

H1299 cells were transfected according to figure labels using polyethylenimine for 24 hours, followed by 21% or 1% O<sub>2</sub> culturing for 24 hours. 786-O and RCC4 cells were cultured in 21% or 1% O<sub>2</sub> for 24 hours. All media was harvested and analyzed using an ELISA kit for TSP-1 (Ray Biotech) with a 10% dilution of conditioned media.

### ***2.14 Immunoprecipitation***

Following transfection and/or treatment as described, cells were lysed in IP Lysis Buffer with protease inhibitor and 20 mM N-ethylmaleimide and incubated for 2 hours at 4° C with Protein-G agarose beads which had been pre-incubated with antibody. Following incubation, beads were washed 3x with IP Wash Buffer for 10 minutes at 4° C (Table 5). After the final wash, 6X Lamelli dye was added to the beads and samples were boiled for 10 minutes at 100° C and separated with SDS-PAGE.

### ***2.15 GFP HUVEC tube formation assay***

H1299 cells were transfected according to the figure panels for 48 hours followed by harvest. 786-O and RCC4 cells were cultured in 21% or 1% O<sub>2</sub> for 48 hours followed by harvest. Growth factor reduced matrigel (Corning) was plated in a 96-well plate and allowed to set according to the manufacturer's guidelines. GFP<sup>+</sup> Human Umbilical Vein

Endothelial Cells were plated on top of the matrigel in 10% EBM-2/EGM-2 (Lonza) and 90% conditioned media. Images were taken and analyzed using an Incucyte by Essen BioScience.

### ***2.16 Bioinformatics analysis of clinical data***

Data was analyzed from KIRC\_TCGA\_PUB downloaded from cbiportal.org. Only samples with wild-type p53 were included. 62 samples with alpha domain mutations in VHL were included and 72 samples with wild type VHL were included.

### ***2.17 His-nedd8 pulldown***

H1299 cells were transfected with His-nedd8 and other plasmids as shown in the figure panels. 24 hours after transfection, cells were treated with MLN4924 or a control for an additional 16 hours. Cells were lysed in denaturing conditions with Nickel Pulldown Lysis Buffer (Table 5) and sonicated. Lysates were incubated with 30  $\mu$ L Ni<sup>2+</sup>-NTA beads (Qiagen) for 2 hours at 4° C with rotation. The beads were washed and eluted with Nickel Pulldown Wash 1-4 and eluted with Nickel Pulldown Elution (Table 5) and subjected to SDS-PAGE.

### ***2.18 In vitro neddylation assay***

500 ng of GST-VHL was incubated with 1  $\mu$ g of His-Mdm2, 30  $\mu$ M nedd8 (Boston Biochem), 200 nM E1 (APPBP1/UBA3, Boston Biochem), 0.5  $\mu$ M E2 (UbcH12, Boston Biochem), and 1.25 mM ATP in Neddylation Reaction Buffer (Table 5) at 37° C for one hour followed by SDS-PAGE.

<b>Buffer</b>	<b>Components</b>	<b>pH</b>
Urea Lysis Buffer	6 M urea 20 mM Tris-HCl 100 mM Na <sub>2</sub> HPO <sub>4</sub> /NaH <sub>2</sub> PO <sub>4</sub>	6.8
IP Lysis Buffer	25 mM Tris-HCl 150 mM NaCl 1% IGEPAL 1% protease inhibitor cocktail 1 mM Na <sub>3</sub> VO <sub>4</sub> 10 mM NaF 1 μM Sodium Pyrophosphate 20 mM N-ethylmaleimide	8.0
IP Wash Buffer	25 mM Tris-HCl 150 mM NaCl 1% IGEPAL	8.0
Nickel Pulldown Lysis Buffer	6 M guanidinium-HCl 100 mM Na <sub>2</sub> HPO <sub>4</sub> /NaH <sub>2</sub> PO <sub>4</sub> 10 mM Tris-HCl 5 mM Imidazole 10 mM β-mercaptoethanol	8.0
Nickel Pulldown Wash 1	6 M guanidinium-HCl 100 mM Na <sub>2</sub> HPO <sub>4</sub> /NaH <sub>2</sub> PO <sub>4</sub> 10 mM Tris-HCl 10 mM β-mercaptoethanol	8.0
Nickel Pulldown Wash 2	8 M urea 100 mM Na <sub>2</sub> HPO <sub>4</sub> /NaH <sub>2</sub> PO <sub>4</sub> 10 mM Tris-HCl 10 mM β-mercaptoethanol	8.0
Nickel Pulldown Wash 3	8 M urea 100 mM Na <sub>2</sub> HPO <sub>4</sub> /NaH <sub>2</sub> PO <sub>4</sub> 10 mM Tris-HCl 10 mM β-mercaptoethanol 0.2% Triton X-100	6.3
Nickel Pulldown Wash 4	8 M urea 100 mM Na <sub>2</sub> HPO <sub>4</sub> /NaH <sub>2</sub> PO <sub>4</sub> 10 mM Tris-HCl 10 mM β-mercaptoethanol 0.1% Triton X-100	6.3
Nickel Pulldown Elution	200 mM Imidazole 5% SDS 150 mM Tris-HCl 30% Glycerol 720 mM β-mercaptoethanol	6.7

Table 6. Description of buffers used

<b>Buffer</b>	<b>Components</b>		<b>pH</b>
Neddylation Reaction Buffer	50 mM	Tris-HCl	7.6
	150 mM	NaCl	
	2.5 mM	MgCl <sub>2</sub>	
5X Acetylation Reaction Buffer	250 mM	Tris-HCl	8.0
	50%	Glycerol	
	0.5 mM	EDTA	
	5 mM	DTT	

Table 6. Description of buffers used, continued



### **3. Mutant and wild-type p53 form complexes with p73 upon phosphorylation by the kinase JNK**

#### ***3.1 Introduction***

The transcription factor family comprising p53, p63, and p73 control the induction of apoptosis in response to cellular stress and developmental cues. The three proteins have distinct as well as overlapping and interdependent functions. Mutations in p53 are common in human tumors; gain-of-function p53 mutants have a dominant-negative effect on wild-type p73 by binding it and inhibiting its ability to bind DNA and thereby preventing its transcriptional induction of apoptotic genes [135, 136]. In mice, knockout of one or both alleles of the individual genes encoding p53, p63, or p73 resulted in reduced cell death in response to DNA-damaging stimuli [137], indicating that all three proteins are necessary to invoke a robust apoptotic response. However, whereas wild-type p63 and p73 form heterodimeric (or higher order) complexes, wild-type p53 reportedly does not [5, 138].

Wild-type p53 has two transactivation domains: TAD1 (amino acids 1-40) and TAD2 (amino acids 43-54). TAD2 is located proximal to the proline-rich domain (PRD; amino acids 63-97) [139, 140], and both TAD2 and the PRD are critical for p53's induction of apoptotic genes [141, 142], whereas TAD1 is reportedly dispensable for this function [143]. Key phosphorylation sites responsible for the induction of apoptotic genes are contained within the PRD (Threonine 81) and TAD2 (Serine 46) [144-148]. Several kinases, such as HIPK2 and p38, reportedly phosphorylate Ser46 [144, 149, 150], and c-Jun N-terminal kinase (JNK) phosphorylates Thr81 [151], yet precisely how

modification of Thr81 regulates p53 activity in the context of apoptosis induction is limited.

The PRD is an important structural domain; prolyl isomerization in this domain regulates the structure of other domains of p53 [152]. Additionally, the PRD is necessary for growth suppression and apoptosis [153, 154]. From the literature, we rationalized that phosphorylation within the PRD may also be sufficient to alter the structure of other domains in p53 and thereby regulate its functional interactions. Our findings support previously published work on genetic knockout mice, the PRD, and mutant p53/p73 complex formation [135, 136], but refine our current understanding of the interaction between wild-type p53 and p73.

### ***3.2 The phosphorylation of p53 by JNK results in the induction of the apoptotic protein PUMA***

Because JNK is a key inducer of p53-mediated apoptosis, and JNK phosphorylates p53 at Thr81, we were first curious whether Thr81 was phosphorylated in mutant p53 in cells. In MDA-MB-468 cells, which have a missense mutation in p53 (R273H), TMD231 cells, which have a missense mutation in p53 (R280K), and MDA-MB-157 cells, which have a truncation mutation in p53 (A88fs\*52), JNK was activated, as determined by immunoblotting with antibodies against phospho-Tyr183/Tyr185 JNK (Figure 4). In addition, mutant p53 was phosphorylated at Thr81 in cells cultured in growth-supporting conditions. Treatment with the DNA topoisomerase inhibitor camptothecin or the protein synthesis inhibitor anisomycin increased phosphorylation of JNK and phos-Thr81. In various cells that have wild-type p53, namely untransformed cell lines NIH3T3 (mouse fibroblast) and HME1 (human mammary epithelial), as well as

human foreskin fibroblast BJ cells and glioblastoma cell lines U87 and SF767, exhibited limited activation of JNK and phosphorylation of p53-Thr81 under growth conditions, but robust induction of both upon camptothecin or anisomycin exposure (Figure 5A). Thus in “normal” cells and tumor cells, JNK is activated and p53 (wild-type or mutant) is phosphorylated at Thr81 in response to cell stress.

We then examined the dependence of JNK activation on the induction of PUMA, the apoptotic downstream target of p53. PUMA abundance was increased by anisomycin treatment in cells that had wild-type p53 (Figure 5B). However, the induction of PUMA was blocked by pretreatment with the small molecule JNK inhibitor SP600125, thereby confirming that activation of JNK was important for induction of the p53 target PUMA. Alongside this increase in PUMA abundance was a significant increase in cell death by ~11-fold, thereby confirming the functional outcome of the pathway (Figure 6).

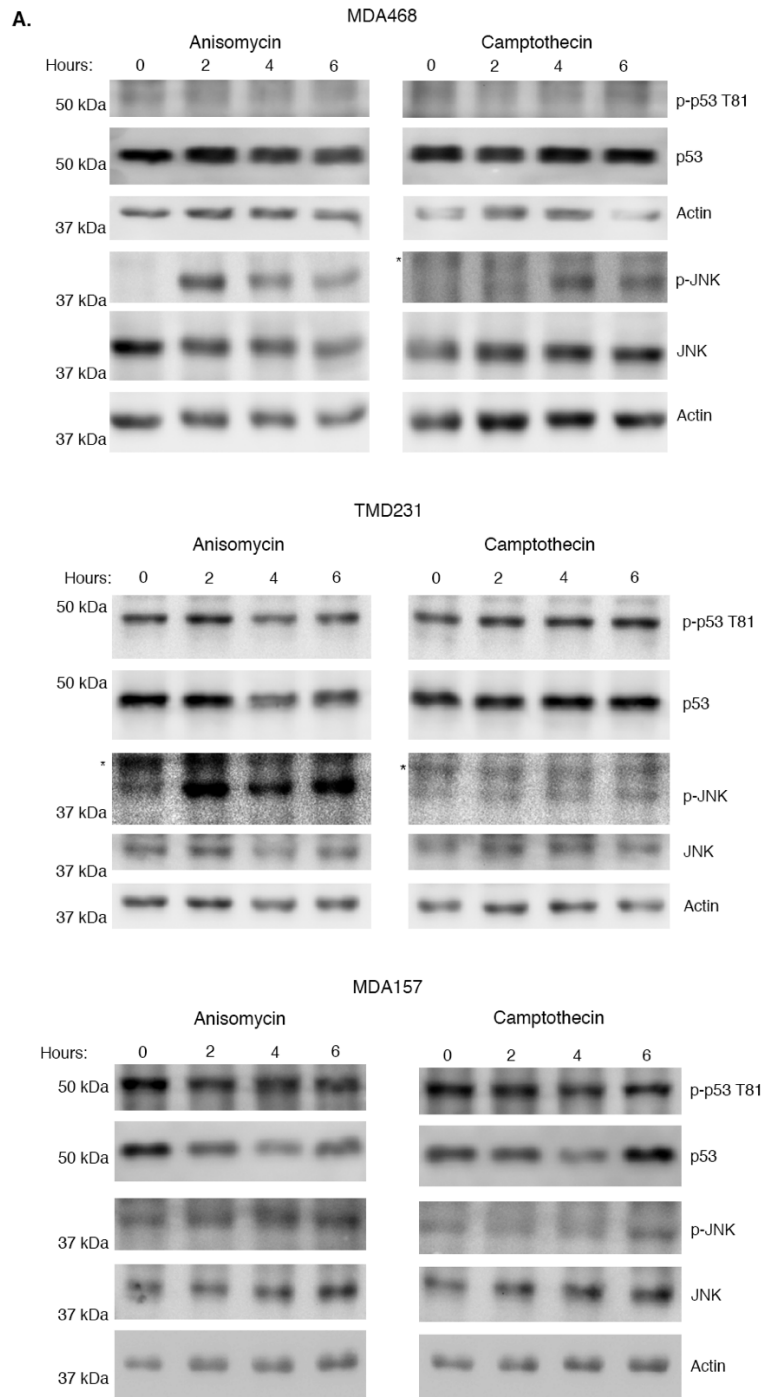


Figure 4. Phosphorylation of Thr81 of mutant p53 in response to JNK activation. (A) Western blot of phosphorylated JNK, phosphorylated Thr81 of p53, and actin in cellular extracts from TMD231, MDA-MB-468 and MDA-MB-157 cells treated with either camptothecin or anisomycin for the indicated times. Blots are representative of three independent experiments. From [1]. Reprinted with permission from AAAS.

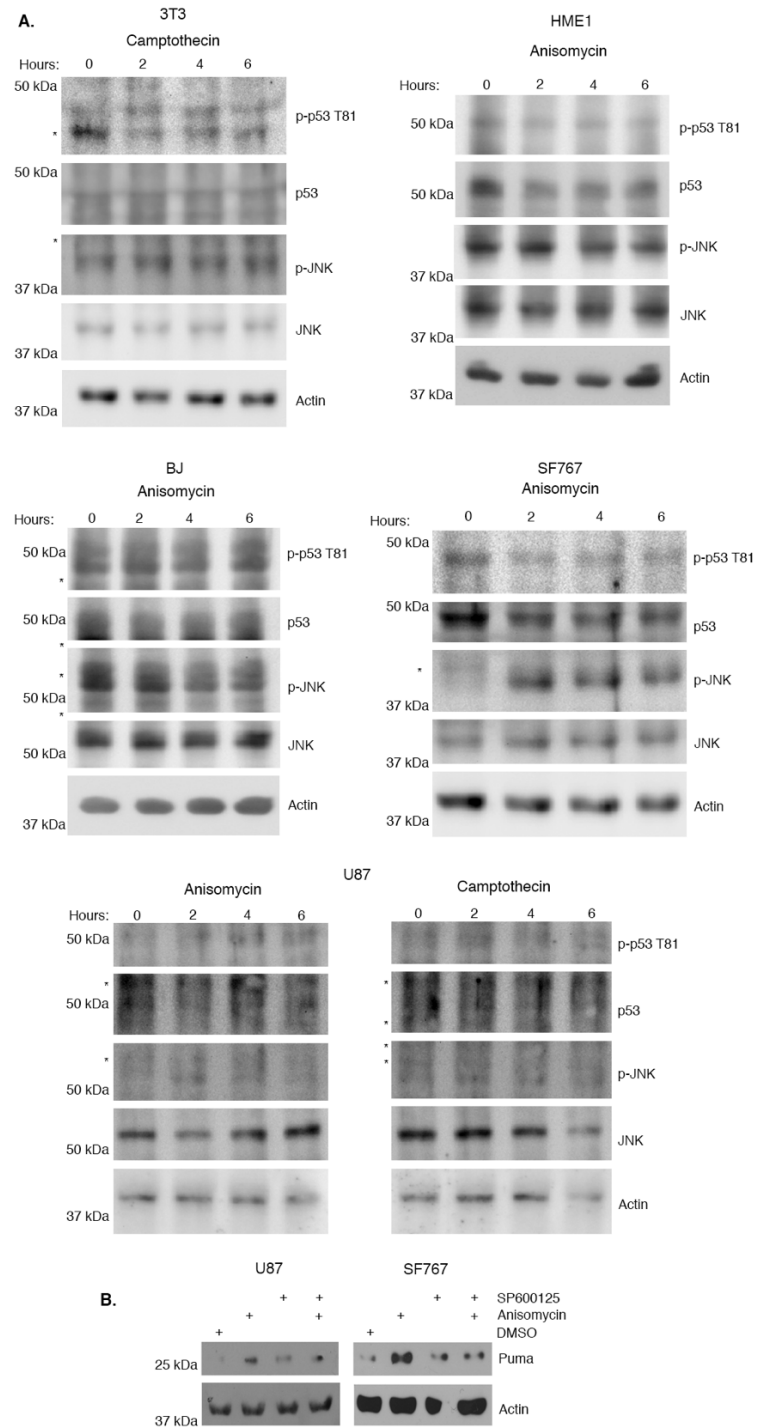


Figure 5. Phosphorylation of Thr81 of wild type p53 in response to JNK activation. (A) Western Blot of phosphorylated JNK or Thr81 of p53 and actin from cellular extract of 3T3, SF767, HME-1, BJ and U87 treated with anisomycin or camptothecin for the indicated times. Blots are representative of three independent experiments. (B) Experiments performed by Kristen Bredhold and Amber Kline. U87 or SF767 cellular extracts from DMSO, SP600125, anisomycin or pretreatment with SP600125 then anisomycin, and western blotted for PUMA and actin. Blots are representative of two independent experiments. From [1]. Reprinted with permission from AAAS.

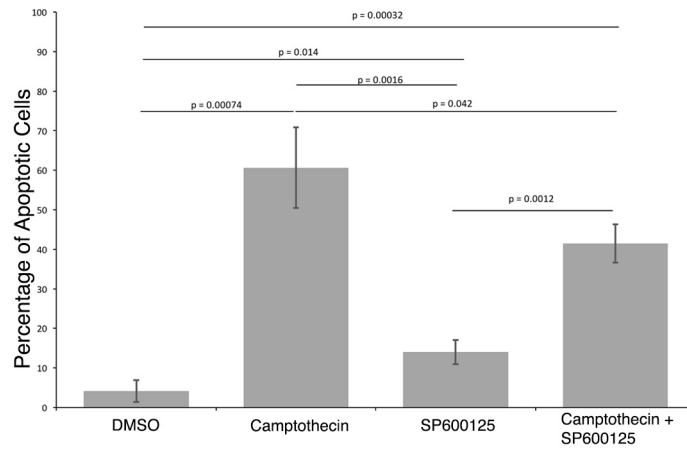


Figure 6. U87 cell death. Experiment performed by Kristen Bredhold. U87 cells were treated with 30  $\mu$ M camptothecin for 6 hours or pretreated with 25  $\mu$ M SP600125 for one hour and then treated with 30  $\mu$ M camptothecin for 6 hours. Cell death was determined by flow cytometry using Annexin V. Error bars represent standard deviation from the mean; P values determined by a two-tailed unpaired t-test. From [1]. Reprinted with permission from AAAS.

### ***3.3 The predicted structure of a Thr81 phosphomimic shows a potential mode of binding to p73***

To gain insight into the structural implications of phosphorylation at Thr81 of p53, we took advantage of a protein structure prediction algorithm, I-TASSER (Iterative Threading ASSEmbly Refinement) [131-133]. Using I-TASSER, we generated predicted protein structure models for wild-type p53, R248W mutant p53 (a common DNA binding domain mutant), and a Thr81 phosphomimic p53 (T81E) (Figure 7). Analysis of wild-type and mutant p53 showed distinct structural differences in the amino and carboxy termini. The Thr81 phosphomimic mutation (T81E) substantially changed the structure of the tetramerization/regulatory (TET/REG) domain compared to that of the unphosphorylated wild-type p53. The TET/REG domain of the T81E model more closely resembled the R248W mutant p53 model than the wild-type p53 model. The R248W mutation of p53 is one of the mutants that binds to p73 [135]. It is probable that it is this structural change in the TET/REG domain that enables p53 to interact with p73, which explains the original finding that wild-type p53 was unable to bind to p73. The results of our structural analysis implies that phosphorylation at Thr81 of p53 is permissive of binding to p73. We also produced in silico structural models of the S46D phosphomimic p53 and a R248W/T81E mutant p53 phosphomimic (Figure 7) to examine if there were any structural changes in these constructs. The TAD2 of the S46D phosphomimic was structurally similar to the T81E phosphomimic but distinct from either of the R248W mutant p53 models. Given that phosphorylation at Ser46 of p53 is needed for a robust apoptotic response, and phosphorylation at Thr81 of p53 causes a structural change similar to that of phosphorylation at Ser46, these data suggest that TAD2 and PRD are

integrated into important structural changes that are associated with induction of apoptotic genes. Compared to mutant p53 alone (R248W), the Thr81 phosphomimic of R248W mutant p53 (R248W/T81E) causes an additional structural change in almost every single functional domain. This suggests that the use of a JNK inhibitor may reduce the binding of mutant p53 to p73 without completely ablating the interaction.



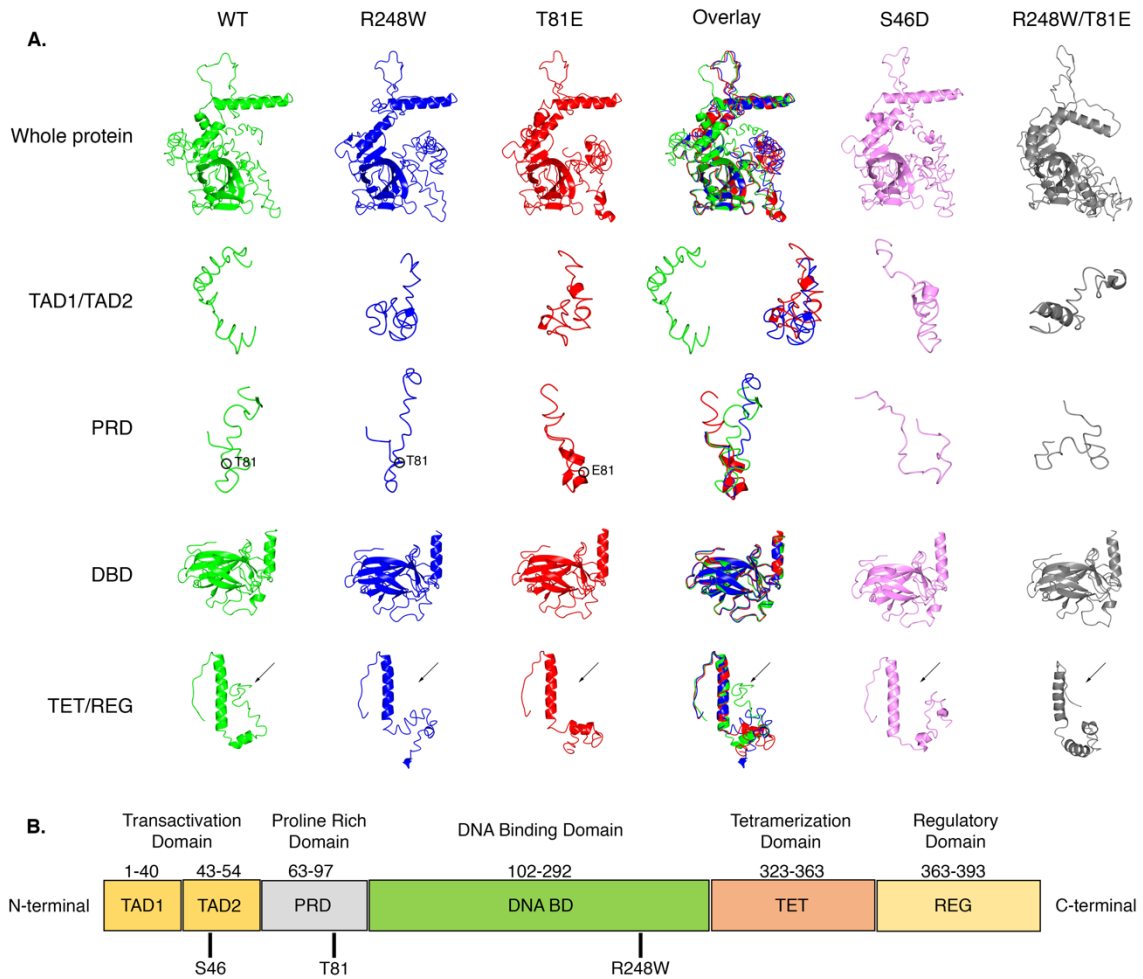


Figure 7. Predicted structure for a Thr81 phosphomimic reveals a possible mode of binding to p73. Structures (A) and amino acid coverage (B) of domains in wild-type and mutant p53. Whole protein represents amino acids 1-393 of p53. Transactivation domains 1 and 2 (TAD1/TAD2) represent amino acids 1-40 and 43-54. The proline rich domain (PRD) represents amino acids 63-97. The tetramerization and regulatory domains (TET/REG) represent amino acids 323-393. T81, Thr81; E, glutamic acid in T81E phosphomimic mutant domain. Arrows represent the region of a conformational change permissive of binding. From [1]. Reprinted with permission from AAAS.

### ***3.4 Phosphorylation of Thr81 of p53 promotes a p53-p73 complex***

Our structural data (Figure 7) combined with previous reports that mutant p53 binds wild-type p73 and the observation of high basal activated JNK and Thr81 phosphorylation of mutant p53 (Figure 4) led us to examine whether blocking JNK with the selective broad-spectrum, small-molecule inhibitor SP600125 could alter the mutant p53-p73 interaction endogenously. Mutant p53 was immunoprecipitated from lysates from TMD231 cells treated with DMSO or SP600125 and blotted for coincident pulldown of p73. We found that p73 co-purified with mutant p53 and that binding decreased by 40% when JNK activity was blocked with SP600125 (Figure 8A). This data suggests that JNK has only a modest effect on the interaction between mutant p53 and p73, which was predicted in the structural data (Figure 7). We next tested whether wild-type p53 and p73 were affected by phosphorylation of p53 by JNK. We transiently transfected H1299 cells with wild-type p53 and HA-tagged p73, then treated the transfected cells with DMSO or anisomycin. Immunoprecipitation of wild-type p53 from cellular extracts shows that p73 co-purified only when JNK was activated with anisomycin (Figure 8B). To provide evidence that phosphorylation of Thr81 was necessary for wild-type p53 to co-purify with p73, we transiently transfected H1299 cells with wild-type p53 or the T81E phosphomimic. Immunoprecipitation of exogenous p53 revealed that T81E, but not wild-type p53, co-purified with endogenous p73 (Figure 9A). Likewise, immunoprecipitation of endogenous p73 from extracts from U87 cells treated with DMSO, anisomycin, SP600125, or pretreated with SP600125 before anisomycin showed that endogenous wild-type p53 co-purified with p73 only when Thr81 was phosphorylated (Figure 8C). These data substantially suggest that Thr81 phosphorylation

in p53 is critical for the formation of a wild-type p53-p73 complex. To definitively show that phosphorylation was crucial for the interaction, we used various p53 phosphomimics (T81E, S46D, T81E-S46D) and p73 produced in bacteria and performed Far-Western analysis to examine the requirement of Thr81 phosphorylation. We fixed recombinant wild-type p53, the phosphomimics, and two positive controls (MDM2 and MDMX) to nitrocellulose, then incubated the membrane with purified p73 and blotted for p73. In support of our cellular data presented above, the in vitro approach confirmed that p73 bound only to T81E and not wild-type p53 or S46D p53 (Figure 9B). We also probed for p53 in a separate lane to show the relative amounts of p53 loaded per well (Figure 9B). Through overexpression, endogenous and recombinant approaches, we conclude that p73 only binds to wild-type p53 that is phosphorylated at Thr81.

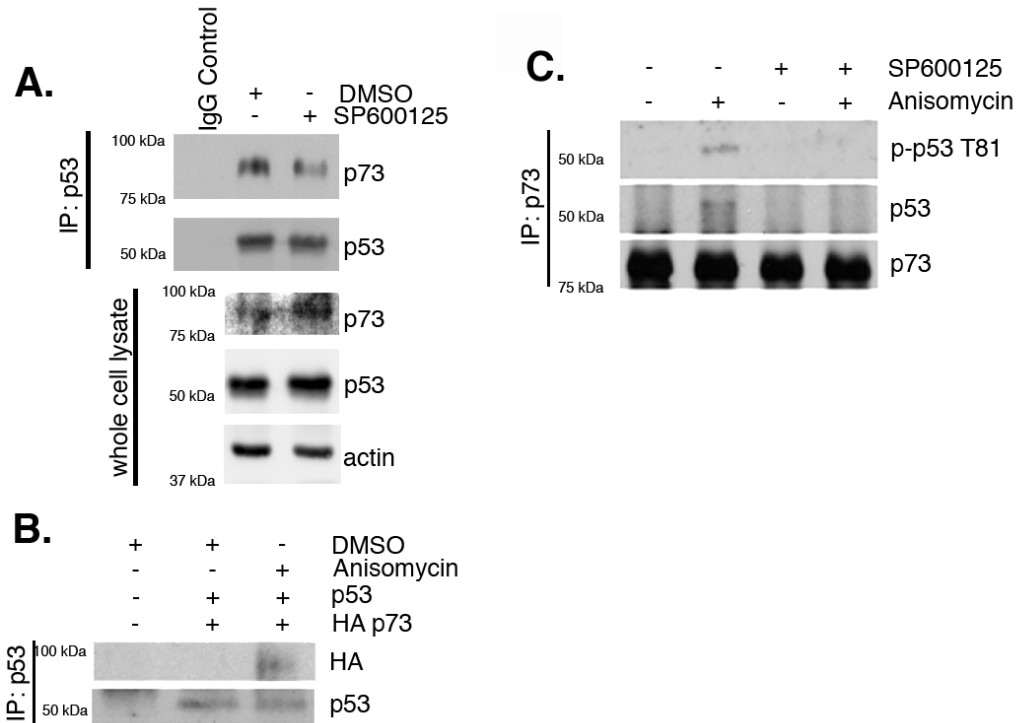


Figure 8. p53-p73 complex formation and activity. (A) Immunoprecipitation of p53 or control IgG from TMD231 cells treated with DMSO or SP600125 and western blotted for p73 and p53. Blots are representative of four independent experiments. (B) Data from Lindsey Mayo. Transient transfection of H1299 cells with p53, HA-p73 and treated with either DMSO or Anisomycin. Western blot of p53 and HA from p53 immunoprecipitated from cellular extracts. Blots are representative of two independent experiments. (C) Data from Lindsey Mayo. Immunoprecipitation of endogenous p73 from U87 cells treated with SP600125, anisomycin or both and western blot of phospho-Thr81, p53, and p73. Blots are representative of two independent experiments. From [1]. Reprinted with permission from AAAS.

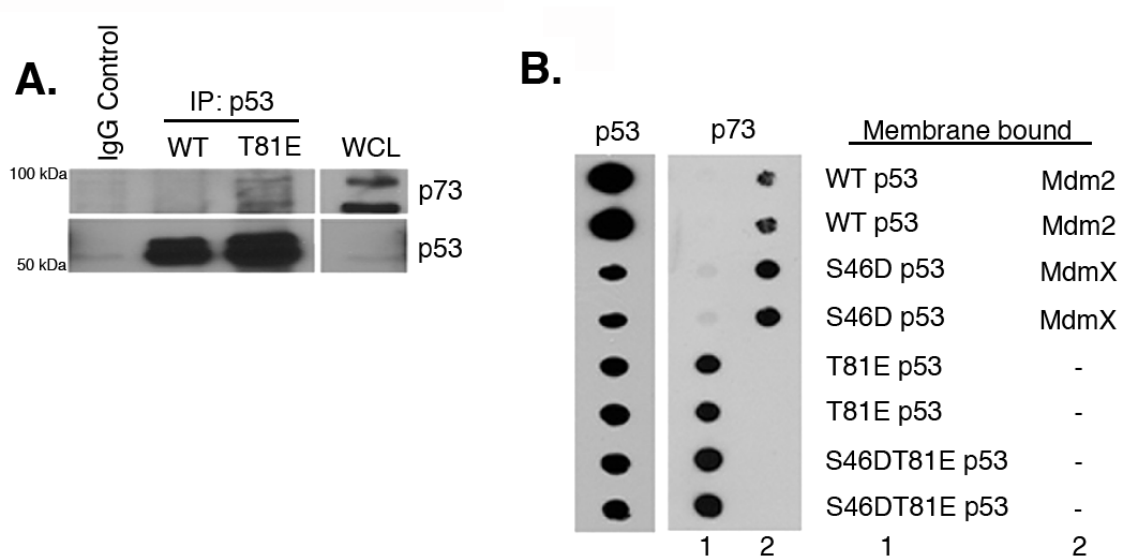


Figure 9. The effect of T81E on p53-p73 complex formation. (A) Data from Lindsey Mayo. Immunoprecipitation of p53 or control IgG and western blot of p53 and p73 from H1299 cells transfected with wild type p53 or T81Ep53. WCL is whole cell lysate from H1299 cells. Blots are representative of two independent experiments. (B) Data from Kristen Bredhold and Amber Kline. Far-Western analysis of p73 binding to p53. Lane 1 corresponds to p53 and the phosphomimics of p53, and lane 2 is Mdm2 and MdmX. Blotting for p73 is detects binding to p53 and Mdm2 and MdmX (right panel). The relative amount of p53 on the membrane is the left panel. Blots are representative of two independent experiments. From [1]. Reprinted with permission from AAAS.

To gain insight into where p53 and p73 interact, confocal immunofluorescence microscopy analysis was performed on MDA157, HME, or TMD231 cells grown on coverslips and treated with anisomycin, SP600125, or DMSO. Anisomycin treatment caused a significant increase of 38% in colocalization between p53 and p73 in the nucleus of p53–wild-type HME cells but not p53-mutant MDA157 cells (Figures 10 and 11, Table 6). Blocking JNK activity with SP600125 in TMD231 cells, which have mutant p53 and high basal activation of JNK, caused a significant decrease in the colocalization of mutant p53 and p73 in the nucleus (Figure 12 and Table 6), which is in accordance with the decrease in binding of mutant p53 and p73 (Figure 8A). To ensure that anisomycin was indeed activating JNK and increasing phosphorylation at Thr81, and that SP600125 was inhibiting JNK and decreasing phosphorylation at Thr81 of p53, the same cells were treated as described in the confocal experiments and lysates were Western blotted for active JNK and phosphorylated Thr81 p53 (Figure 13).

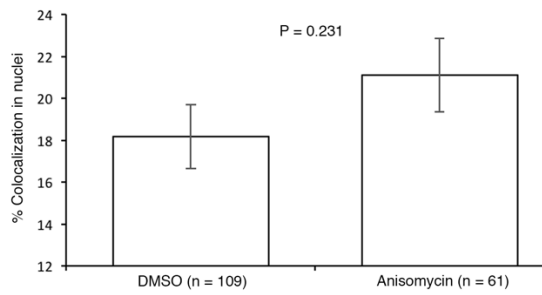
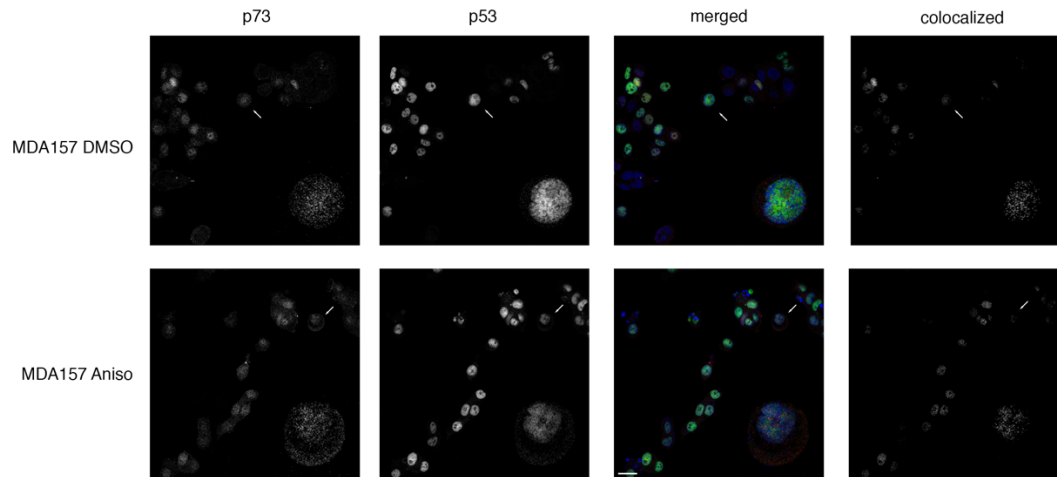


Figure 10. p53 activation and colocalization with p73 in MDA-MB-157 cells. Immunofluorescence of p53-p73 colocalization in MDA157 cells treated with anisomycin or DMSO. Error bars represent standard error of the mean. Significance was determined using a two-tailed unpaired t test. Data is representative of three independent experiments. From [1]. Reprinted with permission from AAAS.

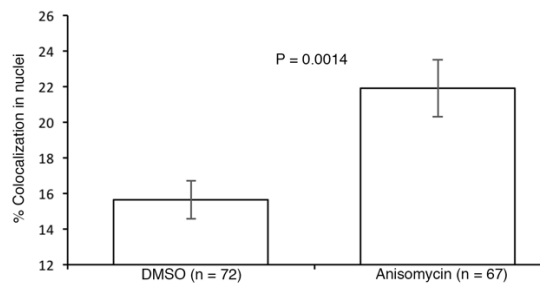
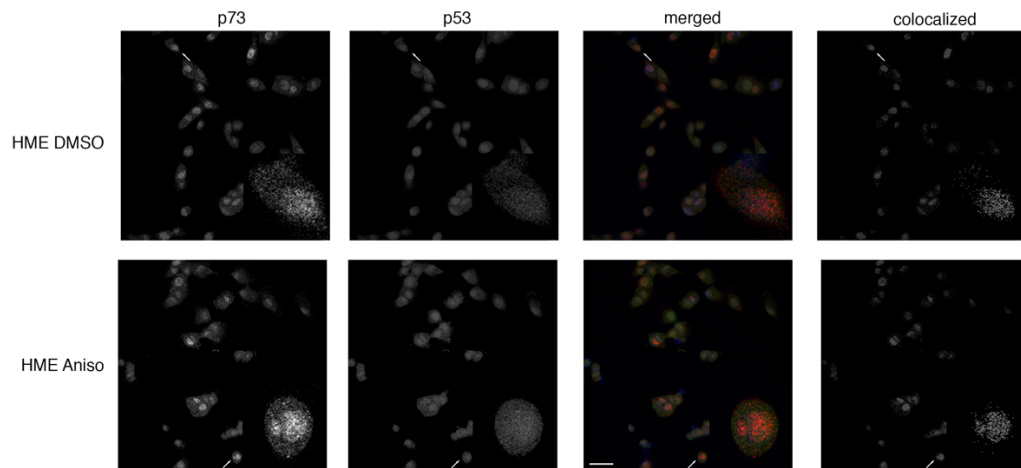


Figure 11. p53 activation and colocalization with p73 in HME1 cells. Immunofluorescence of p53-p73 colocalization in HME cells treated with anisomycin or DMSO. Error bars represent standard error of the mean. Significance was determined using a two-tailed unpaired t test. Data is representative of three independent experiments. From [1]. Reprinted with permission from AAAS.



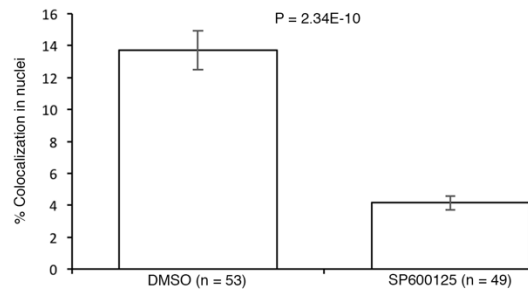
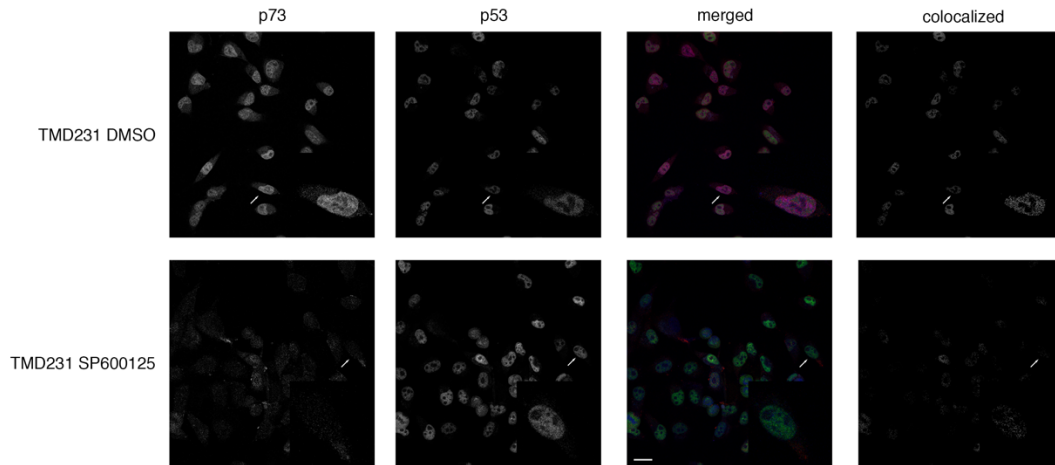


Figure 12. p53 activation and colocalization with p73 in TMD231 cells. Immunofluorescence of p53-p73 colocalization in TMD231 cells treated with SP600125 or DMSO. Error bars represent standard error of the mean. Significance was determined using a two-tailed unpaired t test. Data is representative of three independent experiments. From [1]. Reprinted with permission from AAAS.

	<b>A = p73, B = p53</b>	<b>Manders' A</b>	<b>Standard Error</b>	<b>Manders' B</b>	<b>Standard Error</b>
<b>MDA157</b>	DMSO (n = 109)	0.468	0.021	0.389	0.021
	Anisomycin (n = 61)	0.458	0.023	0.448	0.018
	Significance (p value)	0.763		0.060	
<b>TMD231</b>	DMSO (n = 53)	0.353	0.020	0.404	0.018
	SP600125 (n= 49)	0.114	0.012	0.398	0.009
	Significance (p value)	7.84E-17		0.765	
<b>HME</b>	DMSO (n = 72)	0.519	0.006	0.281	0.017
	Anisomycin (n = 67)	0.560	0.011	0.371	0.024
	Significance (p value)	0.001		0.002	

Table 7. Manders' Coefficients for microscopy colocalization analysis. Mander's A and B coefficients were generated using p73 as channel A and p53 as channel B within the Imaris software. Significance was determined using a two-tailed unpaired t test. From [1]. Reprinted with permission from AAAS.

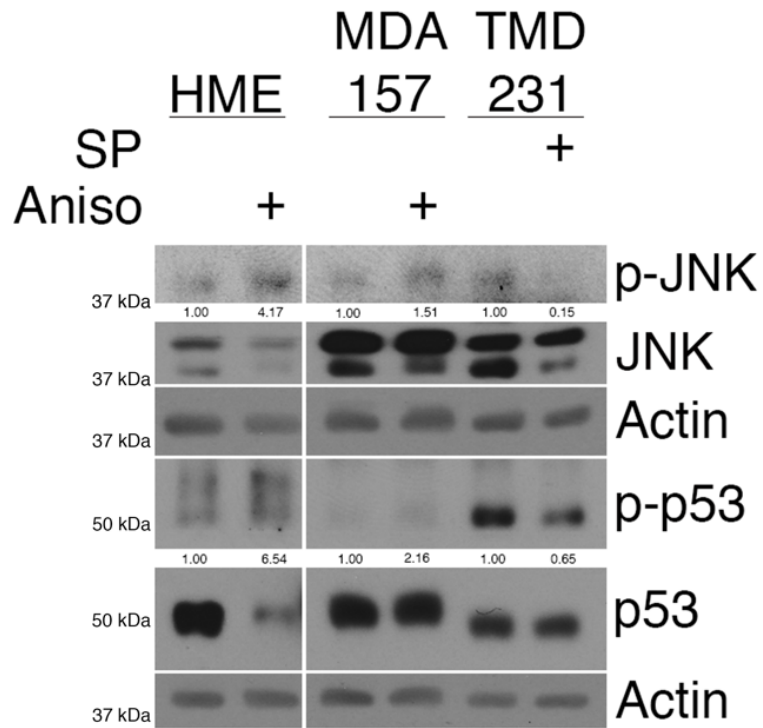


Figure 13. JNK activation or inhibition in HME, MDA157, and TMD231 cell lines. Western blotting for activated JNK (p-JNK) and phosphorylated p53 (at Thr81; p-p53) in whole-cell lysates from HME and MDA157 cells treated with 30  $\mu$ M anisomycin or DMSO for 6 hours and TMD231 cells treated with 25  $\mu$ M SP600125 or DMSO for 6 hours. From [1]. Reprinted with permission from AAAS.

### ***3.5 The JNK-initiated p53-p73 pathway is important for apoptosis***

Phosphorylation of Thr81 of p53 resulted in its interaction with p73 (Figures 8 and 9) and an increased abundance of PUMA (Figure 5B). Therefore, the necessity of p53, p73, and JNK activation for the induction of apoptosis was examined. The removal of p53 in p53–wild-type BJ cells resulted in resistance to JNK-activated cell death by anisomycin treatment (Figure 14A). Specifically, treatment with anisomycin for 9 hours initiated a steady increase in the abundance of BAX and PUMA, which was prevented by shRNA knockdown of p53. In contrast, the abundance of BAX increased after 6 hours of anisomycin treatment; this may be due to the cells overcoming the shRNA knockdown at 6 hours in response to prolonged anisomycin-induced stress (Figure 14A).

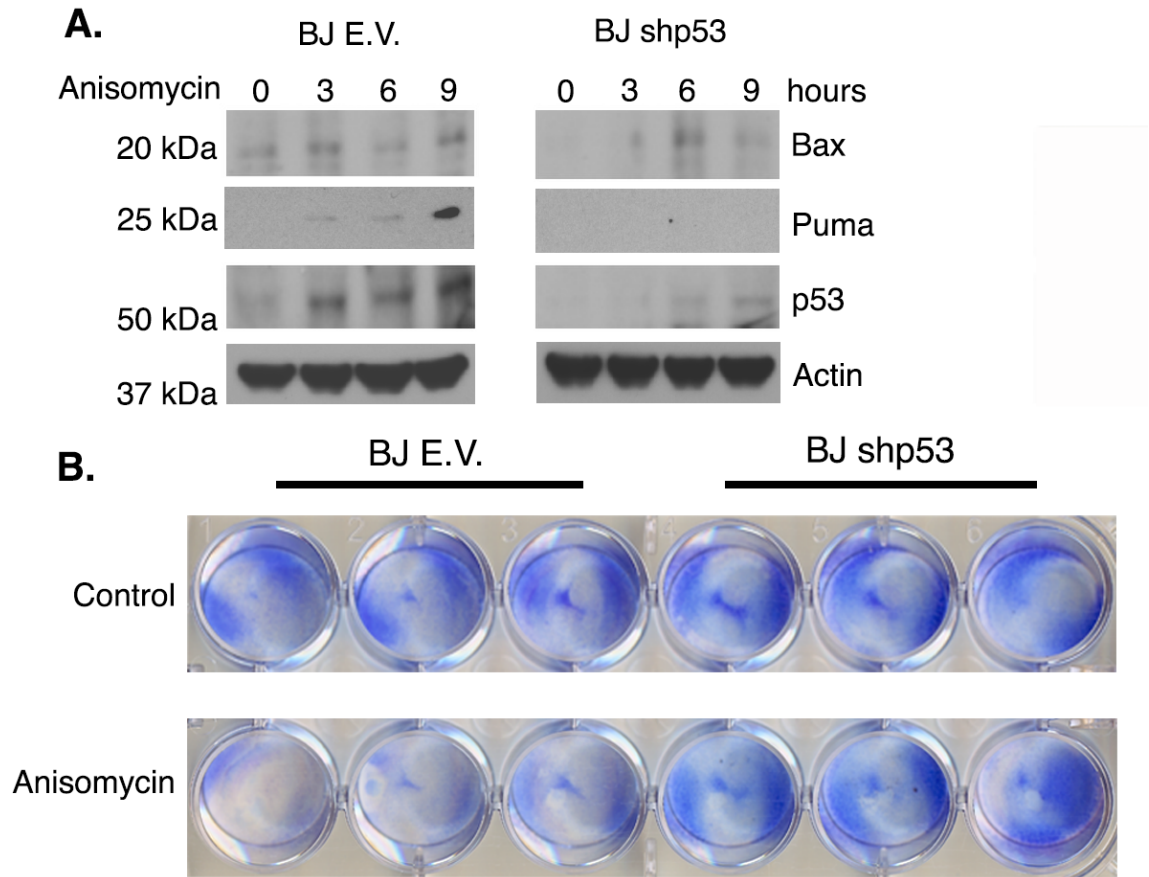


Figure 14. Downstream effects of the p53-p73 pathway. (A) Data from Ciaran McAtarsney. Western blot of Bax, PUMA, p53 and actin in cellular extracts from empty vector control (E.V) and p53-knockdown (shp53) BJ cells treated with anisomycin for the indicated time. Both E.V. and shp53 lanes were developed from the same western blot. Blots are representative of three independent experiments. (B) Data from Ciaran McAtarsney. Cell viability assay of E.V. and shp53 BJ cells stained with Methylene Blue. Cells were treated with DMSO or anisomycin for 9 hours. Data is representative of three independent experiments. From [1]. Reprinted with permission from AAAS.

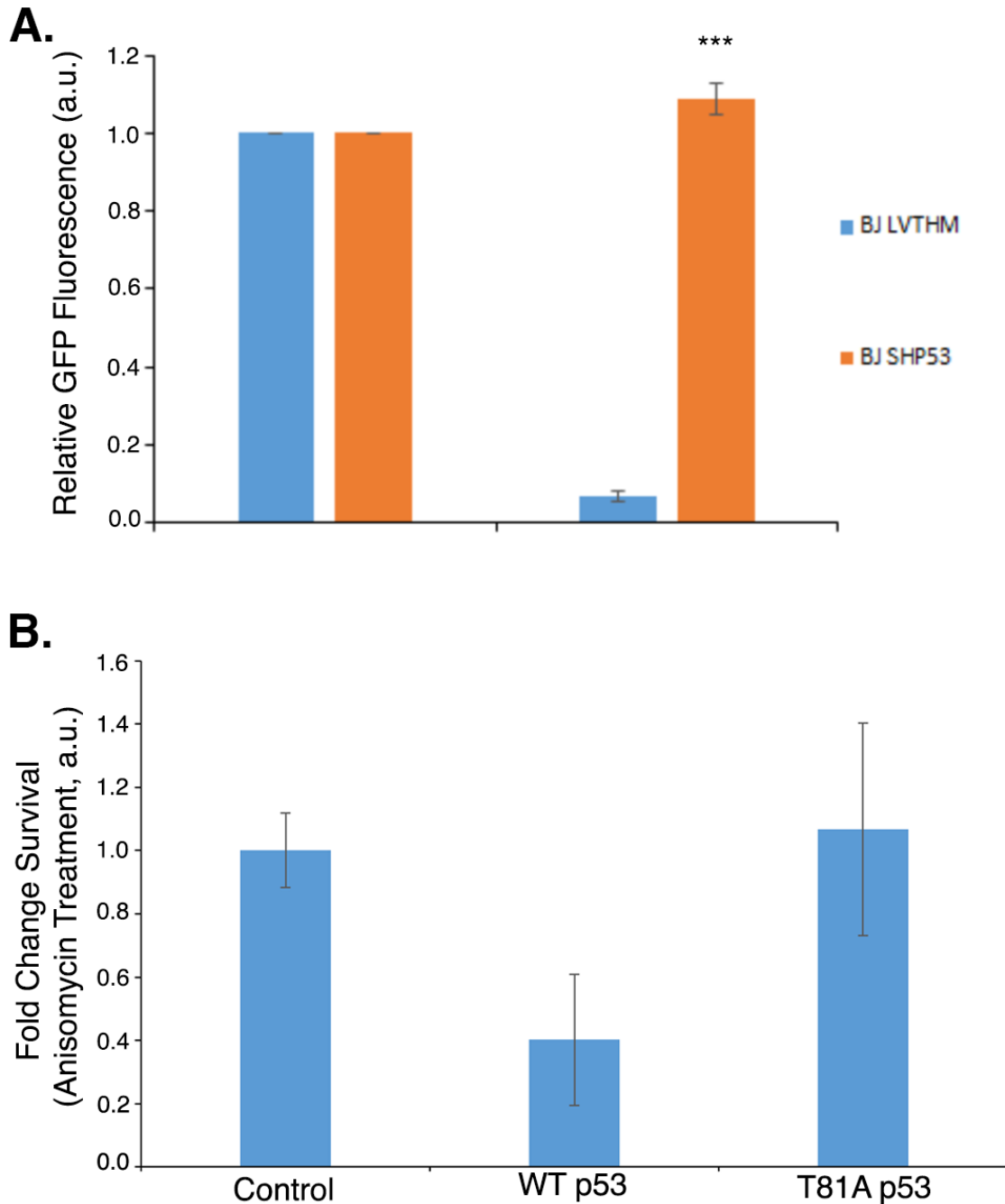


Figure 15. Effects of the p53-p73 pathway on survival. (A) Data from Ciaran McAtarsney. Relative GFP fluorescence was measured in GFP shp53 and LVTHM empty vector BJ cells. Cells were treated with DMSO or anisomycin for 48 hours. Relative fluorescence was derived from DMSO controls. Data is representative of four independent experiments. Significance was determined by a two-tailed unpaired t test (\*\*\*,  $P < 0.005$ ) (B) GFP fluorescence was measured in H1299 cells transfected with GFP alone or GFP and either wild-type or T81A p53, then treated with DMSO or anisomycin. Fold change survival was calculated as the change in survival from DMSO to anisomycin treatment and normalized to the GFP alone control. Error bars represent standard error of the mean. Data is representative of three independent experiments. From [1]. Reprinted with permission from AAAS.

The apoptotic resistance conferred to BJ cells transfected with p53-shRNA was further investigated using a methylene-blue cell death assay (Figure 14B) and by assessing cell number as a factor of green fluorescent protein (GFP) (shRNA vector) signal (Figure 15A). Loss of p53 improved cell viability through anisomycin treatment (Figures 14B and 15A), suggesting that the lack of the p53-p73 complex results in resistance to apoptosis. To test the impact of specifically Thr81 phosphorylation on cell death, GFP and either wild-type p53 or a p53 mutant that cannot be phosphorylated at T81 (T81A) were expressed in H1299 cells and survival was examined by GFP fluorescence after anisomycin treatment. The data revealed an increase in survival of 175% in cells expressing T81A point mutation compared to wild-type p53 (Figure 15B), confirming previously published observations with the T81A mutant [151] and that Thr81 phosphorylation in p53 is critical to cell stress-induced apoptosis.

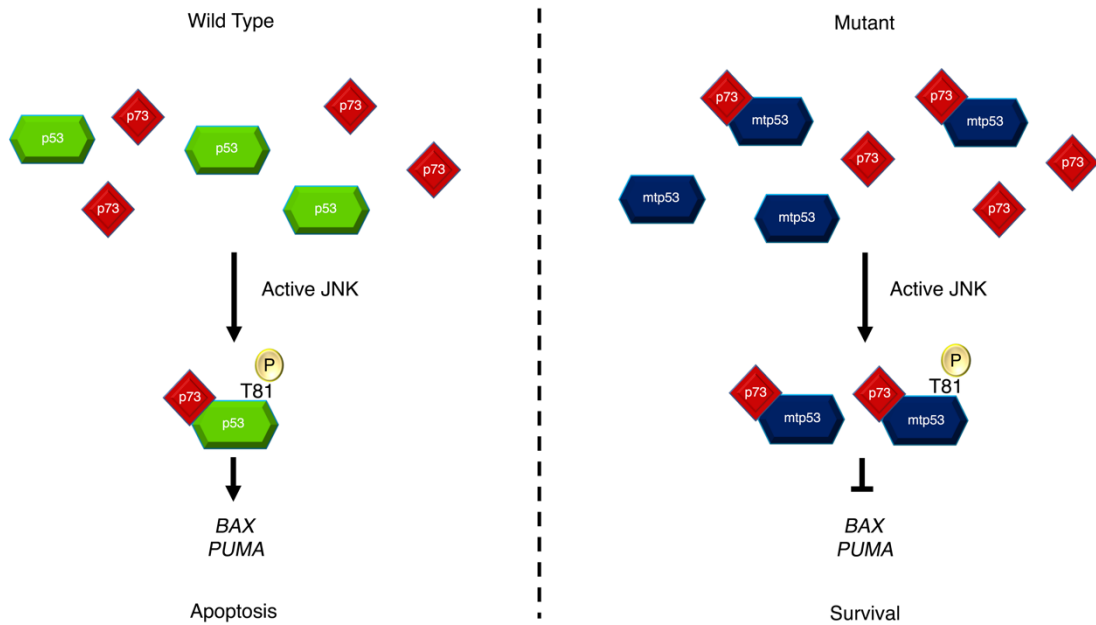


Figure 16. Cell fate is dictated by p53/p73 complex formation. Apoptotic stimuli, for example DNA damage, results in the phosphorylation and activation of JNK. JNK phosphorylates wild-type p53 (green hexagons) at Thr81 causing a structural change in p53 and the subsequent binding of p73 (red diamonds). This complex drives the transcription of PUMA and BAX leading to apoptosis. Mutant p53 (blue hexagons) does not require phosphorylation by JNK to form a complex with p73. Phosphorylation of mutant p53 instead serves to improve the ability of p53 to bind with p73, hence increasing total complex formation. However, PUMA and BAX are not transcribed due to mutant p53's dysfunctional DNA binding domain as well as the sequestering of p73 by complex formation. This decreases the apoptotic signal and promotes tumor survival. Schematic made by Ciaran McAtarsney. From [1]. Reprinted with permission from AAAS.



### ***3.6 Discussion***

The tumor suppressor p53 is highly studied given its role in regulating many cellular activities and responses, including cell cycle arrest, DNA repair, cell death, and metabolism. Its family member p73 has some described overlapping functions; yet, unlike p53, p73 is rarely mutated in human cancer. While p73 is rarely mutated, mutation of p53 may function as a dominant negative to ablate p73 activity [135]. The regulation of p53 is extremely important given that its differential regulation can dictate distinct binding partners and, consequently, distinct outcomes through transcriptional targets, such as PTEN to promote apoptosis versus Mdm2 to promote re-entry into the cell cycle and survival [36, 155]. Increased abundance of PTEN, a protein/lipid phosphatase that inhibits the PI3K (phosphatidylinositol 3-kinase)–AKT (protein kinase B) pathway, can protect p53 from Mdm2-mediated degradation induced by AKT [30, 129, 147, 156, 157]. Thus, p53 can selectively induce PTEN expression and programmed cell death instead of the autoregulatory feedback loop with Mdm2 to promote cell survival [37, 147]. Moreover, PTEN can form a complex with p73 and bind to the *PUMA* promoter to increase its expression, leading to the induction of apoptosis [130]. These molecular and biochemical studies are supported by genetic studies in mice where the loss of p53, p73, or PTEN confers resistance to apoptotic stimuli and an increase in neoplastic development [3, 137, 158-160]. Thus, an effective response to apoptotic stimuli requires the integration of numerous intact tumor suppressors, yet how these tumor suppressors are signaled to form a complex has not previously been clearly defined.

There are well-characterized kinase signaling pathways that phosphorylate p53 and p73 in response to DNA damage, but some phosphorylation sites appear to be

dispensable for the induction of apoptosis. It has been reported by several groups that Ser46 and Thr81 are important for the induction of apoptosis [144, 145, 147, 149]. Homeodomain-interacting protein kinase 2 (HIPK2) and the mitogen-activated protein kinase p38 reportedly phosphorylate Ser46 of p53, whereas JNK, which plays dual roles in cellular proliferation and cell death [161], phosphorylates Thr81 of p53 [144, 145, 147, 149]. One of JNK's substrates is p73, which mediates JNK-induced apoptosis [162], but it was unclear how. Analysis of apoptosis by the JNK-p73 axis in that previous study [162] was performed in cells that maintained expression of wild-type p53, and notably, p53 abundance does not directly correlate with its activity; for example, neddylation of p53 in response to growth factor signaling renders p53 stable but inactive [47].

Untransformed cell lines have an intact apoptotic pathway and deneddylating enzymes, tumor suppressors, active kinases, and post-translational modification enzymes that are activated in response to genotoxic stress that provide a robust induction of apoptosis. There is renewed interest in p53 family member interactions, and several studies have highlighted the importance of the interactions between different family members [163-165]. Our studies have linked the JNK-p53-p73 proteins showing that phosphorylation of p53 at Thr81 by JNK is permissive of a p53-p73 interaction. Notably, our structural modeling analysis revealed that the structure of phosphorylated Thr81 is nearly identical to that of R248W. Therefore, activated JNK can convert wild-type p53 to mimic mutant p53 with regards to binding to p73 by exposing the DNA binding domain. Ser46 is proximal to the proline rich domain in the second transactivation domain, which may be important for additional structural changes to recruit other factors for gene expression. However, we also found that phosphorylation of Ser46 has no effect on binding to p73,

supporting that Ser46 phosphorylation may instead be required for recruiting additional coactivators. The JNK-mediated interaction between wild-type p53 and p73 provides biochemical evidence in support of the existing animal models and gene dose sensitivity of p53 and p73 to apoptosis [3]. We also show that in mutant p53 cells, JNK activity is increased resulting in a mutant p53/wild-type p73 complex with mutant p53 acting as a dominant negative partner of p73. These data are consistent with previous reports showing that mutant p53/p73 form a complex [136]. The p53/p73 complex mediates apoptosis in cells that express wild-type p53, but survival in cells that express mutant p53. Thus, our findings refine our understanding of how cells promote, or in certain contexts circumvent, the p53 apoptotic signaling axis.

In addition to the apoptotic function of p53, the tumor suppressor also plays a major role in the inhibition of angiogenesis [80, 156, 166-172]. The mechanisms governing the activation of p53 for inhibition of angiogenesis have not been thoroughly explored. However, some of the known activators of p53 have been shown to play a role in angiogenesis inhibition independent of p53. For example, in addition to its regulation of HIF $\alpha$  subunits, the Von Hippel-Lindau (VHL) tumor suppressor protein is also able to bind to p53 in response to genotoxic stress, resulting in stabilization and transactivation of p53 [173]. Additionally, while p73 can synergize with p53 in response to JNK activation, it is also able to destabilize HIF1 $\alpha$  in response to hypoxia [174]. While there has been no direct link between these activators of p53 and the ability of p53 to inhibit angiogenesis, these pathways were investigated to determine if there was any mechanism that could activate the anti-angiogenesis activity of p53.

## **4. Mdm2 functions as an angiogenic switch through its regulation of VHL**

### ***4.1 Introduction***

The murine double minute 2 (Mdm2) oncoprotein is detectable in 40-90% of human cancers and is correlated with high-grade metastatic tumors and poor patient outcome [175]. The current paradigm is that the function of Mdm2 is to regulate the tumor suppressor p53 [19, 20]. p53 plays a major role in the DNA damage response and cell cycle arrest by activating transcription of *CDKN1A*, *BAX*, *BBC3* and others [176-178]. p53 can also regulate transcription of genes involved in metabolism, angiogenesis, stemness, migration, and invasion [reviewed in [6]]. In recent years it has come to light that some of the noncanonical p53 targets may be more important for tumor suppression by p53. For instance, p53 mutated at three key lysines that are needed for p53 mediated cell cycle arrest, apoptosis, and senescence is still capable of tumor suppression [179]. Additionally, a mouse model that is deficient in p53-dependent apoptosis is not prone to cancer development [180]. One area of tumor suppression by p53 that is not well understood is its regulation of angiogenesis. p53 is able to activate transcription of several inhibitors of angiogenesis such as *THSB1*, *SERPINE1*, and *COL18A1* and suppress transcription of the proangiogenic *VEGF*, thereby tilting the balance of angiogenesis [166, 168, 170, 172, 181].

Mdm2 can play a role in angiogenesis through several mechanisms. In response to hypoxia, Mdm2 binds directly to hypoxia inducible factor 1 $\alpha$  (HIF1 $\alpha$ ) resulting in increased *VEGF* expression [96-100]. Additionally, Mdm2 can bind to and stabilize the 3' UTR of *VEGF* mRNA [76]. Our lab recently showed that Mdm2 can be converted to a nedd8 E3 ligase in response to phosphorylation by c-Src. Mdm2 can then neddylate p53,

rendering it stable but inactive [47]. Another mechanism of p53 stabilization involves the von Hippel-Lindau tumor suppressor protein (VHL), which binds to p53 and blocks Mdm2-mediated degradation of p53 [173]. VHL is frequently mutated in sporadic clear cell renal cell carcinomas and it plays an important role in hypoxic signaling through its regulation of HIF $\alpha$  subunits [108, 122]. Interestingly, p53 is rarely mutated in renal cell carcinomas, but p53 pathway genes are commonly downregulated suggesting a different mechanism of p53 pathway inhibition [182]. In response to DNA damage, VHL can bind p53 and recruit p300 to acetylate specific lysines of p53, in turn blocking potential ubiquitination sites and activating p53 transcriptional activity of *CDKN1A* and *BAX* [173]. Interestingly, the region of VHL that binds to p53 contains a lysine that has been shown to be neddylated by an unknown E3 ligase [126, 183]. Previously, the neddylation of VHL was shown to be important for the formation of the fibronectin extracellular matrix, but its effect on binding to p53 was not examined.

Because VHL is able to stabilize and activate p53, and Mdm2 can disrupt p53 activity, the impact of Mdm2 on VHL stabilization and activation of p53 was examined. We hypothesize that the VHL-p53 interaction results in an increase in production of inhibitors of angiogenesis and that Mdm2 may disrupt the binding of VHL to p53 through conjugation of nedd8. To this end, we have examined the effect of VHL on p53 antiangiogenic target genes as well as the ability of Mdm2 to disrupt the VHL/p53 pathway. Our study provides an explanation for the changes in p53 pathway genes seen in renal cell carcinomas as well as a reason for p53 tumor suppression in the absence of apoptosis, senescence, or cell cycle arrest.

#### ***4.2 p53 target genes for apoptosis and angiogenesis are altered by VHL status***

The tumor suppressor p53 is able to inhibit cancer progression via several different mechanisms, including the transcription of pro-apoptotic factors and anti-angiogenic factors [166, 170-172, 181]. Activation of p53 is a highly regulated process involving many other tumor suppressor proteins [1, 184]. It has been previously reported that VHL can bind to p53 and increase the transcription of the pro-apoptotic *BAX* and *CDKN1A* [173]. Using a subset of patient data for renal cell carcinomas, we determined the effects of mutations in the domain of VHL that binds to p53 on the mRNA levels of these target genes, as well as several other genes that p53 regulates. Mutations in the  $\alpha$  domain of VHL caused an increase in mRNA for *BAX*, *CDKN1A*, and *BBC3* (Figure 17A). Likewise, the mRNA levels of the antiangiogenic factors *THBS1*, *COL18A1*, and *SERPINE1* were also increased when the  $\alpha$  domain of VHL was mutated (Figure 17B). The change in mRNA expression suggests that there is some modification to the  $\alpha$  domain of VHL that may block its interaction with p53. *THBS1* codes for the protein thrombospondin-1 (TSP-1), a potent inhibitor of angiogenesis that is known to be regulated by p53 [166]. To confirm the importance of VHL on the transcription of *THBS1*, we analyzed the luciferase activity of a TSP-1 reporter in the 786-O and RCC4 cell lines with or without VHL transduction. In both cell lines, transduction with VHL increased the reporter activity by 3-4 fold (Figure 18A). In order to determine if the increase in *THBS1* transcription resulted in an increase in secreted TSP-1 protein, we analyzed conditioned media from 786-O and RCC4 cells for TSP-1 levels. Similar to the reporter activity results, VHL transduction increased the secreted TSP-1 protein levels by

~2 fold (Figure 18B). We also analyzed conditioned media using an angiogenesis microarray and saw consistent results (Figure 19).

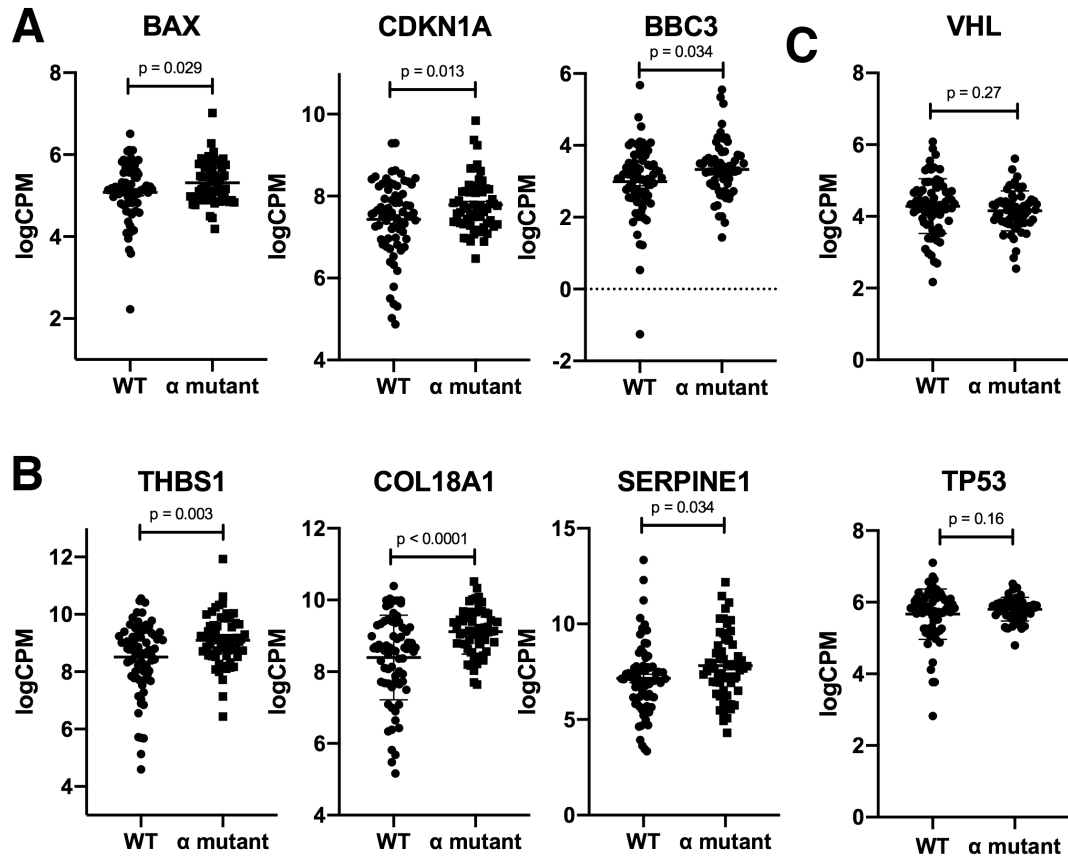


Figure 17. p53 target genes for apoptosis and angiogenesis are altered by VHL status. A) Log counts per million for BAX, CDKN1A, and BBC3. Only samples with wild-type p53 were included in the analysis. WT refers to wild-type VHL status, and  $\alpha$  mutant refers to any point mutation within the  $\alpha$  domain of VHL. Error bars represent SEM. P values were calculated using an unpaired t test. (B) Log counts per million THBS1, COL18A1, and SERPINE1. Only samples with wild-type p53 were included in the analysis. WT refers to wild-type VHL status, and  $\alpha$  mutant refers to any point mutation within the  $\alpha$  domain of VHL. Error bars represent SEM. P values were calculated using an unpaired t test. (C) Log counts per million VHL and TP53. Only samples with wild-type p53 were included in the analysis. WT refers to wild-type VHL status, and  $\alpha$  mutant refers to any point mutation within the  $\alpha$  domain of VHL. Error bars represent SEM. P values were calculated using an unpaired t test.



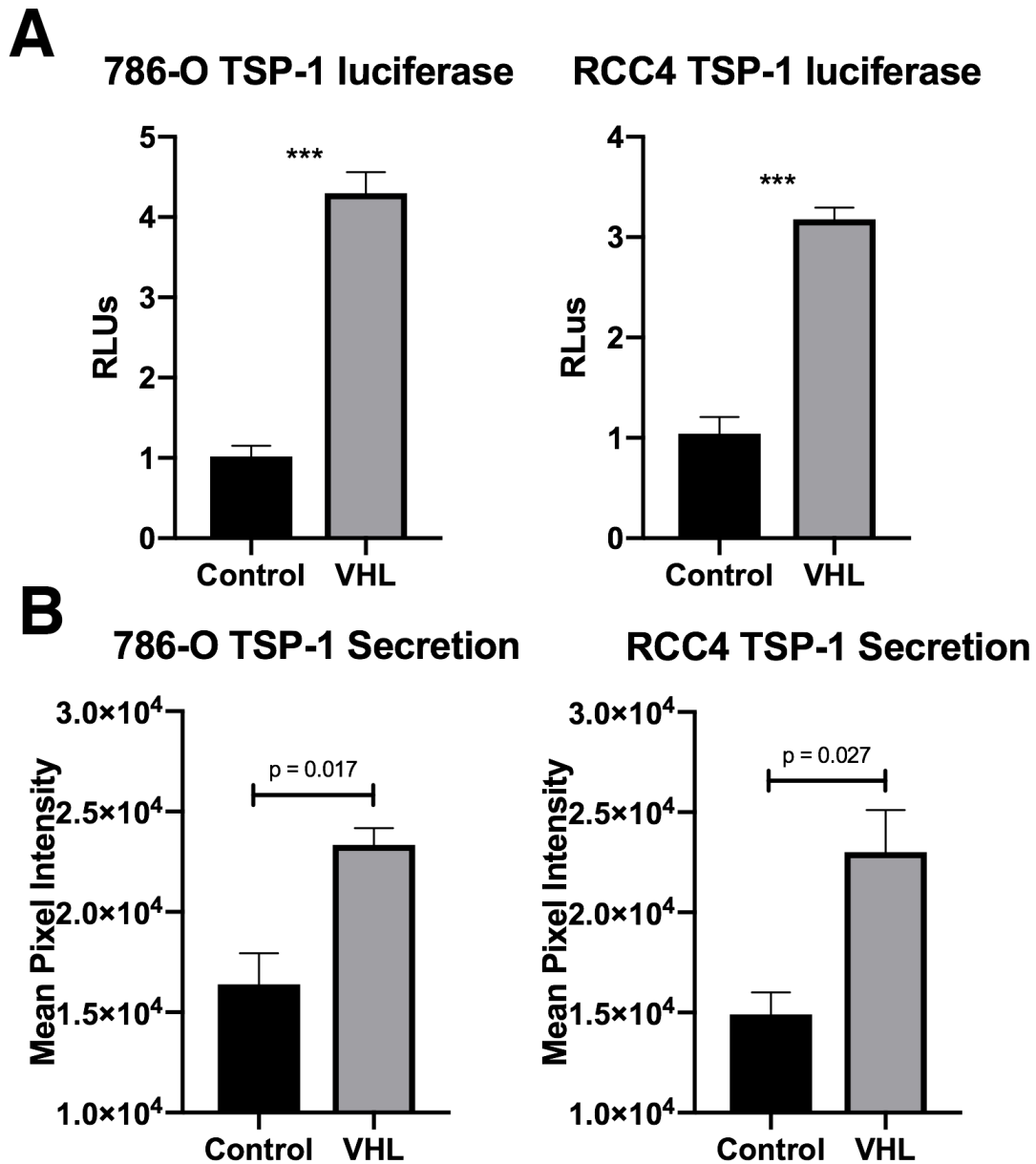


Figure 18. VHL increases transcription of THBS1 and secretion of TSP-1. (A) Luciferase assay in 786-O and RCC4 cells with or without VHL for thrombospondin-1 plotted as relative luciferase units. Means are calculated from three biological replicates. Error bars represent SEM. Statistics were calculated using an unpaired t test (\*\**p*<0.001). (B) Dot blot assay to measure protein level of thrombospondin-1 in media secreted from 786-O or RCC4 cells with or without VHL. Means are calculated from three biological replicates. Error bars represent SEM. Statistics were calculated using an unpaired t test (\*\**p*<0.001).

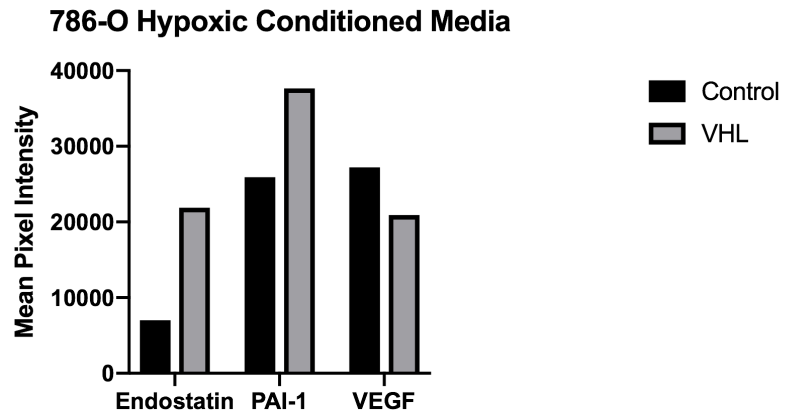


Figure 19. Angiogenesis array with conditioned media from 786-O cells under hypoxia

#### ***4.3 Mdm2 binds to VHL and inhibits VHL-p53 complex formation under hypoxia***

In order to determine what mechanisms may inhibit VHL-p53 complex formation, we expressed exogenous Mdm2, VHL, and p53 in H1299 cells with or without hypoxia and analyzed complex formation by immunoprecipitation. VHL forms a complex with p53 under both normoxia and hypoxia, but that Mdm2 inhibits VHL/p53 complex formation under hypoxia (Figure 20A). We next analyzed complex formation between VHL and Mdm2 in H1299 cells and saw that VHL and Mdm2 form a complex under both normoxia and hypoxia (Figure 20B). Since Mdm2 bound to VHL under both normoxia and hypoxia, but only inhibits VHL-p53 complex formation under hypoxia, we hypothesized that Mdm2 might be causing a posttranslational modification to VHL under hypoxia. Src phosphorylation of Y281 and Y302 of Mdm2 causes Mdm2 to become a neddylation ligase, and Src becomes phosphorylated at Y416 in response to hypoxia [47, 185]. We verified Src activation in our system by analyzing phosphorylation of Y416 in response to hypoxia in the RCC4 cell line and found that Src does become more active after exposure to hypoxia (Figure 20C). Of note, there is a neddylation site at lysine 159 of VHL that overlaps with the region that is required for binding to p53 (Figure 21) [126, 183]. Mdm2 is able to function as a nedd8 E3 ligase under growth conditions [47], so we rationalized that Mdm2 could be neddylation VHL under hypoxia if the right growth conditions are present. To further confirm the effect of Mdm2 on VHL-p53 complex formation, VHL or VHL and Mdm2 were transiently expressed in 786-O cells and stained the cells with VHL and p53 antibody for immunofluorescence. Supporting the immunoprecipitation data, VHL colocalized with p53 under normoxia and Mdm2 inhibited p53/VHL colocalization under hypoxia (Figure 22A and 22B).

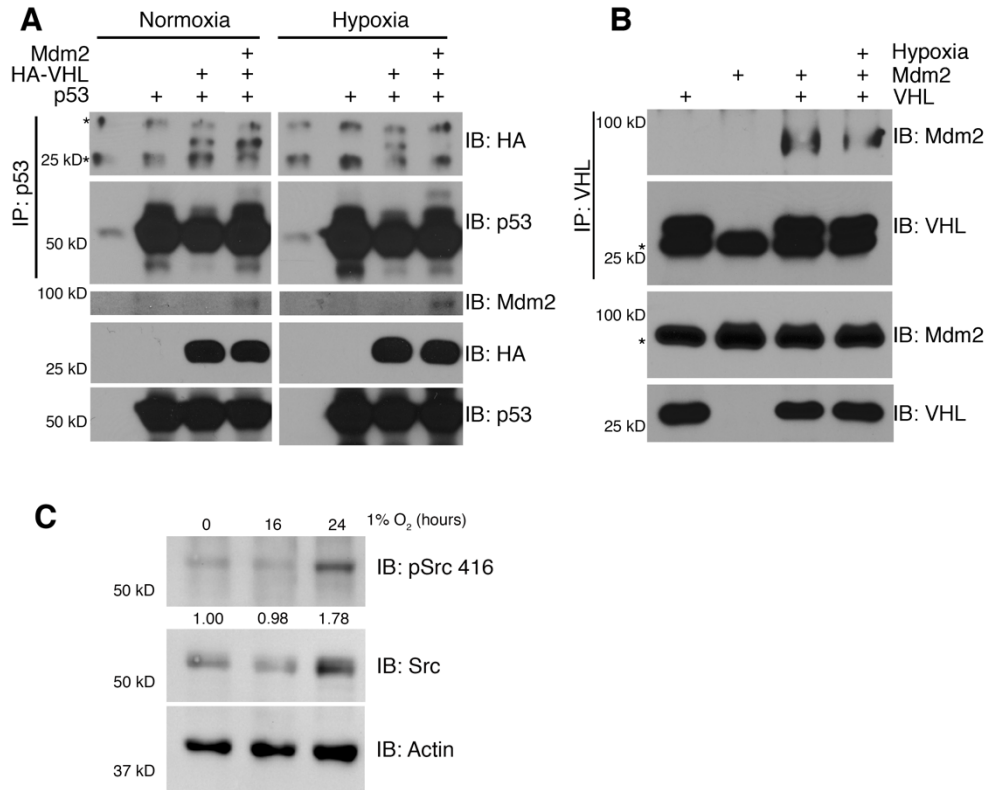


Figure 20. Mdm2 binds to VHL and inhibits VHL-p53 complex formation under hypoxia. (A) Transient transfection in H1299 cells followed by incubation in either normoxia or hypoxia. p53 was immunoprecipitated from cell lysates and subjected to analysis by Western blot. (B) Transient transfection in H1299 cells followed by incubation in either normoxia or hypoxia. VHL was immunoprecipitated from cell lysates and subjected to analysis by Western blot. (C) Hypoxia timecourse in RCC4 cells followed by Western blot.

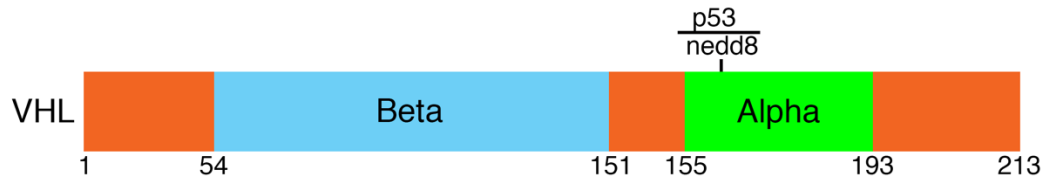


Figure 21. Schematic of VHL protein showing the primary site of neddylation, as well as the region that has been shown to be indispensable for binding to p53.

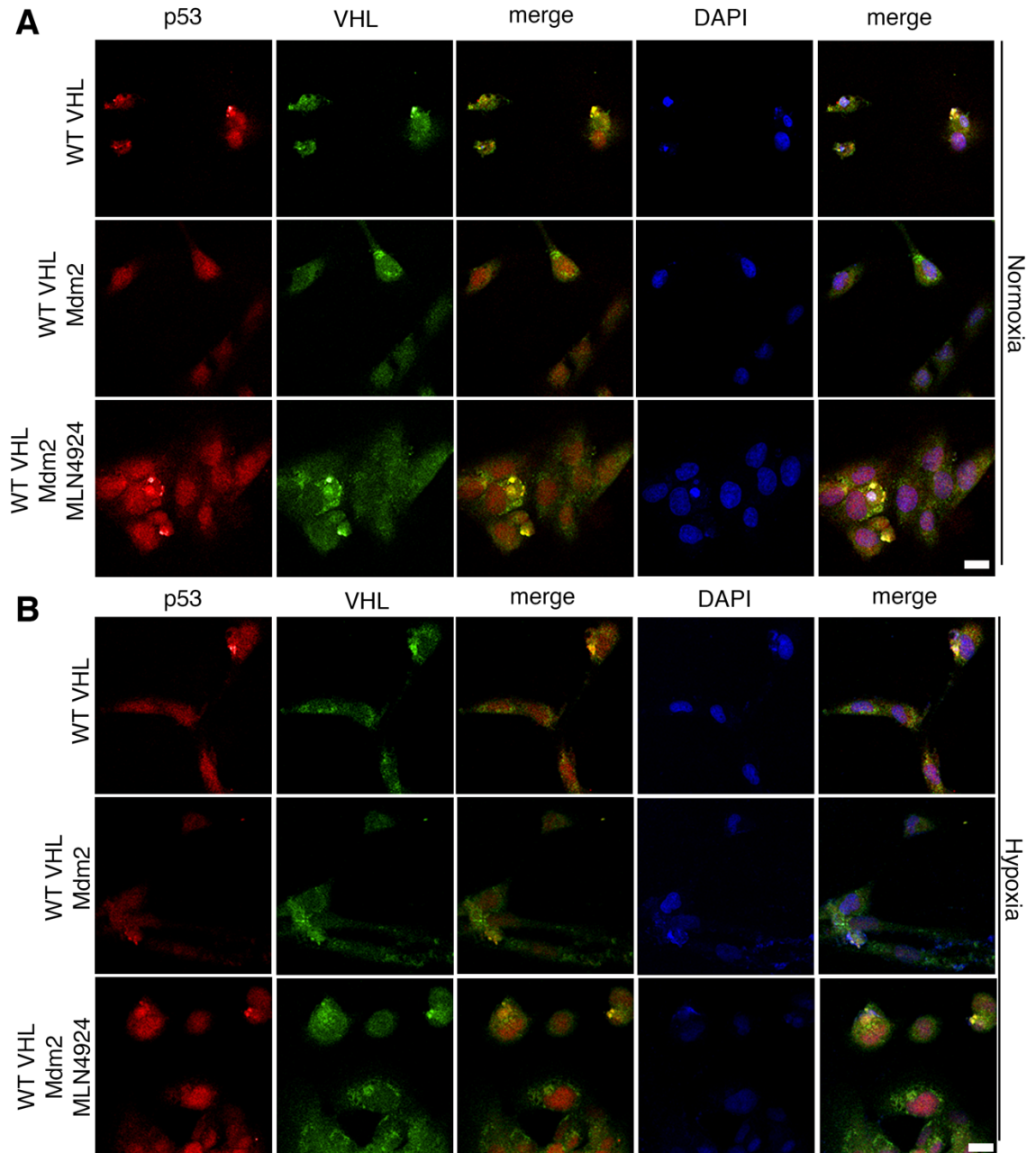


Figure 22. Mdm2 inhibits VHL-p53 complex formation under hypoxia. (A) Transfection of 786-O cells with VHL or VHL and Mdm2 under normoxia. Cells were fixed and stained with p53 or VHL and subjected to immunofluorescence confocal microscopy. Scale bar is 25  $\mu$ m. (B) Transfection of 786-O cells with VHL or VHL and Mdm2 under hypoxia. Cells were fixed and stained with p53 or VHL and subjected to immunofluorescence confocal microscopy. Scale bar is 25  $\mu$ m.

#### ***4.4 Neddylation of VHL by Mdm2 interferes with VHL-p53 complex formation***

To examine the importance K159 neddylation on VHL-p53 complex formation, a K159E point mutant of VHL was utilized. The K159E mutant was isolated from a patient with Type 2C VHL disease, which only develops pheochromocytoma [120, 126]. H1299 cells were transiently transfected with p53 and either WT VHL or K159E VHL under normoxia or hypoxia and analyzed VHL-p53 complex formation by immunoprecipitation (Figure 23A). VHL-p53 complex formation increased with the K159E mutant compared to WT, but this increase was very dramatic under hypoxia which supports VHL becoming neddylated under hypoxia. Treatment with MLN4924, a global neddylation inhibitor, resulted in increased VHL-p53 complex formation in 786-O (Figure 23B) and MCF7 (Figure 23C) cells. To determine if Mdm2 is the nedd8 E3 ligase for VHL, we first examined if Mdm2 binds directly to VHL, and if so what domain of VHL binds to Mdm2 using recombinant proteins produced and purified from E. Coli. The  $\alpha$  domain of VHL interacts directly with Mdm2 (Figure 24A). Purified recombinant proteins were then used in a cell free assay to determine if Mdm2 was able to neddylate VHL. Using GST-VHL, His-Mdm2, His-Src, and neddylation reaction components, we saw that Mdm2 neddylates VHL. In support of previously published data on the activation of Mdm2 [47], the neddylation of VHL is increased with the addition of Src (Figure 24B). To determine if VHL is neddylated by Mdm2 in a tumor cell model, Mdm2 was transiently expressed in 786-O cells that were transduced with WT VHL or a control vector. Immunoprecipitation of nedd8 showed complex formation with VHL when Mdm2 was expressed, and this interaction increased under hypoxia (Figure 24C). Neddylation of VHL was further investigated by transiently expressing components of our system with

His-nedd8 and performed a Ni-NTA pulldown under denaturing conditions. Neddylation of WT VHL was much higher than K159E, CA-Src increased the abundance of the neddylated form of VHL, and MLN4924 reduced the abundance of the neddylated form of VHL (Figure 24D).



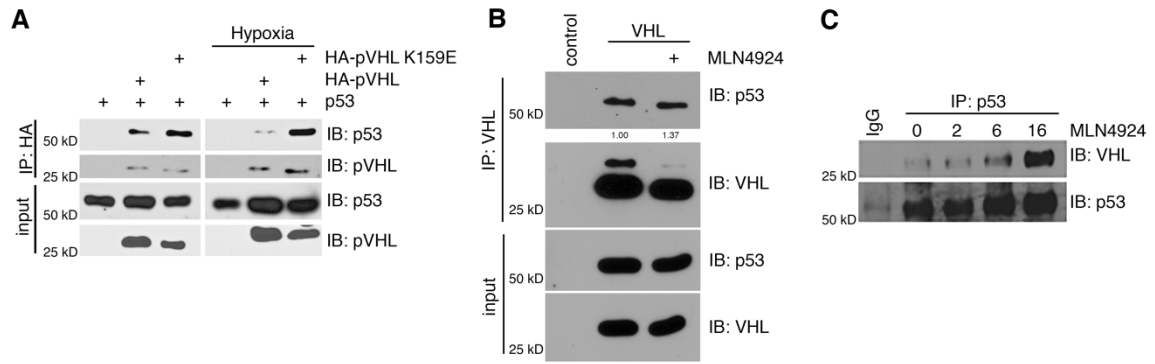


Figure 23. Neddylation impacts p53-VHL complex formation. (A) Transient transfection in H1299 cells under normoxia or hypoxia. Cell lysates were immunoprecipitated for HA and subjected to analysis by Western blot. (B) Immunoprecipitation of VHL from 786-O cells treated with the neddylation inhibitor MLN4924 and Western blotted for p53 and VHL. (C) Data from Lindsey Mayo. Immunoprecipitation of p53 or IgG control from MCF7 cells treated with MLN4924 for various indicated times and Western blotted for VHL and p53.



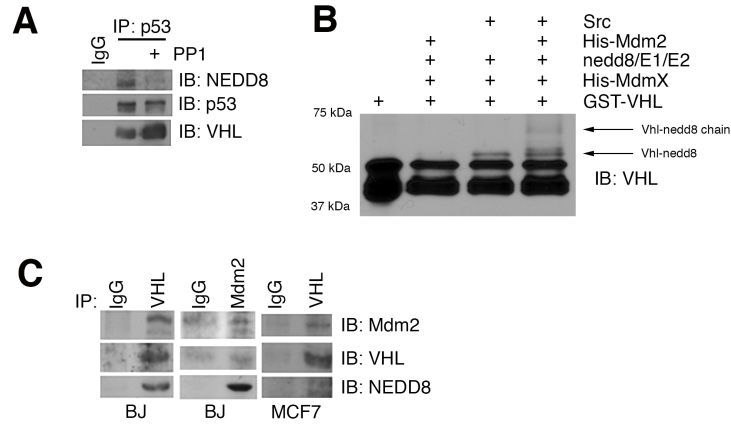


Figure 25. Neddylated VHL by Mdm2 reduces VHL-p53 complex formation. (A) Data from Lindsey Mayo. Immunoprecipitation of p53 or IgG control from MCF7 cells treated with PP1 or a control and Western blotted for nedd8, p53, and VHL. (B) Cell free neddylated assay using recombinant proteins. Reactions were separated by SDS-PAGE and analyzed by Western blot. (C) Data from Lindsey Mayo. Immunoprecipitation of VHL, Mdm2, or IgG control from BJ or MCF7 cell extracts and Western blotted for Mdm2, VHL, and nedd8.

#### ***4.5 VHL colocalizes with p53 under hypoxia or with treatment of MLN4924***

Immunofluorescence confocal microscopy was used to examine the intracellular co-localization of VHL-p53 complex. 786-O cells were transiently transfected with WT VHL, K159E VHL, and Mdm2 and stained with antibody against VHL and p53. Under normal oxygen, WT VHL colocalized with p53 when Mdm2 was not transfected or when Mdm2 was transfected with the addition of the neddylation inhibitor MLN4924 (Figure 26A). The K159E point mutant of VHL colocalized with p53 under all conditions tested in normal oxygen, including when Mdm2 was transfected (Figure 27A). Under hypoxic conditions, WT VHL only colocalized with p53 when cells were treated with MLN4924 (Figure 26B). There was a slight decrease in colocalization of WT VHL and p53 when Mdm2 was co-transfected, but it is likely that endogenous Mdm2 is also inhibiting the interaction between VHL and p53 under hypoxia. There was an increase in colocalization of K159E VHL and p53 under hypoxia as compared to normoxia (Figure 27B). Transfection of Mdm2 with K159E VHL under hypoxia did not interfere with VHL-p53 complex formation. Interestingly, treatment with MLN4924 caused an additional increase in K159E VHL-p53 complex formation under hypoxia, suggesting that there may be additional neddylation sites that are important for the interaction of VHL with p53. To test colocalization in an endogenous system, Caki-1 cells were treated with MLN4924 or DMSO (Control) under normoxia or hypoxia and stained with antibodies against VHL and p53. Similar to the results seen with the 786-O cell line, p53 and VHL formed a complex under normoxia and that complex formation increased with MLN4924 treatment (Figure 28A). Under hypoxia, there was not as much of a loss of complex formation as

seen with 786-O cells, but this could be due to different protein levels of endogenous Mdm2 between cell lines (Figure 28B).

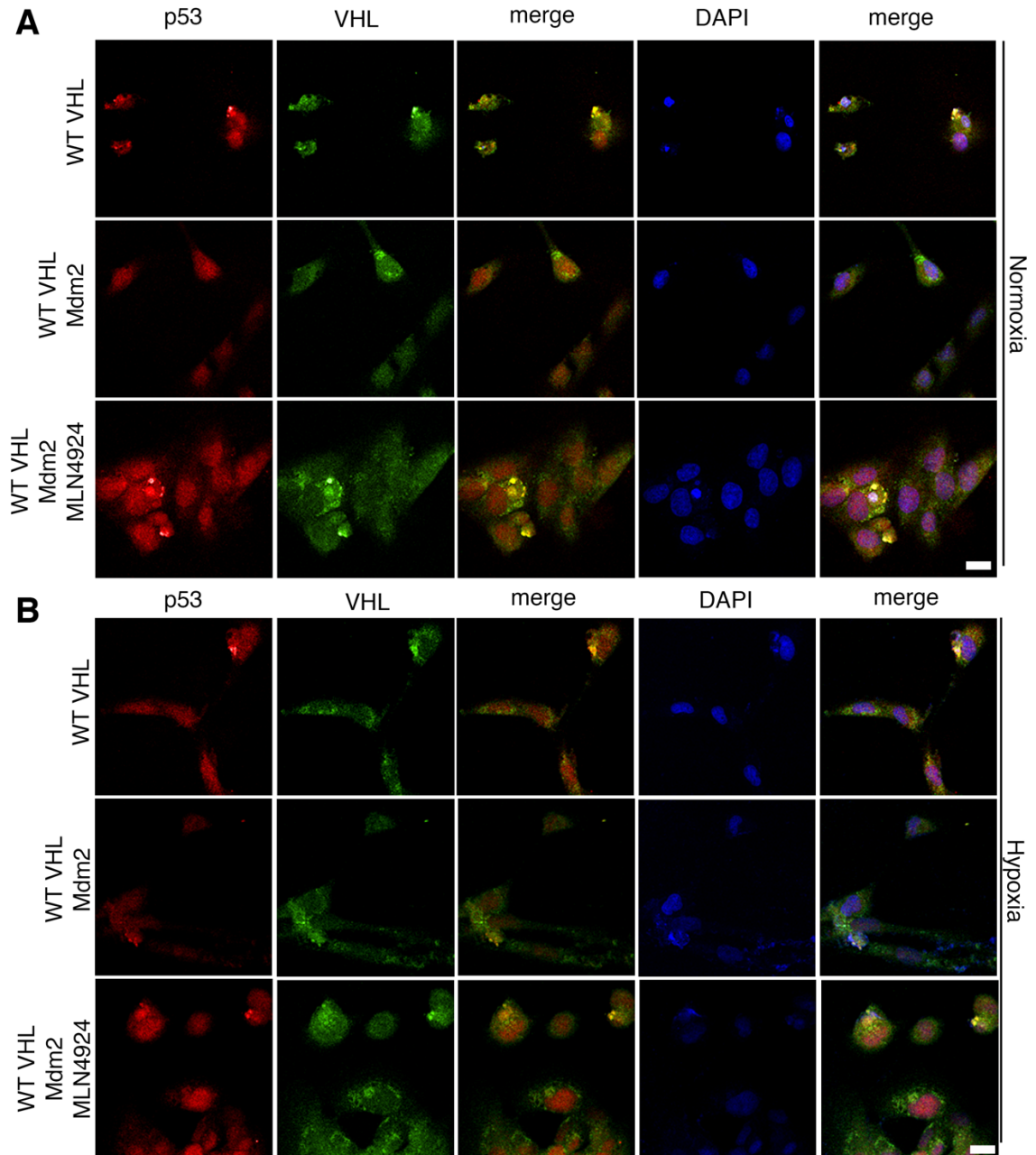


Figure 26. VHL colocalizes with p53 under hypoxia or with treatment of MLN4924. (A) Transfection of 786-O cells with VHL or VHL and Mdm2 under normoxia. Cells were treated with MLN4924 or a control, fixed, and stained with p53 or VHL and subjected to immunofluorescence confocal microscopy. Scale bar is 25  $\mu$ m. (B) Transfection of 786-O cells with K159E VHL or K159E VHL and Mdm2 under normoxia. Cells were treated with MLN4924 or a control, fixed, and stained with p53 or VHL and subjected to immunofluorescence confocal microscopy. Scale bar is 25  $\mu$ m.

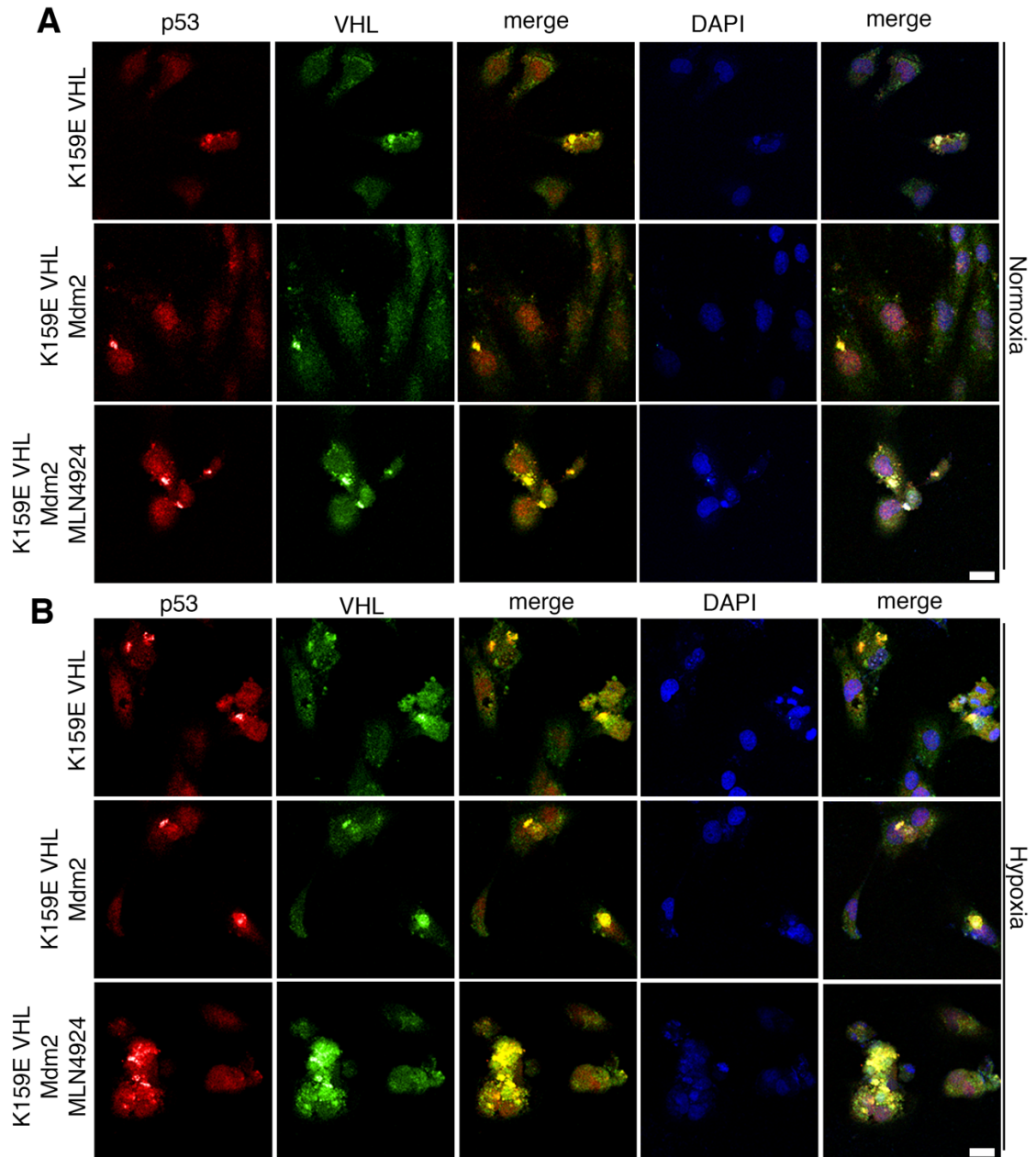


Figure 27. K159E VHL colocalizes with p53 under hypoxia, but also with treatment of MLN4924. (A) Transfection of 786-O cells with VHL or VHL and Mdm2 under hypoxia. Cells were treated with MLN4924 or a control, fixed, and stained with p53 or VHL and subjected to immunofluorescence confocal microscopy. Scale bar is 25  $\mu$ m. (B) Transfection of 786-O cells with K159E VHL or K159E VHL and Mdm2 under hypoxia. Cells were treated with MLN4924 or a control, fixed, and stained with p53 or VHL and subjected to immunofluorescence confocal microscopy. Scale bar is 25  $\mu$ m.

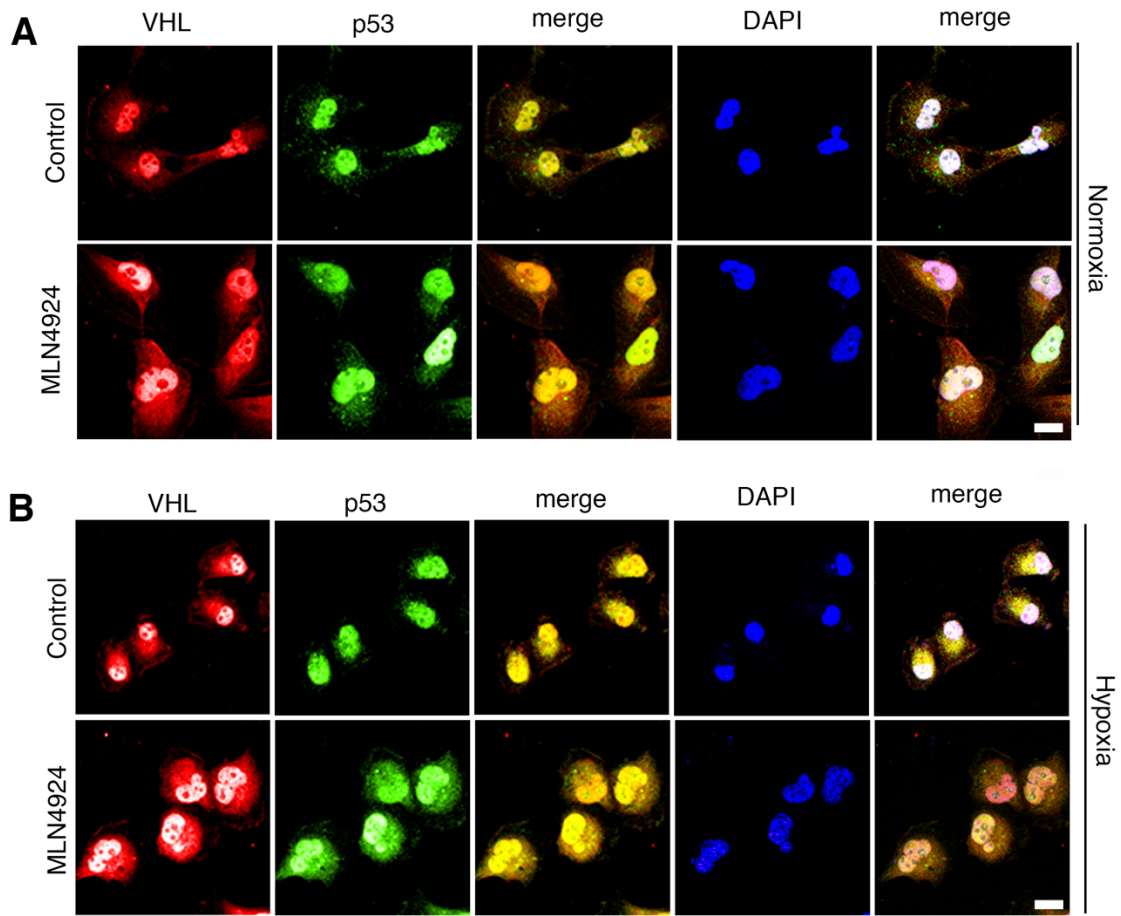


Figure 28. VHL colocalizes with p53 under hypoxia or with treatment of MLN4924. (A) Immunofluorescence microscopy of Caki-1 cells treated with MLN4924 or a control under normoxia. Cells were fixed and stained with VHL and p53. Scale bar is 50  $\mu$ m. (B) Immunofluorescence microscopy of Caki-1 cells treated with MLN4924 or a control under hypoxia. Cells were fixed and stained with VHL and p53. Scale bar is 50  $\mu$ m.



#### ***4.6 VHL increases the acetylation of p53 under hypoxia, leading to increased transcription and secretion of TSP-1***

There are many signals that can activate p53-dependent transcription, but acetylation is necessary in order to change the structure of p53 to expose the DNA binding domain to bind to DNA [reviewed in [186]]. It has previously been shown that VHL activation of p53 results in acetylation at K373/382 of p53 in response to DNA damage [173]. Because the pathway we are focused on is impacted by hypoxia, the role of VHL on acetylation of p53 in response to hypoxia was examined. We found that VHL is required for the acetylation of p53 at K373/382 in response to hypoxia (Figure 29A). To determine if the activation of p53 would lead to increased transcription of *THBS1*, the luciferase activity of a *THBS1* reporter gene in response to hypoxia with or without VHL was examined. VHL reconstitution resulted in a significant increase in *THBS1* transcription, but this increase was negated by hypoxia (Figure 29B). Interestingly, treatment with MLN4924 overcame the hypoxia-dependent decrease in *THBS1* transcription (Figure 29B). To verify that the changes in *THBS1* transcription correlate with a change in secretion, we analyzed the protein levels of secreted TSP-1 by ELISA. As expected, VHL reconstitution increased the secretion of TSP-1 in Caki-1, 786-O, and RCC4 cells (Figure 30). Under hypoxia, TSP-1 secretion was almost identical in control or VHL positive cells. With knockdown p53, however, there was a marked decrease in TSP-1 secretion under hypoxia as compared with control cells with knockdown p53 (Figure 30). These data support our hypothesis that p53 and VHL are both required for a robust induction of TSP-1 in response to hypoxia.

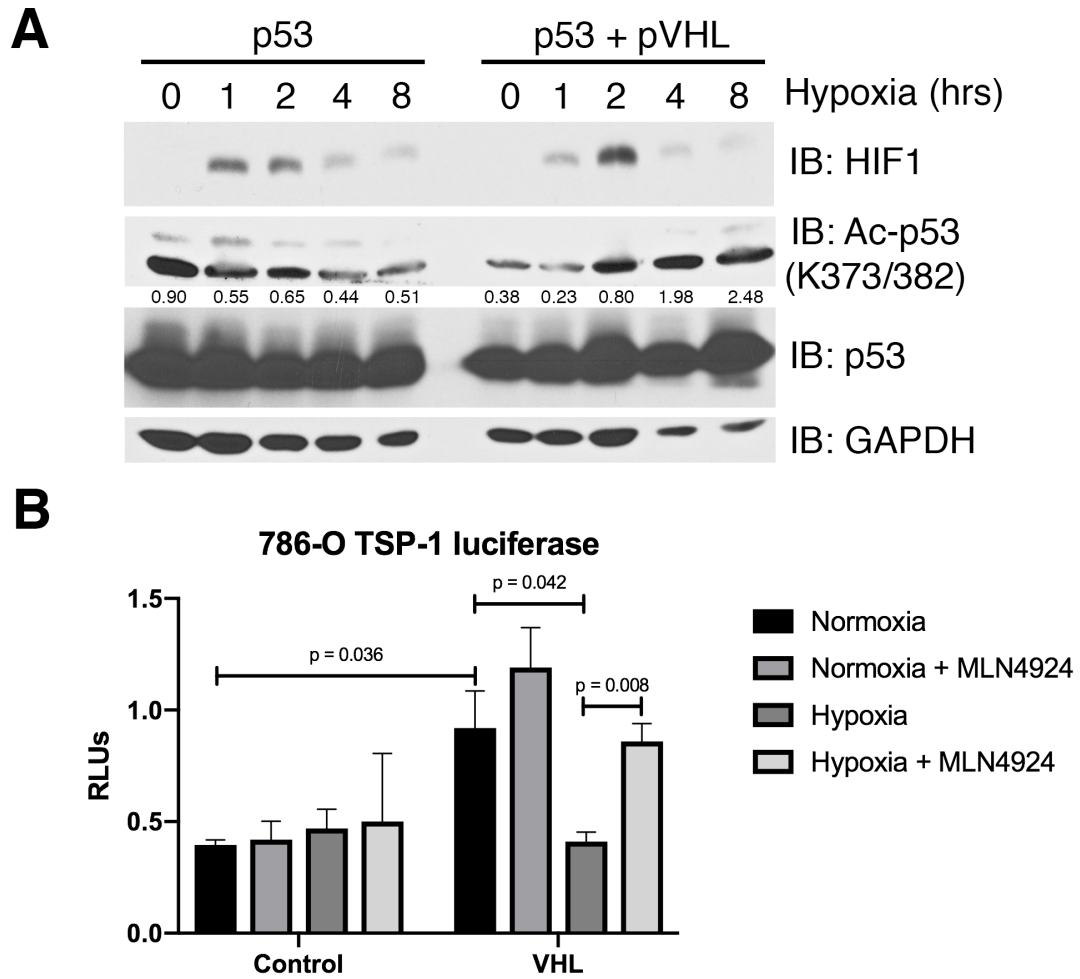


Figure 29. VHL increases the acetylation of p53 under hypoxia, leading to increased transcription of TSP-1. (A) Transient transfection of H1299 cells with p53 or p53 and VHL. Cells were subjected to hypoxia and lysed for analysis by SDS-PAGE and Western blotted for HIF1, Ac-p53 K373/382, p53, and GAPDH. (B) Luciferase assay for thrombospondin-1 in 786-O cells treated with MLN4924 and subjected to hypoxia. Means are plotted as relative luciferase units and calculated from three biological replicates. Error bars represent SEM. Statistics were calculated using an unpaired t test.

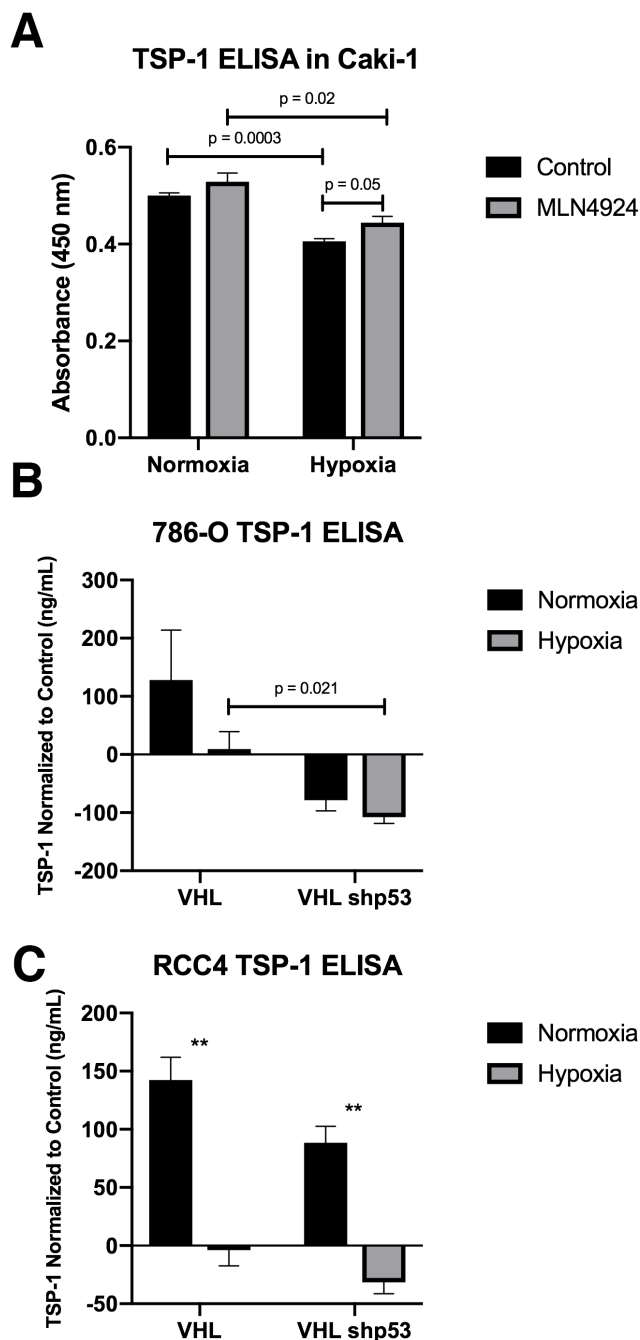


Figure 30. VHL increases the secretion of TSP-1 through p53 transactivation. (A) Enzyme-linked immunosorbent assay for TSP-1 using a 10% dilution of conditioned media from Caki-1 cells under hypoxia and/or MLN4924 treatment. Means from three biological replicates are plotted. Error bars represent SEM. Statistics were calculated using an unpaired t test. (B and C) Enzyme-linked immunosorbent assay for TSP-1 using a 10% dilution of conditioned media from 786-O or RCC4 cells with knockdown p53 under hypoxia. Means from three biological replicates are plotted. Error bars represent SEM. Statistics were calculated using an unpaired t test (\* $p < 0.05$ , \*\* $p < 0.01$ , \*\*\* $p < 0.001$ ).

#### ***4.7 p53 and TSP-1 inhibit Human Umbilical Vein Endothelial Cell network formation***

There are many factors that dictate whether or not angiogenesis will progress in a tumor. While it is evident that TSP-1 secretion is increased, we wanted to gain a more holistic view of how the p53/VHL pathway affects angiogenesis. To this end, H1299 cells were transfected with p53 and either WT VHL or K159R VHL and harvested conditioned media. Human Umbilical Vein Endothelial Cells (HUVECs) were then cultured in the conditioned media on growth factor reduced matrigel to monitor network formation as a readout for angiogenic potential. The addition of K159R VHL resulted in a significant decrease in network branch points compared to p53 alone (Figure 31A and 31B). Additionally, adding an antibody against TSP-1 to the conditioned media reversed this decrease resulting in a significant increase in network branch points. We next knocked down p53 in 786-O and RCC4 cells that had been previously transduced with VHL and harvested conditioned media under normoxia and hypoxia. Conditioned media from 786-O cells with knockdown p53 caused a statistically significant increase in network branch points compared to both normoxia and a vector control under normoxia or hypoxia (Figure 32A). Similar to results seen using conditioned media from H1299 cells, the addition of an antibody to TSP-1 caused an increase in branch point formation. Conditioned media from RCC4 cells induced angiogenesis in a similar pattern, with the exception that hypoxia alone was sufficient to cause an increase in branch point formation in the control cells (Figure 32B). Of note, 786-O cells are naturally null for HIF1 $\alpha$ , but maintain HIF2 $\alpha$ . RCC4 cells maintain both HIF1 $\alpha$  and HIF2 $\alpha$  expression, which may explain the more robust response to hypoxia in that cell line. All of these data are summarized in the schematic in Figure 33.

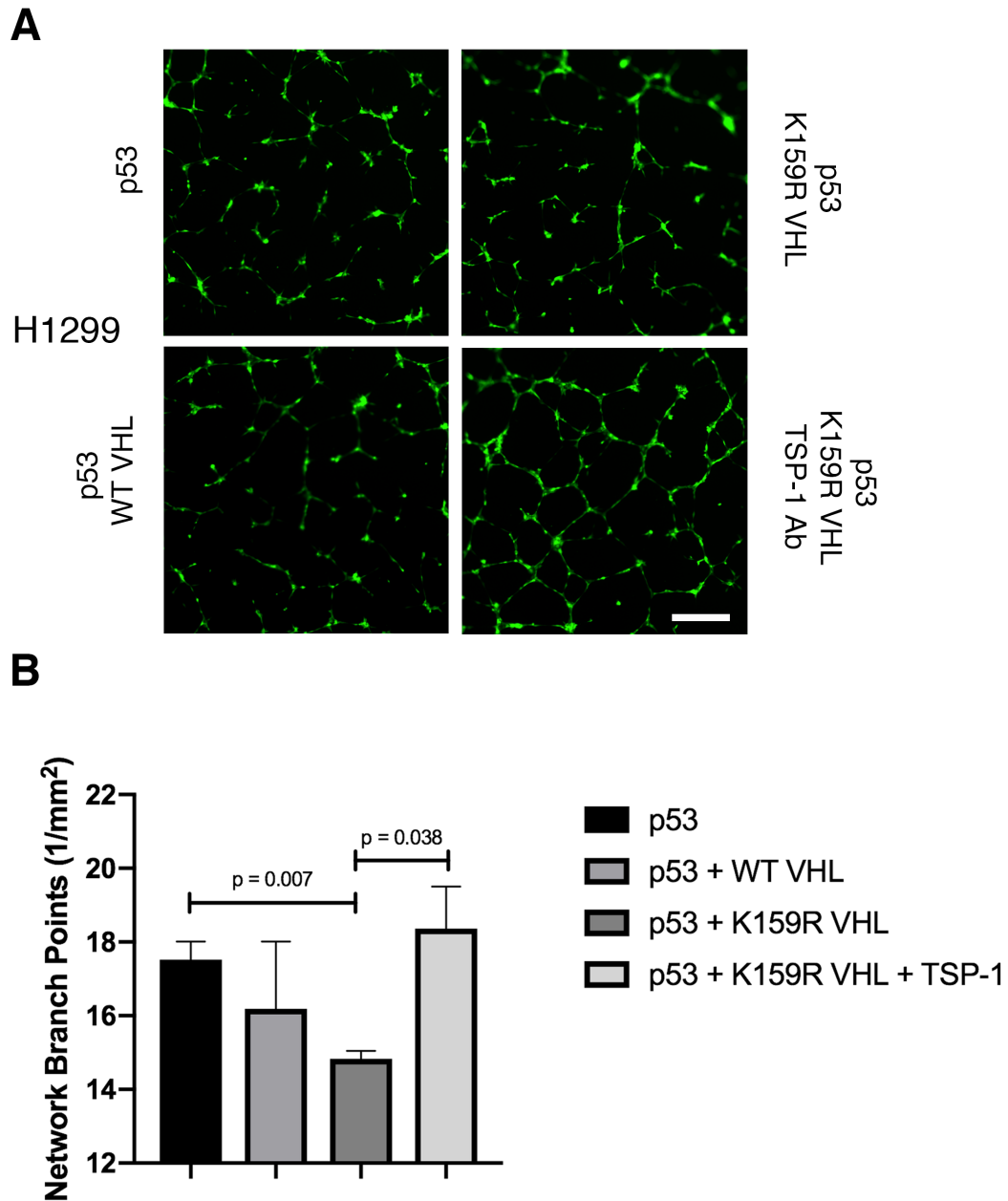


Figure 31. p53 and TSP-1 inhibit Human Umbilical Vein Endothelial Cell network formation through VHL. (A) Network formation assay using conditioned media from transiently transfected H1299 cells. (B) Network branch points were quantified and plotted as the mean of three biological replicates. Error bars represent SEM. Statistics were calculated with an unpaired t test.

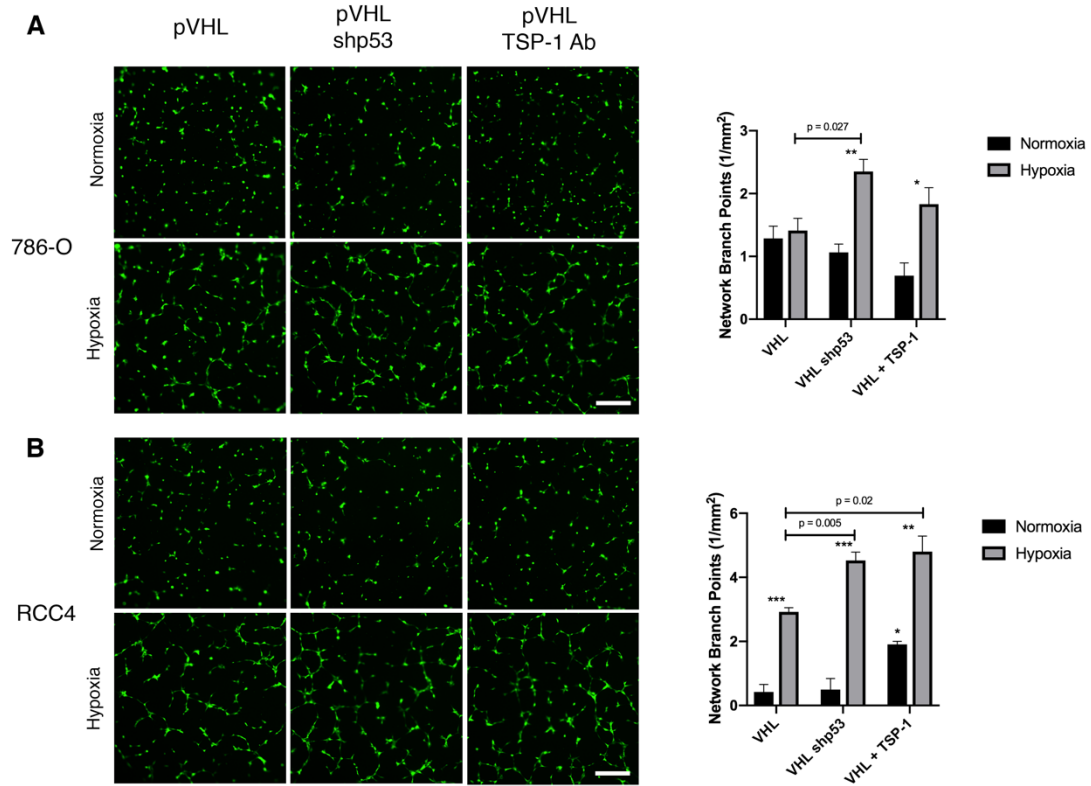


Figure 32. p53 and TSP-1 inhibit Human Umbilical Vein Endothelial Cell network formation. (A) Network formation assay using conditioned media from 786-O cells with VHL, VHL with knockdown p53, or VHL and an antibody against TSP-1 under normoxia or hypoxia. Network branch points were quantified and plotted as the mean of three biological replicates. Error bars represent SEM. Statistics were calculated with an unpaired t test (\* $p < 0.05$ , \*\* $p < 0.01$ , \*\*\* $p < 0.001$ ). (B) Network formation assay using conditioned media from RCC4 cells with VHL, VHL with knockdown p53, or VHL and an antibody against TSP-1 under normoxia or hypoxia. Network branch points were quantified and plotted as the mean of three biological replicates. Error bars represent SEM. Statistics were calculated with an unpaired t test (\* $p < 0.05$ , \*\* $p < 0.01$ , \*\*\* $p < 0.001$ ).

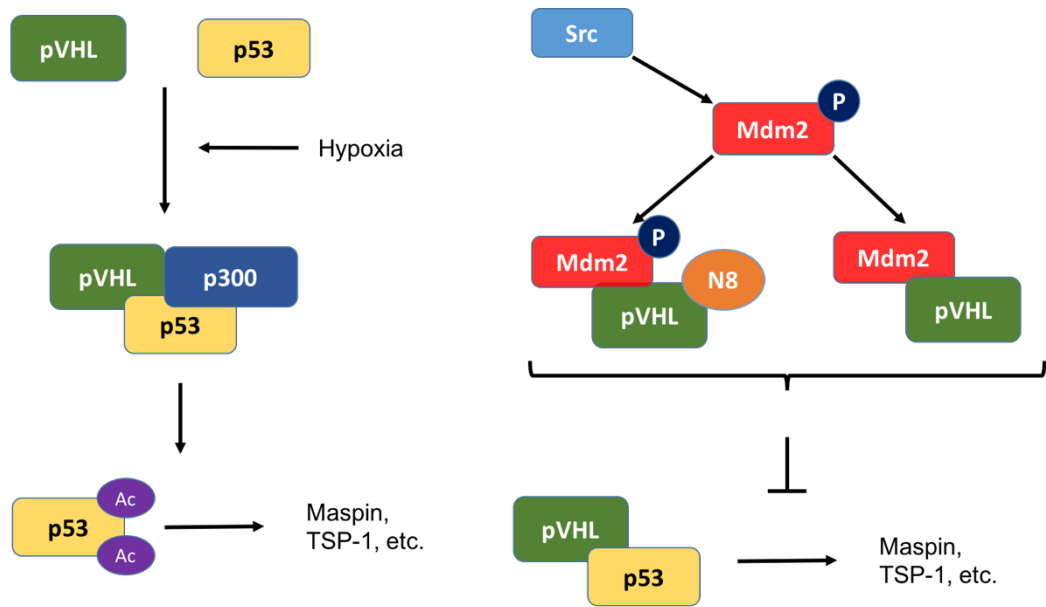


Figure 33. Schematic of the p53-VHL pathway being inhibited by Mdm2. Left: hypoxia results in VHL-p53-p300 complex to acetylate p53 for induction of antiangiogenic genes. Right: Src phosphorylation of Mdm2 results in pVHL neddylation and prevents the p53-VHL complex.

#### **4.8 Discussion**

In this study we describe how an antiangiogenic pathway involving p53 and VHL can be disrupted by the neddylation activity of Mdm2. These data highlight an evolving understanding of both VHL and Mdm2 in the control of angiogenesis. The role of VHL in regulating angiogenesis through HIFs has been well studied and the mechanisms governing that interaction are well understood [108-111, 128, 187]. The impact of Mdm2 on angiogenesis has been previously described, but there is a gap in our understanding of the mechanisms Mdm2 uses to promote angiogenesis. Mdm2 is able to regulate angiogenesis in many ways independent of HIF1 $\alpha$  and *VEGF* stabilization [188-191]. It is probable that there are unknown functions of Mdm2 that can promote angiogenesis in the right signaling environment.

Recent work in our lab suggests that Mdm2 is a driving force for early stage metastasis, which implicates Mdm2 in the vascularization of a tumor as it moves from dormancy to malignancy [101]. In that study, we showed that Mdm2 is a driving force for epithelial to mesenchymal transition as well as early stage metastasis (Figure 34). We have also recently shown that Mdm2 is converted to a neddylation enzyme in response to phosphorylation by the kinase c-Src. In response to various growth conditions c-Src phosphorylates Mdm2, which in turn neddylates p53 to render it stable but inactive [47]. c-Src governs many tumorigenic pathways, including angiogenesis [192]. This led us to examine the effect of the c-Src/Mdm2 pathway on angiogenesis inhibition regulated by p53. Mdm2 has been shown to block the transcriptional activity of p53 independent of its ubiquitination and neddylation functions in an indirect manner, so we decided to investigate coactivators of p53 as potential targets of Mdm2.



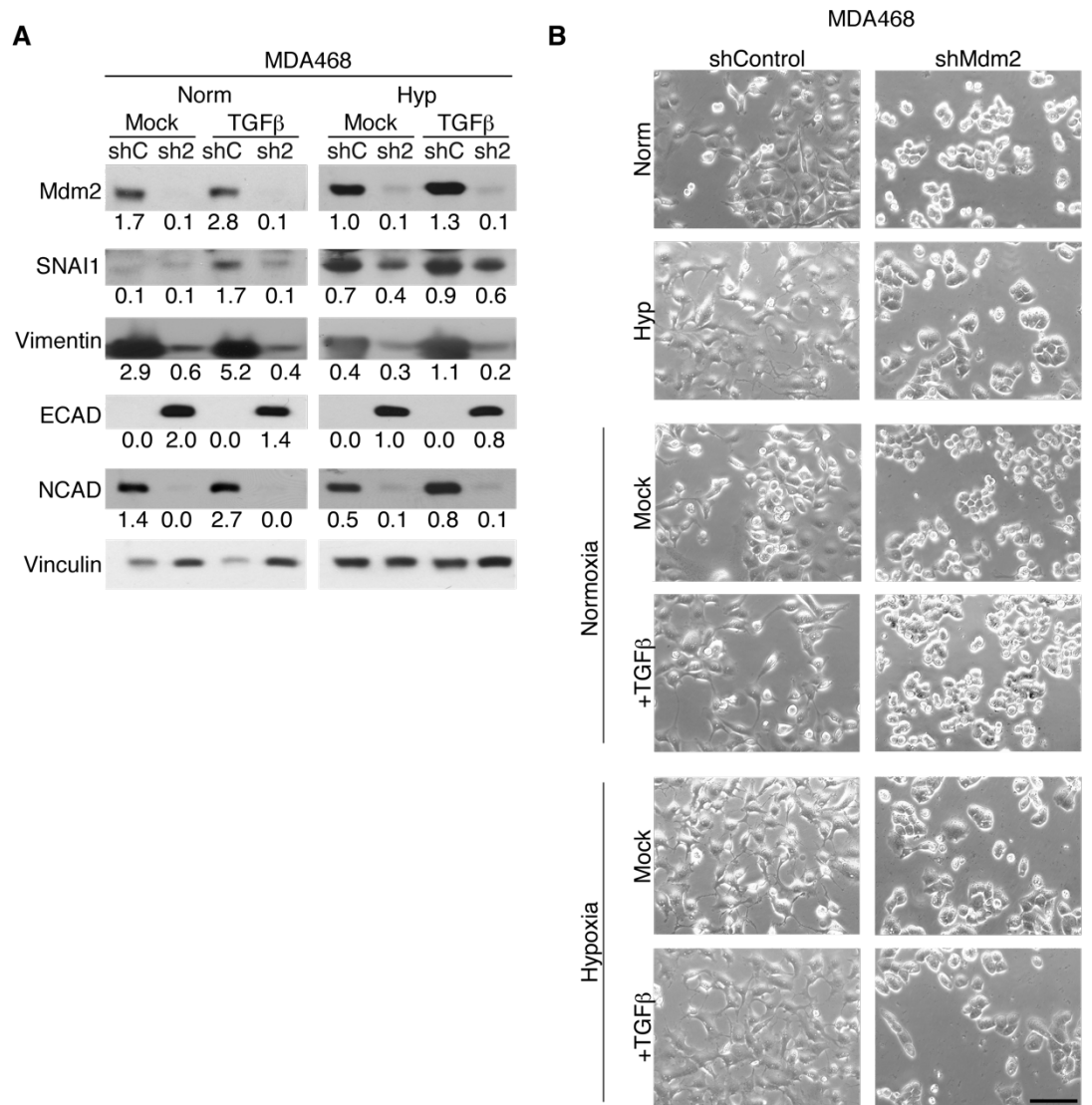


Figure 34. Mdm2 promotes epithelial to mesenchymal transition. (A) MDA-MD-468 cells were transduced with shMdm2 and treated with a control (Mock) or TGFβ in normoxia or hypoxia. Cells were lysed 48 hours after treatment and lysates were separated with SDS-PAGE followed by Western blotting for Mdm2, vinculin, E-cadherin (epithelial marker), and several mesenchymal markers including SNAI1, vimentin, and N-cadherin. (B) Microscopy images of MDA-MB-468 cells with shMdm2 and treated with a control (Mock) or TGFβ. Images were taken 48 hours after treatment and show that Mdm2 is required for a mesenchymal phenotype. Data published in [101]

The canonical function of Mdm2 is its regulation of p53 via ubiquitination and subsequent degradation. In response to DNA damage, p53 activates transcription of Mdm2 which then ubiquitinates p53 in an autoregulatory feedback loop [19, 20]. In addition to its regulation of p53, Mdm2 has many other interactions that impact various coactivators of p53 in order to indirectly impact p53 function [95, 148, 193-197]. The role of p53 in hypoxia has been extensively studied. While there are issues with interpreting the data due to variations in what different groups define as hypoxia (i.e., 0.01% O<sub>2</sub> vs 10% O<sub>2</sub>), the consensus is that HIF1 $\alpha$  binds to p53 in hypoxia and prevents the ubiquitination of p53 by Mdm2 [95, 167, 169, 198-202]. Due to the intricate web of feedback loops and interactions surrounding the p53/Mdm2/HIF/VHL signaling axes, it has been previously suggested that there is some interaction between VHL and Mdm2 that would be important for cancer signaling [173].

In addition to the previously reported genes involved in cell cycle arrest and apoptosis, we show in a subset of patients with clear cell renal cell carcinoma that VHL is important for the activation of p53 for a plethora of genes involved in angiogenesis. It is unclear at the moment if different VHL disease types will have different levels of p53 activation. However, the K159E VHL mutant used in our study was isolated from a patient with a Type 2C VHL disease mutation [126]. Importantly, Type 2C VHL disease does not develop kidney cancer [120]. The mutations for different VHL disease types are categorized based on the clinical presentation of the disease as opposed to the location of the mutation on the gene [118]. It will be interesting to see in the future how different VHL disease mutants respond to this signaling pathway. Every mutant of VHL that has been tested has a defect in binding to fibronectin. Neddylation of VHL is required for

binding to fibronectin, but VHL in complex with fibronectin is not neddylated [126]. It is possible that some disease causing mutations of VHL may actually protect against kidney cancer by changing the binding activity of the protein.

p53 is rarely mutated in renal cell carcinoma, but many target genes of p53 are downregulated in these tumors [182]. For many years, there were conflicting reports on the effect of p53 upregulation and subsequent Mdm2 upregulation in renal cell carcinomas. However, a consensus has recently emerged that shows a correlation between p53 upregulation and disease progression [reviewed in [203]]. This correlation suggests that there are other pathways involved in shutting down the wild type p53 signaling axis. VHL is a likely source of p53 dysregulation as it is highly mutated in renal cell carcinoma and is a known coactivator of p53 [173]. But that does not explain the incidence of tumors that maintain both wild type p53 and VHL. Renal cell carcinoma patients with high protein levels of both p53 and Mdm2 have the poorest overall survival [204]. This data, combined with our study, highlights the importance of Mdm2 signaling in renal cell carcinoma. We have presented one mechanism that Mdm2 uses to disrupt normal p53 signaling to promote angiogenesis and tumor progression. Additionally, Mdm2 is able to neddylate p53, which increases the stability of p53 but makes it inactive [47]. The neddylation of p53 by Mdm2 could be part of the reason why high levels of wild type p53 are associated with poor outcomes in ccRCC. It is likely that there are other mechanisms to guarantee redundancy in the function of Mdm2, and these are currently being explored. Our study provides the impetus for Mdm2 to be considered as a prognostic marker and potential therapeutic target in renal cell carcinomas.

## **5. Discussion and Future Directions**

### ***5.1 Contributions to the field and status of research***

The field of p53 research has been studying the interplay between different p53 family members since the characterization of p53 as a tumor suppressor. I elaborated on some of these interactions in the section on p53 family members, but until recently this field has been hindered by a mischaracterization of p53/p73 interaction. In 1999, Di Como et al. published findings that suggested mutant p53 (specifically R175H and R248W) could bind to p73 and inhibit the tumor suppressive functions of p73 [135]. This research led to the widespread belief that mutations of *TP53* confer a gain of function to the protein by functioning as an oncoprotein and inhibiting the other p53 family members, p63 and p73 [135, 136]. The field as a whole had accepted these findings as dogma, and research progressed to investigate mutant p53 gain of function mutations [205, 206]. However, reexamination of the original study by Di Como et al. led us to believe that there may be some crucial components missing.

The p53 protein is highly regulated at the posttranslational level and these modifications often dictate the function of p53 in specific contexts. Di Como et al. examined the p53/p73 interaction under conditions of transient transfection, but they did not investigate specific signaling pathways. Furthermore, the immunoprecipitations done in this study were performed 48 hours after transfection. The p53 apoptotic response can be very rapid, so it is also possible that they simply missed the window of time in which p53 and p73 interact. Our study of p53 family member interactions focused on specific signaling events that might cause wild type p53 to interact with p73. We analyzed various phosphorylation sites that are known to be important for apoptosis, and then examined

p53-p73 complex formation under cell signaling conditions when those sites would be phosphorylated. As expected, we identified a phosphorylation site that is important for p53/p73 interaction. When the kinase JNK is active, wild type p53 is phosphorylated at Thr81, resulting in a conformational change that is reflective of mutant p53 and is permissive of binding to p73. The interaction between wild type p53 and p73 results in a synergistic induction of apoptosis [1].

Our study helps to refine the dogma of p53 family member interactions. It provides the impetus to reexamine the implications of p53 family member interactions in different contexts, and corrects the long held belief in the field that wild type p53 does not interact with p73. The p53 pathway has been the focus of many therapeutic efforts to treat cancer, though this approach has seen little success to date. Our data add another level of information to the enigma of targeting p53, and provides a fresh take on this well-known pathway. In addition to the synergistic effect of wild type p53 and p73 working together, our lab is interested in other mechanisms of p53 activation and regulation of p53 activation at the posttranslational level. This work led us to examine a somewhat unique situation that is seen clinically in clear cell renal cell carcinomas.

In ccRCC, *TP53* mutations are very rare, but p53 target genes are still downregulated [182]. Another common feature of ccRCC is mutation of the VHL protein [122]. In 2006, Roe et al. showed that VHL could bind to p53 in response to DNA damage, resulting in the stabilization and transactivation of p53 [173]. They did not, however, examine the p53/VHL pathway in hypoxia, which is a major component of the highly vascularized RCC tumors. We showed that in response to hypoxia, VHL binds to p53 and activates transcription of anti-angiogenesis p53 target genes. Additionally, the

p53/VHL interaction is inhibited by neddylation of VHL at K159 by Mdm2. Mdm2 neddylates VHL in the region of the protein that is required for its binding with p53, effectively blocking this interaction. Clinical data from our study supports our hypothesis that mutations in the alpha domain of VHL, which binds directly to Mdm2, results in increased RNA expression of p53 target genes involved in inhibiting angiogenesis.

Due to the unique characteristics in the p53 pathway in ccRCC, many groups have attempted to identify methods to use the status of p53 and/or Mdm2 as a prognostic marker for these patients [203, 204]. These studies offer conflicting reports on the use of either p53 or Mdm2 as effective indicators of disease free progression or overall survival. We introduce another potential method of predicting outcomes in ccRCC through the utilization of immunohistochemistry for activated (Ac-K382) p53 and TSP-1 protein levels. This staining approach could be an effective method of determining the angiogenic potential of a tumor. Another aspect of the p53/VHL pathway that is still under investigation, is the involvement of the Mdm2 family member, MdmX.

MdmX is known to support the ubiquitin and nedd8 E3 ligase activity of Mdm2 [48, 207-209]. In another study from our lab, I showed that phosphorylation of Mdm2 by Src at Y281 and Y302 results in increased binding between Mdm2 and MdmX (Figure 35). Phosphorylation of Mdm2 at Y281 and Y302 by Src converts Mdm2 to a neddylating E3 ligase and MdmX is able to increase the efficiency of Mdm2-mediated neddylation of p53 [47, 48]. Following this logic, we presumed that MdmX may also increase the nedd8 E3 ligase activity of Mdm2 in order to neddylate VHL. Indeed, in a cell free assay using recombinant proteins, there was a marked increase in the neddylated form of VHL when MdmX was included in the reaction (Figure 36). These findings

support a potentially important function of Mdm2 and MdmX in the progression of ccRCC by inhibiting the VHL-p53 pathway.

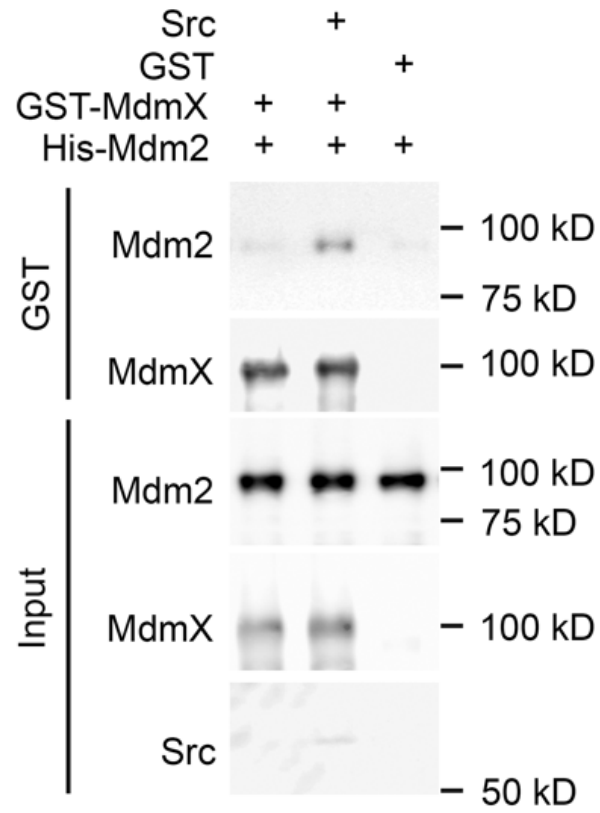


Figure 35. Phosphorylation of Mdm2 by Src increases binding to MdmX. GST-pulldown for MdmX using Src, GST, GST-MdmX, and His-Mdm2 and Western blotted for Mdm2, MdmX, and Src. Data published in [48]



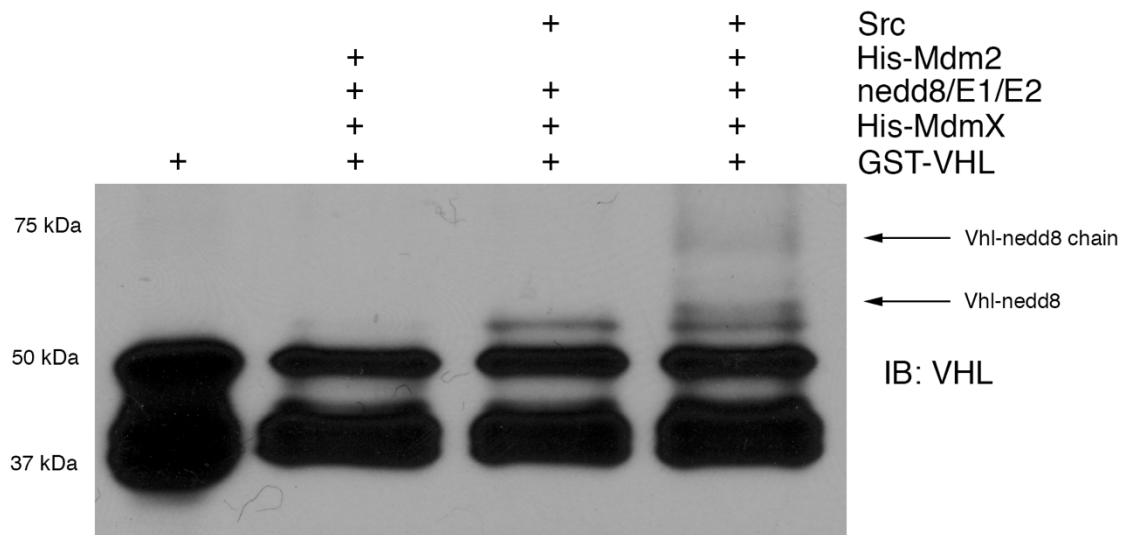


Figure 36. MdmX increases the Mdm2-mediated neddylation of VHL. Cell free neddylation assay using recombinant proteins. Reactions were separated by SDS-PAGE and analyzed by Western blot.

## ***5.2 Evidence for an Mdm2-VHL feedback loop***

While researching the effect of VHL mutations on various p53 pathway target genes, I noticed that mRNA for *MDM2* was increased in the alpha mutation group (Figure 37). Since p53 can activate transcription of *MDM2*, this is not entirely surprising. However, *MDM2* mRNA is ordinarily not altered significantly in tumors, even if there is a large change in corresponding protein abundance [39]. We decided to investigate the change in *MDM2* mRNA to determine if VHL was somehow altering the transcription of *MDM2*. To this end, we utilized a reporter gene for the P2 promoter of *MDM2*, which is the promoter responsible for transcription above basal levels. The luciferase activity of 786-O cells with or without VHL under normoxia and hypoxia was tested. *MDM2* is known to undergo a transient increase in transcription in response to hypoxia, and we saw this increase in our own data (Figure 38). We also saw that cells with VHL had a marked decrease in *MDM2* P2 promoter activity compared to the control. The impact of VHL on *MDM2* P2 promoter activity was somewhat surprising to us as other groups have postulated the existence of a VHL-Mdm2 feedback loop, but no data has been published on an Mdm2/VHL pathway.

To determine if steady state RNA levels were affected by VHL, RNA was harvested from 786-O cells with or without VHL subjected to normoxia or hypoxia and performed PCR following reverse transcription. We first used primers for the start site of *MDM2* and a site 639 bases downstream to amplify the gene. While the overall level of RNA was no different between all conditions tested, we did notice the appearance of a lower migrating band of *MDM2* RNA (Figure 39A).

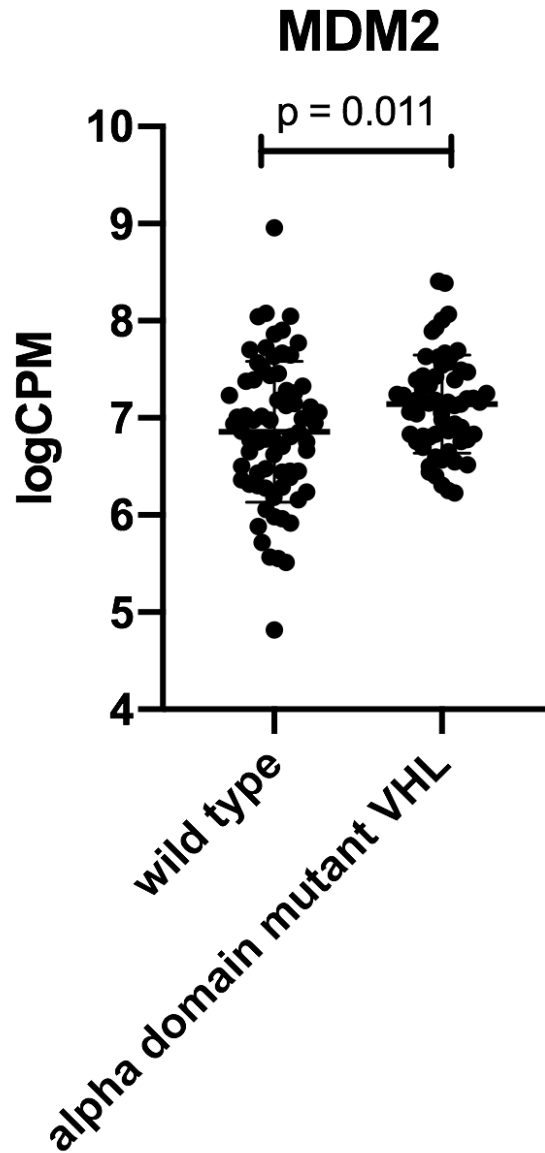


Figure 37. *MDM2* mRNA levels are affected by the mutation status of VHL. Log counts per million for *MDM2*. Only samples with wild-type p53 were included in the analysis. Error bars represent SEM. P values were calculated using an unpaired t test.

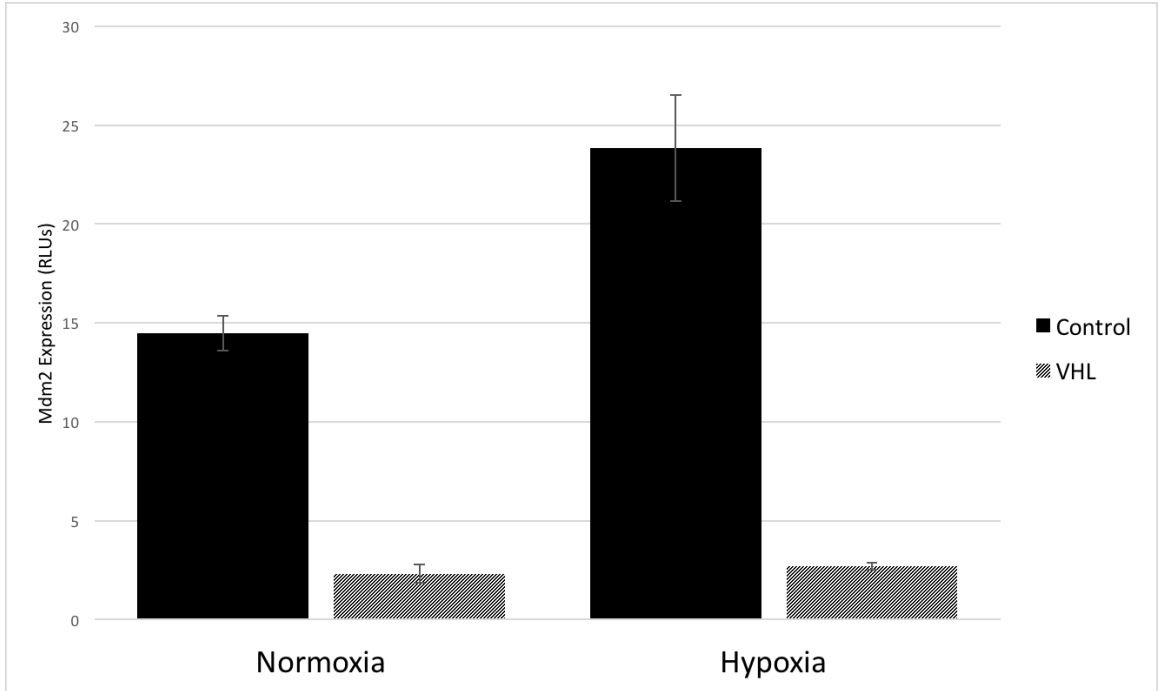


Figure 38. VHL inhibits the P2 promoter of Mdm2 in normoxia and hypoxia. Luciferase assay for the P2 promoter of Mdm2 in 786-O cells treated subjected to hypoxia. Means are plotted as relative luciferase units and calculated from three biological replicates. Error bars represent the standard deviation.

There are many alternatively spliced isoforms of *MDM2*, and these isoforms are especially active in cancer or in conditions of stress, such as hypoxia [210-212]. From the difference in size of the RNA bands combined with available information on different splice forms of *MDM2*, we were able to form a hypothesis as to which, if any, splice form this band corresponded to. We hypothesized that the lower migrating band represented isoform F of *MDM2* (Figure 39B and 39C). Of note, isoform F is almost identical to the full length version except for its loss of the p53 binding domain. To test our hypothesis, the same sample was amplified with primers directed at 174 bases downstream of the start site and 639 bases downstream of the start site. The primer directed at 174 bases downstream of the start site would not be able to bind to the lower band of *MDM2* if it corresponded to isoform F. Amplification with this primer set resulted in the loss of the lower band of *MDM2*, supporting our hypothesis for the induction of isoform F (Figure 39A and 39C). Since it is lacking most of the p53 binding domain, we believe that isoform F of Mdm2 will have a much different function than full length Mdm2. It is possible that isoform F functions primarily to regulate VHL, creating a feedback loop within this already complex system. While the region of Mdm2 that binds to VHL is currently unknown, the acidic domain of Mdm2 is a likely candidate. The three lysine residues within the  $\alpha$  domain of VHL, which is the region of VHL that binds to Mdm2, would create a positive charge on the protein in that region. This positive charge may be sufficient to attract the negatively charged acidic domain of Mdm2. If this is indeed the case, then the isoform F of Mdm2 should maintain its full binding capacity for VHL.

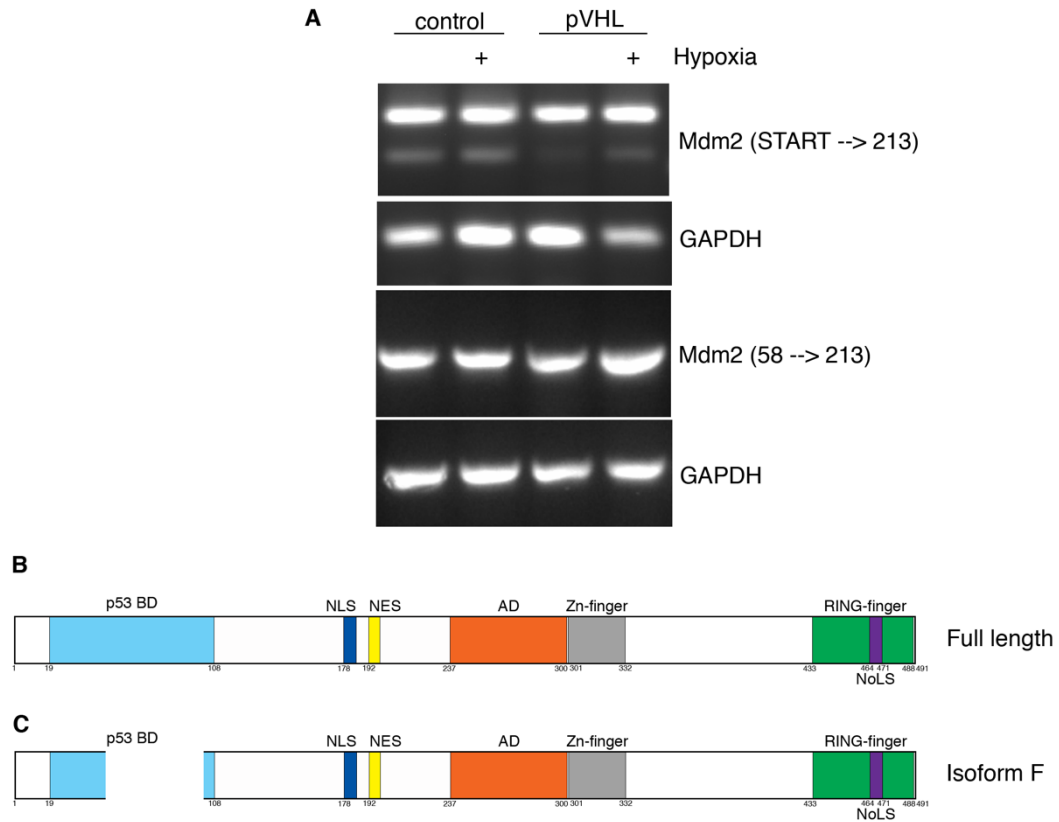


Figure 39. VHL and hypoxia cause the expression of an alternatively spliced isoform of MDM2. (A) RNA was harvested from 786-O cells with or without VHL in normoxia or hypoxia and PCR for Mdm2 was performed following reverse transcription. START →213 corresponds to a primer pair directed to the start site of MDM2 and another site 639 bases downstream. 58 → represents a primer pair directed to sites 174 and 639 base pairs downstream of the start site. (B) Map of the full length Mdm2 protein. (C) Map of the alternatively spliced isoform F Mdm2 protein.

In order to test if these changes at the RNA level corresponded to a change at the protein level, 786-O cells with or without VHL were subjected to a time course of normoxia or hypoxia and analyzed Mdm2 protein by Western blot. Mdm2 protein was less abundant with VHL present, and that a lower migrating band of Mdm2 protein began to appear as hypoxia progressed (Figure 40). The size of the lower migrating band corresponds to the previously determined apparent size of isoform F [210]. To determine if the pathway leading to the potential isoform F was indeed some sort of feedback loop, we examined the ability of Mdm2 to ubiquitinate VHL, as is the case with the autoregulatory feedback loop between Mdm2 and p53. H1299 cells were transiently transfected with Mdm2, VHL, Abl, and His-ubiquitin, followed by an Ni-NTA pulldown under denaturing conditions. Mdm2 is able to ubiquitinate VHL, and this ubiquitination increases with Abl transfection (Figure 41). Abl phosphorylates Mdm2 and activates its ubiquitin E3 ligase function.

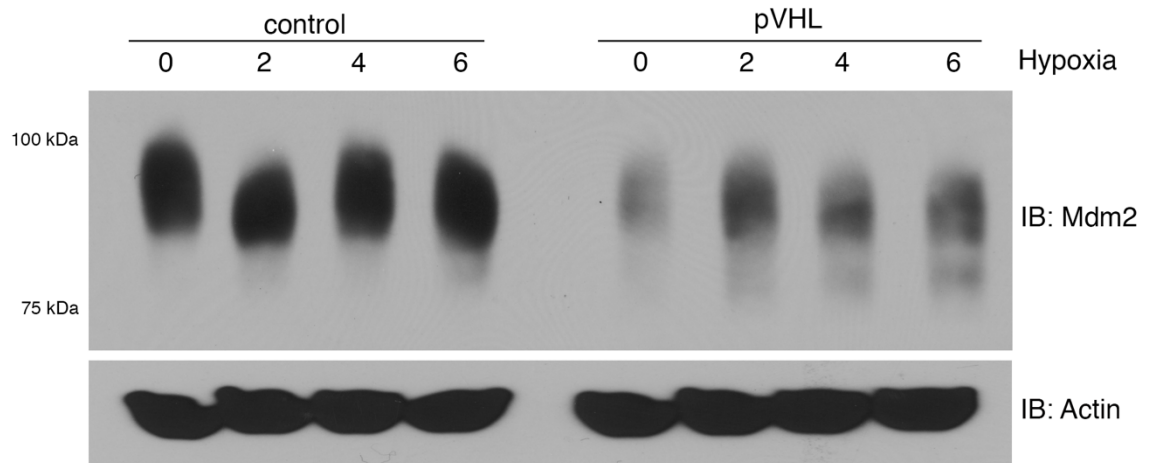


Figure 40. VHL and hypoxia cause the expression of an alternatively spliced isoform of Mdm2 protein. 786-O cells were subjected to a time course of normoxia or hypoxia and harvested at the indicated times. Lysates were separated with SDS-PAGE and Western blotted for Mdm2 and actin.



H1299

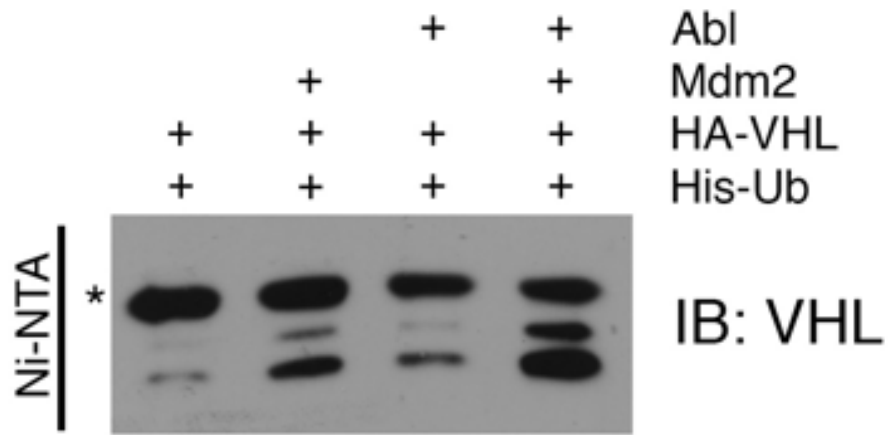


Figure 41. Mdm2 ubiquitinates VHL. Ni-NTA pulldown for His-nedd8 in H1299 cells in a transient transfection. Samples were separated with SDS-PAGE and analyzed by Western blot for VHL.

These data support an alternative feedback loop for Mdm2 and VHL. VHL both inhibits transcription of *MDM2* and increases the abundance of an alternative isoform of Mdm2 that is unable to bind to p53. Conversely, Mdm2 ubiquitinates and destabilizes VHL. The mechanisms governing the Mdm2-VHL feedback loop are still being investigated, as is the function of the Mdm2 isoform F. It is possible that isoform F of Mdm2 is responsible for regulation of VHL, as it has lost its ability to bind to p53. The inhibition of transcription from the P2 promoter of *MDM2* could be happening through the transcription factor Sp1. VHL has been shown to bind to Sp1, resulting in inhibition of the transcription of *VEGF* [213, 214]. The P2 promoter of *MDM2* contains a binding site for Sp1 [215], so it is possible that VHL is reducing the transcription of both *MDM2* and *VEGF* by binding Sp1 and sequestering it away from the promoters of these genes. A naturally occurring single nucleotide polymorphism (SNP) of the *MDM2* promoter (SNP309) has been shown to increase its affinity for Sp1, resulting in increased risk for cancer [215]. Interestingly, a second SNP at 285 of the *MDM2* promoter has been shown to reduce the risk of breast, ovarian, and endometrial cancer. SNP285 occurs in a region where an estrogen response element overlaps with the Sp1 binding site, suggesting that the Mdm2 pathway may have large implications in gender-specific tumor formation [216]. In addition to the inhibition of the P2 promoter of *MDM2* by VHL, we also believe that the P1 promoter is becoming active under hypoxia due to the fact that the lower migrating band of Mdm2 mRNA and protein was also seen in the vector control cells. PTEN has previously been shown to inhibit the P1 promoter of *MDM2* independently of p53 [217]. Recent data suggests that hypoxia is able to modulate the activity of PTEN, resulting in an increase in EMT [218, 219]. These data support our model where VHL

inhibits the P2 promoter of *MDM2*, and hypoxia activates the P1 promoter by alleviating the PTEN inhibition. Other groups have shown that elevated *MDM2* from the P1 promoter is correlated with poor prognosis in glioblastomas and pancreatic ductal adenocarcinomas [220, 221]. Our lab recently published that Mdm2 is able to promote EMT independently of p53, and it is possible that this function is due in part to elevated P1 transcription of *MDM2* [101]. As previously mentioned, the isoform of Mdm2 that we believe is being produced under hypoxia has lost the p53 binding domain, but maintains the region of binding to VHL and would also maintain the EMT promoting functions. The Mdm2-VHL alternative feedback loop is an ongoing project in the lab, but the current findings and hypothesis are presented in (Figure 42).

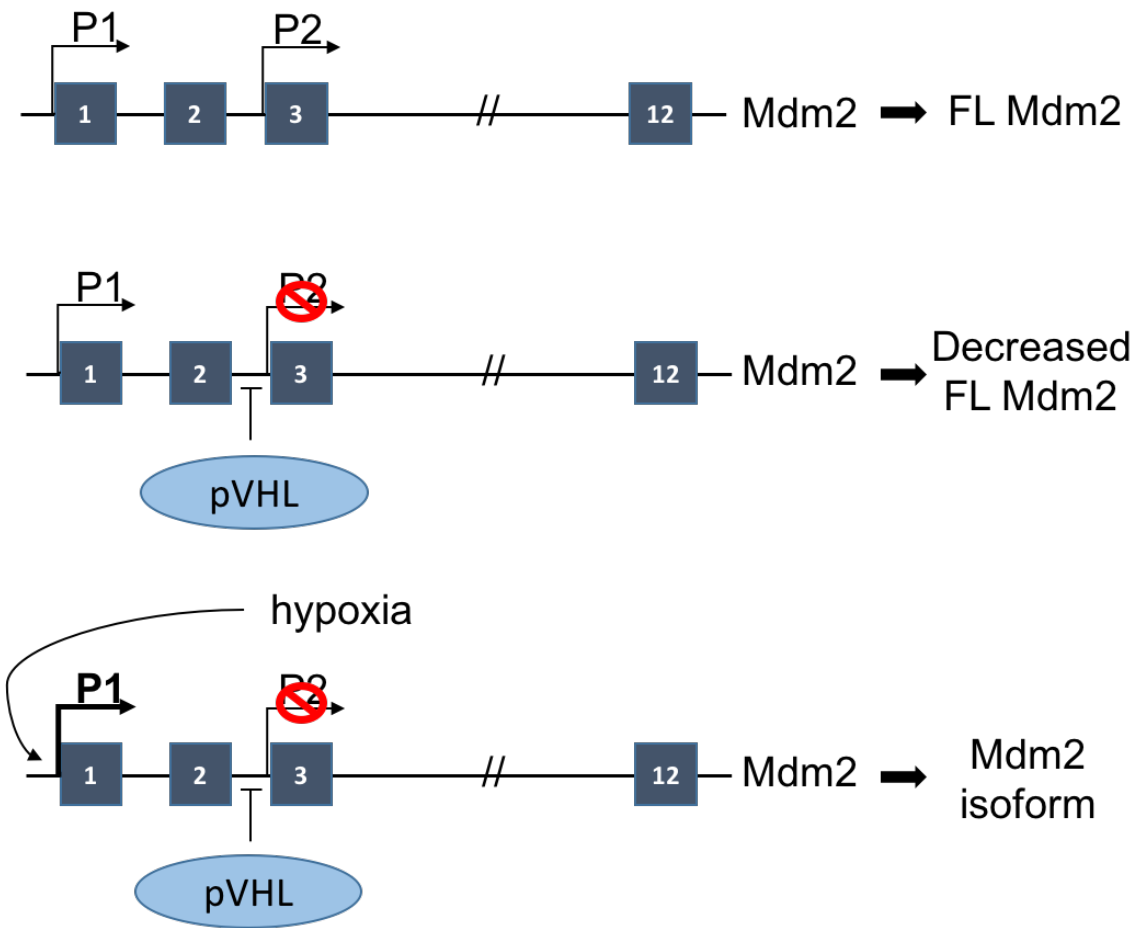


Figure 42. Schematic of the VHL-Mdm2 alternative feedback loop.

### ***5.3 Conclusions and summary of findings***

These data contribute new information on the activation of the tumor suppressor protein p53. Different signaling pathways and cell stresses have been examined for the role they play in activating downstream, p53-dependent responses. The work herein has provided an explanation for the inhibition of p53 pathway targets in tumors that have wild type p53, such as ccRCC. The p53-VHL pathway could also be active in tumors that maintain wild type p53, wild type VHL, and normal protein levels of Mdm2. My research highlights the importance of cell signaling conditions in tumors as opposed to the mutation status alone. The pathways presented in this dissertation can both suppress and promote tumor progression regardless of the mutation status of the tumor. Additionally, there are many intricate and overlapping methods of activating these pathways. For instance, while Mdm2 can neddylate VHL directly to inhibit its interaction with p53, Mdm2 is also able to neddylate p53 directly. Whether through neddylation of VHL or neddylation of p53, Mdm2 is able to block transcriptional activity of p53 through its neddylation function. Mdm2 is also able to ubiquitinate both p53 and p73, resulting in degradation of both. If p53 is protected from Mdm2-mediated ubiquitination by VHL or ATM, then Mdm2 is still able to inhibit the p53-p73 pathway by ubiquitinating p73. These redundant mechanisms are abundant in cell signaling.

Another overlapping mechanism of angiogenesis suppression occurs between VHL and p73. In normoxia, VHL destabilizes HIF1 $\alpha$  via ubiquitination which blocks its proangiogenic functions. In hypoxic conditions HIF1 $\alpha$  is relieved of VHL-mediated degradation and is free to activate transcription of proangiogenic target genes such as *VEGF*. However, under hypoxia p73 is able to bind to Mdm2 and recruit it to HIF1 $\alpha$  in

order to promote ubiquitination of HIF1 $\alpha$  [174]. The regulation of Mdm2 by p73 is in part due to the regulation of SIAH1, an E3 ubiquitin ligase for p73. In normoxia, SIAH1 ubiquitinates p73 and promotes its degradation. But in hypoxia, stabilized HIF1 $\alpha$  can bind to SIAH1 and inhibit its suppression of p73, which in turn allows p73 to promote ubiquitination of HIF1 $\alpha$  through Mdm2 [174, 222, 223]. The ubiquitination of HIF1 $\alpha$  via p73 stabilization is independent of VHL [222], highlighting the fact that there are multiple tumor suppressors tasked with overlapping, but independent, functions to keep tumors from growing. Of note, the experiment showing that p73 stabilization under hypoxia is independent of VHL was done transiently in H1299 cells with siRNA against VHL. Since transient transfection can also cause a DNA damage response, it is possible that VHL would be important for p73 stabilization in different signaling conditions or that stabilization of p73 by VHL would become more evident with a better knockdown of VHL.

In summary, I have shown new mechanisms of p53 activation by the tumor suppressor proteins p73 and VHL. In response to cell stress that activates the kinase JNK, p53 and p73 form a complex that has synergistic activity in promoting apoptosis. JNK is responsive to a wide variety of cell stress including growth factors, DNA damage, and oxidative stress caused by hypoxia. I have shown another mechanism of p53 activation in response to hypoxia that involves the tumor suppressor protein VHL. VHL binds to p53 and activates transcription of a variety of anti-angiogenic targets of p53 in order to suppress blood vessel formation and tumor growth. The VHL-p53 pathway has also been shown to be active in response to DNA damage [173]. Combined, our data show two unique and potentially overlapping mechanisms of p53 activation which can both be

potentially disrupted by the oncoprotein Mdm2 through ubiquitination or neddylation of p73 and VHL. Our work provides a fresh take on the oncogenic functions of Mdm2 and gives rationale for considering new approaches in targeting Mdm2 therapeutically.

## References

1. Wolf, E.R., et al., *Mutant and wild-type p53 form complexes with p73 upon phosphorylation by the kinase JNK*. *Sci Signal*, 2018. **11**(524).
2. Belyi, V.A., et al., *The origins and evolution of the p53 family of genes*. *Cold Spring Harb Perspect Biol*, 2010. **2**(6): p. a001198.
3. Flores, E.R., et al., *p63 and p73 are required for p53-dependent apoptosis in response to DNA damage*. *Nature*, 2002. **416**(6880): p. 560-4.
4. Moll, U.M. and N. Slade, *p63 and p73: roles in development and tumor formation*. *Mol Cancer Res*, 2004. **2**(7): p. 371-86.
5. Joerger, A.C., et al., *Structural evolution of p53, p63, and p73: implication for heterotetramer formation*. *Proc Natl Acad Sci U S A*, 2009. **106**(42): p. 17705-10.
6. Joerger, A.C. and A.R. Fersht, *The p53 Pathway: Origins, Inactivation in Cancer, and Emerging Therapeutic Approaches*. *Annu Rev Biochem*, 2016. **85**: p. 375-404.
7. Ariffin, H., et al., *Whole-genome sequencing analysis of phenotypic heterogeneity and anticipation in Li-Fraumeni cancer predisposition syndrome*. *Proc Natl Acad Sci U S A*, 2014. **111**(43): p. 15497-501.
8. Birch, J.M., et al., *Linkage studies in a Li-Fraumeni family with increased expression of p53 protein but no germline mutation in p53*. *Br J Cancer*, 1994. **70**(6): p. 1176-81.
9. Ryeom, S. and J. Folkman, *Role of endogenous angiogenesis inhibitors in Down syndrome*. *J Craniofac Surg*, 2009. **20 Suppl 1**: p. 595-6.
10. Sulak, M., et al., *TP53 copy number expansion is associated with the evolution of increased body size and an enhanced DNA damage response in elephants*. *Elife*, 2016. **5**.
11. Lane, D.P. and L.V. Crawford, *T antigen is bound to a host protein in SV40-transformed cells*. *Nature*, 1979. **278**(5701): p. 261-3.
12. Linzer, D.I. and A.J. Levine, *Characterization of a 54K dalton cellular SV40 tumor antigen present in SV40-transformed cells and uninfected embryonal carcinoma cells*. *Cell*, 1979. **17**(1): p. 43-52.
13. Michalovitz, D., O. Halevy, and M. Oren, *Conditional inhibition of transformation and of cell proliferation by a temperature-sensitive mutant of p53*. *Cell*, 1990. **62**(4): p. 671-80.
14. Momand, J., et al., *The mdm-2 oncogene product forms a complex with the p53 protein and inhibits p53-mediated transactivation*. *Cell*, 1992. **69**(7): p. 1237-45.
15. Barak, Y., et al., *mdm2 expression is induced by wild type p53 activity*. *EMBO J*, 1993. **12**(2): p. 461-8.
16. Barak, Y. and M. Oren, *Enhanced binding of a 95 kDa protein to p53 in cells undergoing p53-mediated growth arrest*. *EMBO J*, 1992. **11**(6): p. 2115-21.
17. Oliner, J.D., et al., *Oncoprotein MDM2 conceals the activation domain of tumour suppressor p53*. *Nature*, 1993. **362**(6423): p. 857-60.
18. White, D.E., et al., *Mouse double minute 2 associates with chromatin in the presence of p53 and is released to facilitate activation of transcription*. *Cancer Res*, 2006. **66**(7): p. 3463-70.



19. Haupt, Y., et al., *Mdm2 promotes the rapid degradation of p53*. Nature, 1997. **387**(6630): p. 296-9.
20. Kubbutat, M.H., S.N. Jones, and K.H. Vousden, *Regulation of p53 stability by Mdm2*. Nature, 1997. **387**(6630): p. 299-303.
21. Honda, R., H. Tanaka, and H. Yasuda, *Oncoprotein MDM2 is a ubiquitin ligase E3 for tumor suppressor p53*. FEBS Lett, 1997. **420**(1): p. 25-7.
22. Kussie, P.H., et al., *Structure of the MDM2 oncoprotein bound to the p53 tumor suppressor transactivation domain*. Science, 1996. **274**(5289): p. 948-53.
23. Lin, J., et al., *Several hydrophobic amino acids in the p53 amino-terminal domain are required for transcriptional activation, binding to mdm-2 and the adenovirus 5 E1B 55-kD protein*. Genes Dev, 1994. **8**(10): p. 1235-46.
24. Rippin, T.M., et al., *Recognition of DNA by p53 core domain and location of intermolecular contacts of cooperative binding*. J Mol Biol, 2002. **319**(2): p. 351-8.
25. Jain, A.K. and M.C. Barton, *Making sense of ubiquitin ligases that regulate p53*. Cancer Biol Ther, 2010. **10**(7): p. 665-72.
26. Khetchoumian, K., et al., *Loss of Trim24 (Tif1alpha) gene function confers oncogenic activity to retinoic acid receptor alpha*. Nat Genet, 2007. **39**(12): p. 1500-6.
27. Allton, K., et al., *Trim24 targets endogenous p53 for degradation*. Proc Natl Acad Sci U S A, 2009. **106**(28): p. 11612-6.
28. Sheng, Y., et al., *Molecular basis of Pirh2-mediated p53 ubiquitylation*. Nat Struct Mol Biol, 2008. **15**(12): p. 1334-42.
29. Chen, D., et al., *ARF-BP1/Mule is a critical mediator of the ARF tumor suppressor*. Cell, 2005. **121**(7): p. 1071-83.
30. Mayo, L.D. and D.B. Donner, *A phosphatidylinositol 3-kinase/Akt pathway promotes translocation of Mdm2 from the cytoplasm to the nucleus*. Proc Natl Acad Sci U S A, 2001. **98**(20): p. 11598-603.
31. Jackson, M.W., et al., *Hdm2 nuclear export, regulated by insulin-like growth factor-I/MAPK/p90Rsk signaling, mediates the transformation of human cells*. J Biol Chem, 2006. **281**(24): p. 16814-20.
32. Shinozaki, T., et al., *Functional role of Mdm2 phosphorylation by ATR in attenuation of p53 nuclear export*. Oncogene, 2003. **22**(55): p. 8870-80.
33. Pomerantz, J., et al., *The Ink4a tumor suppressor gene product, p19Arf, interacts with MDM2 and neutralizes MDM2's inhibition of p53*. Cell, 1998. **92**(6): p. 713-23.
34. Kamijo, T., et al., *Functional and physical interactions of the ARF tumor suppressor with p53 and Mdm2*. Proc Natl Acad Sci U S A, 1998. **95**(14): p. 8292-7.
35. Tao, W. and A.J. Levine, *P19(ARF) stabilizes p53 by blocking nucleocytoplasmic shuttling of Mdm2*. Proc Natl Acad Sci U S A, 1999. **96**(12): p. 6937-41.
36. Mayo, L.D., et al., *PTEN protects p53 from Mdm2 and sensitizes cancer cells to chemotherapy*. J Biol Chem, 2002. **277**(7): p. 5484-9.
37. Wu, X., et al., *The p53-mdm-2 autoregulatory feedback loop*. Genes Dev, 1993. **7**(7A): p. 1126-32.

38. Mendrysa, S.M. and M.E. Perry, *The p53 tumor suppressor protein does not regulate expression of its own inhibitor, MDM2, except under conditions of stress.* Mol Cell Biol, 2000. **20**(6): p. 2023-30.
39. Araki, S., et al., *TGF-beta1-induced expression of human Mdm2 correlates with late-stage metastatic breast cancer.* J Clin Invest, 2010. **120**(1): p. 290-302.
40. Phelps, M., et al., *p53-independent activation of the hdm2-P2 promoter through multiple transcription factor response elements results in elevated hdm2 expression in estrogen receptor alpha-positive breast cancer cells.* Cancer Res, 2003. **63**(10): p. 2616-23.
41. Zeng, Y., et al., *Inhibition of all-trans retinoic acid on MDM2 gene expression in astrocytoma cell line SHG-44.* Neurosci Bull, 2008. **24**(5): p. 297-304.
42. Chen, H., et al., *Vitamin D directly regulates Mdm2 gene expression in osteoblasts.* Biochem Biophys Res Commun, 2013. **430**(1): p. 370-4.
43. Brekman, A., et al., *A p53-independent role of Mdm2 in estrogen-mediated activation of breast cancer cell proliferation.* Breast Cancer Res, 2011. **13**(1): p. R3.
44. Qi, J.S., et al., *Regulation of the mdm2 oncogene by thyroid hormone receptor.* Mol Cell Biol, 1999. **19**(1): p. 864-72.
45. Kinyamu, H.K. and T.K. Archer, *Estrogen receptor-dependent proteasomal degradation of the glucocorticoid receptor is coupled to an increase in mdm2 protein expression.* Mol Cell Biol, 2003. **23**(16): p. 5867-81.
46. Xirodimas, D.P., et al., *Mdm2-mediated NEDD8 conjugation of p53 inhibits its transcriptional activity.* Cell, 2004. **118**(1): p. 83-97.
47. Batuello, C.N., et al., *Src phosphorylation converts Mdm2 from a ubiquitinating to a neddyating E3 ligase.* Proc Natl Acad Sci U S A, 2015. **112**(6): p. 1749-54.
48. Hauck, P.M., et al., *The fate of murine double minute X (MdmX) is dictated by distinct signaling pathways through murine double minute 2 (Mdm2).* Oncotarget, 2017. **8**(61): p. 104455-104466.
49. Huang, Q., et al., *MDMX acidic domain inhibits p53 DNA binding in vivo and regulates tumorigenesis.* Proc Natl Acad Sci U S A, 2018. **115**(15): p. E3368-E3377.
50. Bates, S. and K.H. Vousden, *p53 in signaling checkpoint arrest or apoptosis.* Curr Opin Genet Dev, 1996. **6**(1): p. 12-8.
51. de Stanchina, E., et al., *E1A signaling to p53 involves the p19(ARF) tumor suppressor.* Genes Dev, 1998. **12**(15): p. 2434-42.
52. Honda, R. and H. Yasuda, *Association of p19(ARF) with Mdm2 inhibits ubiquitin ligase activity of Mdm2 for tumor suppressor p53.* EMBO J, 1999. **18**(1): p. 22-7.
53. Wang, S.P., et al., *p53 controls cancer cell invasion by inducing the MDM2-mediated degradation of Slug.* Nat Cell Biol, 2009. **11**(6): p. 694-704.
54. Cahilly-Snyder, L., et al., *Molecular analysis and chromosomal mapping of amplified genes isolated from a transformed mouse 3T3 cell line.* Somat Cell Mol Genet, 1987. **13**(3): p. 235-44.
55. Fakharzadeh, S.S., S.P. Trusko, and D.L. George, *Tumorigenic potential associated with enhanced expression of a gene that is amplified in a mouse tumor cell line.* EMBO J, 1991. **10**(6): p. 1565-9.

56. Finlay, C.A., *The mdm-2 oncogene can overcome wild-type p53 suppression of transformed cell growth.* Mol Cell Biol, 1993. **13**(1): p. 301-6.
57. Seger, Y.R., et al., *Transformation of normal human cells in the absence of telomerase activation.* Cancer Cell, 2002. **2**(5): p. 401-13.
58. Jones, S.N., et al., *Rescue of embryonic lethality in Mdm2-deficient mice by absence of p53.* Nature, 1995. **378**(6553): p. 206-8.
59. Montes de Oca Luna, R., D.S. Wagner, and G. Lozano, *Rescue of early embryonic lethality in mdm2-deficient mice by deletion of p53.* Nature, 1995. **378**(6553): p. 203-6.
60. Leveillard, T., et al., *MDM2 expression during mouse embryogenesis and the requirement of p53.* Mech Dev, 1998. **74**(1-2): p. 189-93.
61. Jones, S.N., et al., *Overexpression of Mdm2 in mice reveals a p53-independent role for Mdm2 in tumorigenesis.* Proc Natl Acad Sci U S A, 1998. **95**(26): p. 15608-12.
62. Fu, W., et al., *MDM2 acts downstream of p53 as an E3 ligase to promote FOXO ubiquitination and degradation.* J Biol Chem, 2009. **284**(21): p. 13987-4000.
63. Hsieh, J.K., et al., *RB regulates the stability and the apoptotic function of p53 via MDM2.* Mol Cell, 1999. **3**(2): p. 181-93.
64. Loughran, O. and N.B. La Thangue, *Apoptotic and growth-promoting activity of E2F modulated by MDM2.* Mol Cell Biol, 2000. **20**(6): p. 2186-97.
65. Martin, K., et al., *Stimulation of E2F1/DP1 transcriptional activity by MDM2 oncoprotein.* Nature, 1995. **375**(6533): p. 691-4.
66. Tang, Y.A., et al., *MDM2 overexpression deregulates the transcriptional control of RB/E2F leading to DNA methyltransferase 3A overexpression in lung cancer.* Clin Cancer Res, 2012. **18**(16): p. 4325-33.
67. Wunderlich, M. and S.J. Berberich, *Mdm2 inhibition of p53 induces E2F1 transactivation via p21.* Oncogene, 2002. **21**(28): p. 4414-21.
68. Xiao, Z.X., et al., *Interaction between the retinoblastoma protein and the oncoprotein MDM2.* Nature, 1995. **375**(6533): p. 694-8.
69. Zhang, Z., et al., *Stabilization of E2F1 protein by MDM2 through the E2F1 ubiquitination pathway.* Oncogene, 2005. **24**(48): p. 7238-47.
70. Alt, J.R., et al., *Mdm2 binds to Nbs1 at sites of DNA damage and regulates double strand break repair.* J Biol Chem, 2005. **280**(19): p. 18771-81.
71. Bouska, A., et al., *Mdm2 promotes genetic instability and transformation independent of p53.* Mol Cell Biol, 2008. **28**(15): p. 4862-74.
72. Chen, X., et al., *MDM2 promotes invasion and metastasis in invasive ductal breast carcinoma by inducing matrix metalloproteinase-9.* PLoS One, 2013. **8**(11): p. e78794.
73. Rajabi, P., P. Karimian, and M. Heidarpour, *The relationship between MDM2 expression and tumor thickness and invasion in primary cutaneous malignant melanoma.* J Res Med Sci, 2012. **17**(5): p. 452-5.
74. Yang, J.Y., et al., *MDM2 promotes cell motility and invasiveness by regulating E-cadherin degradation.* Mol Cell Biol, 2006. **26**(19): p. 7269-82.
75. Zhang, X., et al., *Transcription factor NFAT1 activates the mdm2 oncogene independent of p53.* J Biol Chem, 2012. **287**(36): p. 30468-76.

76. Zhou, S., et al., *MDM2 regulates vascular endothelial growth factor mRNA stabilization in hypoxia*. Mol Cell Biol, 2011. **31**(24): p. 4928-37.
77. Dubs-Poterszman, M.C., B. Tocque, and B. Wasylyk, *MDM2 transformation in the absence of p53 and abrogation of the p107 G1 cell-cycle arrest*. Oncogene, 1995. **11**(11): p. 2445-9.
78. Lundgren, K., et al., *Targeted expression of MDM2 uncouples S phase from mitosis and inhibits mammary gland development independent of p53*. Genes Dev, 1997. **11**(6): p. 714-25.
79. Hanahan, D. and R.A. Weinberg, *Hallmarks of cancer: the next generation*. Cell, 2011. **144**(5): p. 646-74.
80. Levine, A.J. and M. Oren, *The first 30 years of p53: growing ever more complex*. Nat Rev Cancer, 2009. **9**(10): p. 749-58.
81. Momand, J. and G.P. Zambetti, *Analysis of the proportion of p53 bound to mdm-2 in cells with defined growth characteristics*. Oncogene, 1996. **12**(11): p. 2279-89.
82. Cao, L., et al., *Independent binding of the retinoblastoma protein and p107 to the transcription factor E2F*. Nature, 1992. **355**(6356): p. 176-9.
83. Hurford, R.K., Jr., et al., *pRB and p107/p130 are required for the regulated expression of different sets of E2F responsive genes*. Genes Dev, 1997. **11**(11): p. 1447-63.
84. Takahashi, Y., J.B. Rayman, and B.D. Dynlacht, *Analysis of promoter binding by the E2F and pRB families in vivo: distinct E2F proteins mediate activation and repression*. Genes Dev, 2000. **14**(7): p. 804-16.
85. Ginsberg, D., et al., *E2F-4, a new member of the E2F transcription factor family, interacts with p107*. Genes Dev, 1994. **8**(22): p. 2665-79.
86. O'Connor, D.J., et al., *Physical and functional interactions between p53 and cell cycle co-operating transcription factors, E2F1 and DP1*. EMBO J, 1995. **14**(24): p. 6184-92.
87. Jin, Y., et al., *MDM2 promotes p21waf1/cip1 proteasomal turnover independently of ubiquitylation*. EMBO J, 2003. **22**(23): p. 6365-77.
88. Wunderlich, M., et al., *MdmX represses E2F1 transactivation*. Cell Cycle, 2004. **3**(4): p. 472-8.
89. Cress, W.D. and J.R. Nevins, *Interacting domains of E2F1, DP1, and the adenovirus E4 protein*. J Virol, 1994. **68**(7): p. 4213-9.
90. Du, W., et al., *Rapamycin inhibits IGF-1-mediated up-regulation of MDM2 and sensitizes cancer cells to chemotherapy*. PLoS One, 2013. **8**(4): p. e63179.
91. Slack, A., et al., *The p53 regulatory gene MDM2 is a direct transcriptional target of MYCN in neuroblastoma*. Proc Natl Acad Sci U S A, 2005. **102**(3): p. 731-6.
92. Zhang, D.H., et al., *Expression and significance of MMP-9 and MDM2 in the oncogenesis of lung cancer in rats*. Asian Pac J Trop Med, 2014. **7**(7): p. 585-8.
93. Shi, W.D., et al., *Identification of liver metastasis-related genes in a novel human pancreatic carcinoma cell model by microarray analysis*. Cancer Lett, 2009. **283**(1): p. 84-91.
94. Van den Steen, P.E., et al., *Biochemistry and molecular biology of gelatinase B or matrix metalloproteinase-9 (MMP-9)*. Crit Rev Biochem Mol Biol, 2002. **37**(6): p. 375-536.

95. Chen, D., et al., *Direct interactions between HIF-1 alpha and Mdm2 modulate p53 function*. J Biol Chem, 2003. **278**(16): p. 13595-8.
96. Joshi, S., A.R. Singh, and D.L. Durden, *MDM2 regulates hypoxic hypoxia-inducible factor 1alpha stability in an E3 ligase, proteasome, and PTEN-phosphatidylinositol 3-kinase-AKT-dependent manner*. J Biol Chem, 2014. **289**(33): p. 22785-97.
97. Nieminen, A.L., et al., *Mdm2 and HIF-1alpha interaction in tumor cells during hypoxia*. J Cell Physiol, 2005. **204**(2): p. 364-9.
98. Bardos, J.I., N.M. Chau, and M. Ashcroft, *Growth factor-mediated induction of HDM2 positively regulates hypoxia-inducible factor 1alpha expression*. Mol Cell Biol, 2004. **24**(7): p. 2905-14.
99. Carroll, V.A. and M. Ashcroft, *Regulation of angiogenic factors by HDM2 in renal cell carcinoma*. Cancer Res, 2008. **68**(2): p. 545-52.
100. LaRusch, G.A., et al., *Nutlin3 blocks vascular endothelial growth factor induction by preventing the interaction between hypoxia inducible factor 1alpha and Hdm2*. Cancer Res, 2007. **67**(2): p. 450-4.
101. Hauck, P.M., et al., *Early-Stage Metastasis Requires Mdm2 and Not p53 Gain of Function*. Mol Cancer Res, 2017. **15**(11): p. 1598-1607.
102. Gao, C., et al., *Context-dependent roles of MDMX (MDM4) and MDM2 in breast cancer proliferation and circulating tumor cells*. Breast Cancer Res, 2019. **21**(1): p. 5.
103. Semenza, G.L., *Oxygen sensing, hypoxia-inducible factors, and disease pathophysiology*. Annu Rev Pathol, 2014. **9**: p. 47-71.
104. Makino, Y., et al., *Inhibitory PAS domain protein (IPAS) is a hypoxia-inducible splicing variant of the hypoxia-inducible factor-3alpha locus*. J Biol Chem, 2002. **277**(36): p. 32405-8.
105. Heikkila, M., et al., *Roles of the human hypoxia-inducible factor (HIF)-3alpha variants in the hypoxia response*. Cell Mol Life Sci, 2011. **68**(23): p. 3885-901.
106. Kumar, H., et al., *Differential regulation of HIF-3alpha in LPS-induced BV-2 microglial cells: Comparison and characterization with HIF-1alpha*. Brain Res, 2015. **1610**: p. 33-41.
107. Koh, M.Y. and G. Powis, *Passing the baton: the HIF switch*. Trends Biochem Sci, 2012. **37**(9): p. 364-72.
108. Ivan, M., et al., *HIFalpha targeted for VHL-mediated destruction by proline hydroxylation: implications for O2 sensing*. Science, 2001. **292**(5516): p. 464-8.
109. Jaakkola, P., et al., *Targeting of HIF-alpha to the von Hippel-Lindau ubiquitylation complex by O2-regulated prolyl hydroxylation*. Science, 2001. **292**(5516): p. 468-72.
110. Lonergan, K.M., et al., *Regulation of hypoxia-inducible mRNAs by the von Hippel-Lindau tumor suppressor protein requires binding to complexes containing elongins B/C and Cul2*. Mol Cell Biol, 1998. **18**(2): p. 732-41.
111. Ohh, M., et al., *Ubiquitination of hypoxia-inducible factor requires direct binding to the beta-domain of the von Hippel-Lindau protein*. Nat Cell Biol, 2000. **2**(7): p. 423-7.

112. Leonardi, E., A. Murgia, and S.C. Tosatto, *Adding structural information to the von Hippel-Lindau (VHL) tumor suppressor interaction network*. FEBS Lett, 2009. **583**(22): p. 3704-10.
113. Holmquist-Mengelbier, L., et al., *Recruitment of HIF-1alpha and HIF-2alpha to common target genes is differentially regulated in neuroblastoma: HIF-2alpha promotes an aggressive phenotype*. Cancer Cell, 2006. **10**(5): p. 413-23.
114. Koh, M.Y., et al., *The hypoxia-associated factor switches cells from HIF-1alpha to HIF-2alpha-dependent signaling promoting stem cell characteristics, aggressive tumor growth and invasion*. Cancer Res, 2011. **71**(11): p. 4015-27.
115. Semenza, G.L. and G.L. Wang, *A nuclear factor induced by hypoxia via de novo protein synthesis binds to the human erythropoietin gene enhancer at a site required for transcriptional activation*. Mol Cell Biol, 1992. **12**(12): p. 5447-54.
116. Ziello, J.E., I.S. Jovin, and Y. Huang, *Hypoxia-Inducible Factor (HIF)-1 regulatory pathway and its potential for therapeutic intervention in malignancy and ischemia*. Yale J Biol Med, 2007. **80**(2): p. 51-60.
117. Beroukhi, R., et al., *Patterns of gene expression and copy-number alterations in von-hippel lindau disease-associated and sporadic clear cell carcinoma of the kidney*. Cancer Res, 2009. **69**(11): p. 4674-81.
118. Kaelin, W.G., *Von Hippel-Lindau disease*. Annu Rev Pathol, 2007. **2**: p. 145-73.
119. Kaelin, W.G., Jr., *Molecular basis of the VHL hereditary cancer syndrome*. Nat Rev Cancer, 2002. **2**(9): p. 673-82.
120. Zbar, B., et al., *Germline mutations in the Von Hippel-Lindau disease (VHL) gene in families from North America, Europe, and Japan*. Hum Mutat, 1996. **8**(4): p. 348-57.
121. van Leeuwen, R.S., et al., *Von Hippel-Lindau Syndrome*, in *GeneReviews*(R), M.P. Adam, et al., Editors. 1993: Seattle (WA).
122. Kim, W.Y. and W.G. Kaelin, *Role of VHL gene mutation in human cancer*. J Clin Oncol, 2004. **22**(24): p. 4991-5004.
123. Cockman, M.E., et al., *Hypoxia inducible factor-alpha binding and ubiquitylation by the von Hippel-Lindau tumor suppressor protein*. J Biol Chem, 2000. **275**(33): p. 25733-41.
124. Hacker, K.E., C.M. Lee, and W.K. Rathmell, *VHL type 2B mutations retain VBC complex form and function*. PLoS One, 2008. **3**(11): p. e3801.
125. Ding, Z., et al., *Genetic and pharmacological strategies to refunctionalize the von Hippel Lindau R167Q mutant protein*. Cancer Res, 2014. **74**(11): p. 3127-36.
126. Stickle, N.H., et al., *pVHL modification by NEDD8 is required for fibronectin matrix assembly and suppression of tumor development*. Mol Cell Biol, 2004. **24**(8): p. 3251-61.
127. Iliopoulos, O., et al., *Tumour suppression by the human von Hippel-Lindau gene product*. Nat Med, 1995. **1**(8): p. 822-6.
128. Ivan, M. and W.G. Kaelin, Jr., *The von Hippel-Lindau tumor suppressor protein*. Curr Opin Genet Dev, 2001. **11**(1): p. 27-34.
129. Maehama, T. and J.E. Dixon, *PTEN: a tumour suppressor that functions as a phospholipid phosphatase*. Trends Cell Biol, 1999. **9**(4): p. 125-8.

130. Lehman, J.A., et al., *Induction of apoptotic genes by a p73-phosphatase and tensin homolog (p73-PTEN) protein complex in response to genotoxic stress*. J Biol Chem, 2011. **286**(42): p. 36631-40.
131. Roy, A., A. Kucukural, and Y. Zhang, *I-TASSER: a unified platform for automated protein structure and function prediction*. Nat Protoc, 2010. **5**(4): p. 725-38.
132. Yang, J., et al., *The I-TASSER Suite: protein structure and function prediction*. Nat Methods, 2015. **12**(1): p. 7-8.
133. Zhang, Y., *I-TASSER server for protein 3D structure prediction*. BMC Bioinformatics, 2008. **9**: p. 40.
134. McNicholas, S., et al., *Presenting your structures: the CCP4mg molecular-graphics software*. Acta Crystallogr D Biol Crystallogr, 2011. **67**(Pt 4): p. 386-94.
135. Di Como, C.J., C. Gaiddon, and C. Prives, *p73 function is inhibited by tumor-derived p53 mutants in mammalian cells*. Mol Cell Biol, 1999. **19**(2): p. 1438-49.
136. Gaiddon, C., et al., *A subset of tumor-derived mutant forms of p53 down-regulate p63 and p73 through a direct interaction with the p53 core domain*. Mol Cell Biol, 2001. **21**(5): p. 1874-87.
137. Flores, E.R., et al., *Tumor predisposition in mice mutant for p63 and p73: evidence for broader tumor suppressor functions for the p53 family*. Cancer Cell, 2005. **7**(4): p. 363-73.
138. Davison, T.S., et al., *p73 and p63 are homotetramers capable of weak heterotypic interactions with each other but not with p53*. J Biol Chem, 1999. **274**(26): p. 18709-14.
139. Zhu, J., et al., *Differential regulation of cellular target genes by p53 devoid of the PXXP motifs with impaired apoptotic activity*. Oncogene, 1999. **18**(12): p. 2149-55.
140. Zhu, J., et al., *Definition of the p53 functional domains necessary for inducing apoptosis*. J Biol Chem, 2000. **275**(51): p. 39927-34.
141. Ruaro, E.M., et al., *A proline-rich motif in p53 is required for transactivation-independent growth arrest as induced by Gas1*. Proc Natl Acad Sci U S A, 1997. **94**(9): p. 4675-80.
142. Venot, C., et al., *The requirement for the p53 proline-rich functional domain for mediation of apoptosis is correlated with specific PIG3 gene transactivation and with transcriptional repression*. EMBO J, 1998. **17**(16): p. 4668-79.
143. Zhu, J., et al., *Identification of a novel p53 functional domain that is necessary for mediating apoptosis*. J Biol Chem, 1998. **273**(21): p. 13030-6.
144. D'Orazi, G., et al., *Homeodomain-interacting protein kinase-2 phosphorylates p53 at Ser 46 and mediates apoptosis*. Nat Cell Biol, 2002. **4**(1): p. 11-9.
145. Fuchs, S.Y., et al., *MEKK1/JNK signaling stabilizes and activates p53*. Proc Natl Acad Sci U S A, 1998. **95**(18): p. 10541-6.
146. Hofmann, T.G., et al., *Regulation of p53 activity by its interaction with homeodomain-interacting protein kinase-2*. Nat Cell Biol, 2002. **4**(1): p. 1-10.
147. Mayo, L.D., et al., *Phosphorylation of human p53 at serine 46 determines promoter selection and whether apoptosis is attenuated or amplified*. J Biol Chem, 2005. **280**(28): p. 25953-9.

148. Wang, Y., K.M. Debatin, and H. Hug, *HIPK2 overexpression leads to stabilization of p53 protein and increased p53 transcriptional activity by decreasing Mdm2 protein levels*. BMC Mol Biol, 2001. **2**: p. 8.
149. Bulavin, D.V., et al., *Phosphorylation of human p53 by p38 kinase coordinates N-terminal phosphorylation and apoptosis in response to UV radiation*. EMBO J, 1999. **18**(23): p. 6845-54.
150. Saito, S., et al., *ATM mediates phosphorylation at multiple p53 sites, including Ser(46), in response to ionizing radiation*. J Biol Chem, 2002. **277**(15): p. 12491-4.
151. Buschmann, T., et al., *Jun NH2-terminal kinase phosphorylation of p53 on Thr-81 is important for p53 stabilization and transcriptional activities in response to stress*. Mol Cell Biol, 2001. **21**(8): p. 2743-54.
152. Berger, M., et al., *Mutations in proline 82 of p53 impair its activation by Pin1 and Chk2 in response to DNA damage*. Mol Cell Biol, 2005. **25**(13): p. 5380-8.
153. Baptiste, N., et al., *The proline-rich domain of p53 is required for cooperation with anti-neoplastic agents to promote apoptosis of tumor cells*. Oncogene, 2002. **21**(1): p. 9-21.
154. Walker, K.K. and A.J. Levine, *Identification of a novel p53 functional domain that is necessary for efficient growth suppression*. Proc Natl Acad Sci U S A, 1996. **93**(26): p. 15335-40.
155. Stambolic, V., et al., *Regulation of PTEN transcription by p53*. Mol Cell, 2001. **8**(2): p. 317-25.
156. Eitel, J.A., et al., *PTEN and p53 are required for hypoxia induced expression of maspin in glioblastoma cells*. Cell Cycle, 2009. **8**(6): p. 896-901.
157. Li, A.G., et al., *Mechanistic insights into maintenance of high p53 acetylation by PTEN*. Mol Cell, 2006. **23**(4): p. 575-87.
158. Talos, F., et al., *p73 suppresses polyploidy and aneuploidy in the absence of functional p53*. Mol Cell, 2007. **27**(4): p. 647-59.
159. Di Cristofano, A., et al., *Pten is essential for embryonic development and tumour suppression*. Nat Genet, 1998. **19**(4): p. 348-55.
160. Suzuki, A., et al., *High cancer susceptibility and embryonic lethality associated with mutation of the PTEN tumor suppressor gene in mice*. Curr Biol, 1998. **8**(21): p. 1169-78.
161. Davis, R.J., *Signal transduction by the c-Jun N-terminal kinase*. Biochem Soc Symp, 1999. **64**: p. 1-12.
162. Jones, E.V., M.J. Dickman, and A.J. Whitmarsh, *Regulation of p73-mediated apoptosis by c-Jun N-terminal kinase*. Biochem J, 2007. **405**(3): p. 617-23.
163. Gebel, J., et al., *Mechanism of TAp73 inhibition by DeltaNp63 and structural basis of p63/p73 hetero-tetramerization*. Cell Death Differ, 2016. **23**(12): p. 1930-1940.
164. Kehrloesser, S., et al., *Intrinsic aggregation propensity of the p63 and p73 TI domains correlates with p53R175H interaction and suggests further significance of aggregation events in the p53 family*. Cell Death Differ, 2016. **23**(12): p. 1952-1960.
165. Chillemi, G., et al., *Structural Evolution and Dynamics of the p53 Proteins*. Cold Spring Harb Perspect Med, 2017. **7**(4).



166. Dameron, K.M., et al., *Control of angiogenesis in fibroblasts by p53 regulation of thrombospondin-1*. Science, 1994. **265**(5178): p. 1582-4.
167. Graeber, T.G., et al., *Hypoxia induces accumulation of p53 protein, but activation of a G1-phase checkpoint by low-oxygen conditions is independent of p53 status*. Mol Cell Biol, 1994. **14**(9): p. 6264-77.
168. Kamat, C.D., et al., *Mutant p53 facilitates pro-angiogenic, hyperproliferative phenotype in response to chronic relative hypoxia*. Cancer Lett, 2007. **249**(2): p. 209-19.
169. Mizuno, S., et al., *p53 Gene deficiency promotes hypoxia-induced pulmonary hypertension and vascular remodeling in mice*. Am J Physiol Lung Cell Mol Physiol, 2011. **300**(5): p. L753-61.
170. Mukhopadhyay, D., L. Tsiokas, and V.P. Sukhatme, *Wild-type p53 and v-Src exert opposing influences on human vascular endothelial growth factor gene expression*. Cancer Res, 1995. **55**(24): p. 6161-5.
171. Nishimori, H., et al., *A novel brain-specific p53-target gene, BAI1, containing thrombospondin type 1 repeats inhibits experimental angiogenesis*. Oncogene, 1997. **15**(18): p. 2145-50.
172. Zou, Z., et al., *p53 regulates the expression of the tumor suppressor gene maspin*. J Biol Chem, 2000. **275**(9): p. 6051-4.
173. Roe, J.S., et al., *p53 stabilization and transactivation by a von Hippel-Lindau protein*. Mol Cell, 2006. **22**(3): p. 395-405.
174. Amelio, I., et al., *TAp73 opposes tumor angiogenesis by promoting hypoxia-inducible factor 1alpha degradation*. Proc Natl Acad Sci U S A, 2015. **112**(1): p. 226-31.
175. Rayburn, E., et al., *MDM2 and human malignancies: expression, clinical pathology, prognostic markers, and implications for chemotherapy*. Curr Cancer Drug Targets, 2005. **5**(1): p. 27-41.
176. el-Deiry, W.S., et al., *WAF1, a potential mediator of p53 tumor suppression*. Cell, 1993. **75**(4): p. 817-25.
177. Han, J., et al., *Expression of bbc3, a pro-apoptotic BH3-only gene, is regulated by diverse cell death and survival signals*. Proc Natl Acad Sci U S A, 2001. **98**(20): p. 11318-23.
178. Miyashita, T. and J.C. Reed, *Tumor suppressor p53 is a direct transcriptional activator of the human bax gene*. Cell, 1995. **80**(2): p. 293-9.
179. Li, T., et al., *Tumor suppression in the absence of p53-mediated cell-cycle arrest, apoptosis, and senescence*. Cell, 2012. **149**(6): p. 1269-83.
180. Liu, G., et al., *Chromosome stability, in the absence of apoptosis, is critical for suppression of tumorigenesis in Trp53 mutant mice*. Nat Genet, 2004. **36**(1): p. 63-8.
181. Miled, C., et al., *A genomic map of p53 binding sites identifies novel p53 targets involved in an apoptotic network*. Cancer Res, 2005. **65**(12): p. 5096-104.
182. Gurova, K.V., et al., *p53 pathway in renal cell carcinoma is repressed by a dominant mechanism*. Cancer Res, 2004. **64**(6): p. 1951-8.
183. Russell, R.C. and M. Ohh, *NEDD8 acts as a 'molecular switch' defining the functional selectivity of VHL*. EMBO Rep, 2008. **9**(5): p. 486-91.

184. Somasundaram, K., et al., *BRCA1 signals ARF-dependent stabilization and coactivation of p53*. *Oncogene*, 1999. **18**(47): p. 6605-14.
185. Mukhopadhyay, D., et al., *Hypoxic induction of human vascular endothelial growth factor expression through c-Src activation*. *Nature*, 1995. **375**(6532): p. 577-81.
186. Reed, S.M. and D.E. Quelle, *p53 Acetylation: Regulation and Consequences*. *Cancers (Basel)*, 2014. **7**(1): p. 30-69.
187. Stebbins, C.E., W.G. Kaelin, Jr., and N.P. Pavletich, *Structure of the VHL-ElonginC-ElonginB complex: implications for VHL tumor suppressor function*. *Science*, 1999. **284**(5413): p. 455-61.
188. Venkatesan, T., et al., *MDM2 Overexpression Modulates the Angiogenesis-Related Gene Expression Profile of Prostate Cancer Cells*. *Cells*, 2018. **7**(5).
189. Xiong, J., et al., *Effects of MDM2 inhibitors on vascular endothelial growth factor-mediated tumor angiogenesis in human breast cancer*. *Angiogenesis*, 2014. **17**(1): p. 37-50.
190. Patterson, D.M., et al., *Effect of MDM2 and vascular endothelial growth factor inhibition on tumor angiogenesis and metastasis in neuroblastoma*. *Angiogenesis*, 2011. **14**(3): p. 255-66.
191. Ding, X., et al., *A DHX9-lncRNA-MDM2 interaction regulates cell invasion and angiogenesis of cervical cancer*. *Cell Death Differ*, 2018.
192. Eliceiri, B.P., et al., *Selective requirement for Src kinases during VEGF-induced angiogenesis and vascular permeability*. *Mol Cell*, 1999. **4**(6): p. 915-24.
193. Bohlman, S. and J.J. Manfredi, *p53-independent effects of Mdm2*. *Subcell Biochem*, 2014. **85**: p. 235-46.
194. Ganguli, G. and B. Wasylyk, *p53-independent functions of MDM2*. *Mol Cancer Res*, 2003. **1**(14): p. 1027-35.
195. Kadakia, M., C. Slader, and S.J. Berberich, *Regulation of p63 function by Mdm2 and MdmX*. *DNA Cell Biol*, 2001. **20**(6): p. 321-30.
196. Wang, X.Q., et al., *A possible role of p73 on the modulation of p53 level through MDM2*. *Cancer Res*, 2001. **61**(4): p. 1598-603.
197. Zeng, X., et al., *MDM2 suppresses p73 function without promoting p73 degradation*. *Mol Cell Biol*, 1999. **19**(5): p. 3257-66.
198. An, W.G., et al., *Stabilization of wild-type p53 by hypoxia-inducible factor 1alpha*. *Nature*, 1998. **392**(6674): p. 405-8.
199. Hammond, E.M., et al., *Hypoxia links ATR and p53 through replication arrest*. *Mol Cell Biol*, 2002. **22**(6): p. 1834-43.
200. Hansson, L.O., et al., *Two sequence motifs from HIF-1alpha bind to the DNA-binding site of p53*. *Proc Natl Acad Sci U S A*, 2002. **99**(16): p. 10305-9.
201. Pan, Y., et al., *p53 cannot be induced by hypoxia alone but responds to the hypoxic microenvironment*. *Oncogene*, 2004. **23**(29): p. 4975-83.
202. Sanchez-Puig, N., D.B. Veprintsev, and A.R. Fersht, *Binding of natively unfolded HIF-1alpha ODD domain to p53*. *Mol Cell*, 2005. **17**(1): p. 11-21.
203. Noon, A.P., et al., *p53 and MDM2 in renal cell carcinoma: biomarkers for disease progression and future therapeutic targets?* *Cancer*, 2010. **116**(4): p. 780-90.

204. Haitel, A., et al., *mdm2 expression as a prognostic indicator in clear cell renal cell carcinoma: comparison with p53 overexpression and clinicopathological parameters*. Clin Cancer Res, 2000. **6**(5): p. 1840-4.
205. Brosh, R. and V. Rotter, *When mutants gain new powers: news from the mutant p53 field*. Nat Rev Cancer, 2009. **9**(10): p. 701-13.
206. Vousden, K.H. and X. Lu, *Live or let die: the cell's response to p53*. Nat Rev Cancer, 2002. **2**(8): p. 594-604.
207. Singh, R.K., S. Iyappan, and M. Scheffner, *Hetero-oligomerization with MdmX rescues the ubiquitin/Nedd8 ligase activity of RING finger mutants of Mdm2*. J Biol Chem, 2007. **282**(15): p. 10901-7.
208. Uldrijan, S., W.J. Pannekoek, and K.H. Vousden, *An essential function of the extreme C-terminus of MDM2 can be provided by MDMX*. EMBO J, 2007. **26**(1): p. 102-12.
209. Okamoto, K., Y. Taya, and H. Nakagama, *Mdmx enhances p53 ubiquitination by altering the substrate preference of the Mdm2 ubiquitin ligase*. FEBS Lett, 2009. **583**(17): p. 2710-4.
210. Tamborini, E., et al., *Analysis of the molecular species generated by MDM2 gene amplification in liposarcomas*. Int J Cancer, 2001. **92**(6): p. 790-6.
211. Steinman, H.A., et al., *An alternative splice form of Mdm2 induces p53-independent cell growth and tumorigenesis*. J Biol Chem, 2004. **279**(6): p. 4877-86.
212. Bartel, F., et al., *MDM2 and its splice variant messenger RNAs: expression in tumors and down-regulation using antisense oligonucleotides*. Mol Cancer Res, 2004. **2**(1): p. 29-35.
213. Cohen, H.T., et al., *An important von Hippel-Lindau tumor suppressor domain mediates Sp1-binding and self-association*. Biochem Biophys Res Commun, 1999. **266**(1): p. 43-50.
214. Mukhopadhyay, D., et al., *The von Hippel-Lindau tumor suppressor gene product interacts with Sp1 to repress vascular endothelial growth factor promoter activity*. Mol Cell Biol, 1997. **17**(9): p. 5629-39.
215. Bond, G.L., et al., *A single nucleotide polymorphism in the MDM2 promoter attenuates the p53 tumor suppressor pathway and accelerates tumor formation in humans*. Cell, 2004. **119**(5): p. 591-602.
216. Knappskog, S., et al., *SNP285C modulates oestrogen receptor/Sp1 binding to the MDM2 promoter and reduces the risk of endometrial but not prostatic cancer*. Eur J Cancer, 2012. **48**(13): p. 1988-96.
217. Chang, C.J., D.J. Freeman, and H. Wu, *PTEN regulates Mdm2 expression through the P1 promoter*. J Biol Chem, 2004. **279**(28): p. 29841-8.
218. Kohnoh, T., et al., *Hypoxia-induced modulation of PTEN activity and EMT phenotypes in lung cancers*. Cancer Cell Int, 2016. **16**: p. 33.
219. Nakashima, H., et al., *Involvement of the transcription factor twist in phenotype alteration through epithelial-mesenchymal transition in lung cancer cells*. Mol Carcinog, 2012. **51**(5): p. 400-10.
220. Dimitriadi, M., et al., *p53-independent mechanisms regulate the P2-MDM2 promoter in adult astrocytic tumours*. Br J Cancer, 2008. **99**(7): p. 1144-52.

221. Grochola, L.F., et al., *Elevated transcript levels from the MDM2 P1 promoter and low p53 transcript levels are associated with poor prognosis in human pancreatic ductal adenocarcinoma*. *Pancreas*, 2011. **40**(2): p. 265-70.
222. Dulloo, I., et al., *Hypoxia-inducible TAp73 supports tumorigenesis by regulating the angiogenic transcriptome*. *Nat Cell Biol*, 2015. **17**(4): p. 511-23.
223. Sabapathy, K., *p73: a Positive or Negative Regulator of Angiogenesis, or Both?* *Mol Cell Biol*, 2015. **36**(6): p. 848-54.

## Curriculum Vitae

**Eric R. Wolf**

### Education

Indiana University, Indianapolis, IN  
Ph.D., Biochemistry and Molecular Biology, July 2019

Purdue University, Indianapolis, IN  
B.S., Biomedical Engineering, May 2014

### Research Experience

Ph.D. Research, Indiana University, Department of Biochemistry and Molecular Biology, Indianapolis, IN. August 2014 - July 2019

Overlapping projects to examine the regulation of p53 activation

- 1) Mechanisms regulating the binding of wild-type p53 to p73
- 2) Signaling required for VHL activation of p53 in hypoxia

Advisor: Lindsey Mayo, PhD

### Oral Research Presentations

**E.R. Wolf**, L.D. Mayo. VHL restricts angiogenesis via activation of p53. Indiana University School of Medicine, Department of Biochemistry and Molecular Biology Student Seminar. October, 2018.

**E.R. Wolf**, L.D. Mayo. WT p53 complexes with p73 to induce cell death. Indiana University School of Medicine, Department of Biochemistry and Molecular Biology Student Seminar. October, 2017.

### Posters

**E.R. Wolf**, C.P. McAtarsney, K.E. Bredhold, A.M. Kline, L.D. Mayo, Mutant and wild-type p53 form complexes with p73 upon phosphorylation by the kinase JNK [abstract]. In: Indiana University Cancer Center Annual Research Day (2018)

D.J. Olivos, M. Chtcherbinine, **E.R. Wolf**, C.P. McAtarsney, L.D. Mayo, MDM2 induces cell fusion in breast cancer and osteosarcoma [abstract]. In: Proceedings of the American Association for Cancer Research Annual Meeting 2017; 2017 Apr 1-5; Washington, DC. Philadelphia (PA): AACR; Cancer Res 2017;77(13 Suppl):Abstract nr 2552

## **Publications**

**E.R. Wolf**, L.D. Mayo. Mdm2 functions as the angiogenic switch through its regulation of VHL. *Submitted*.

**E.R. Wolf**, C. P. McAtarsney, K.E. Bredhold, A.M. Kline, L.D. Mayo, Mutant and wild-type p53 form complexes with p73 upon phosphorylation by the kinase JNK. *Sci. Signal*.11, eaao4170 (2018)

P.M. Hauck, **E.R. Wolf**, D.J. Olivos, C.N. Batuello, K.C. McElyea, C.P. McAtarsney, R.M. Cournoyer, G.E. Sandusky, L.D. Mayo, Early stage metastasis requires Mdm2 and not p53 gain of function. *Mol. Cancer Res.* 15(11), 1598-1607 (2017)

P.M. Hauck, **E.R. Wolf**, D.J. Olivos, C.P. McAtarsney, L.D. Mayo. The fate of murine double minute X (MdmX) is dictated by distinct signaling pathways through murine double minute 2 (Mdm2). *Oncotarget.* 8, 104455-104466 (2017)

## **Honors and Awards**

Peggy Gibson Award (2018)

Simon Cancer Center Cancer Biology Training Program Fellowship (2017-2018)

Indiana University Graduate Fellowship (2014-2015)